New bacterial pathway of 4- and 5-chlorosalicylate degradation via 4-chlorocatechol and maleylacetate in a *Pseudomonas* strain

Von der Gemeinsamen Naturwissenschaftlichen Fakultät
der Technischen Universität Carolo-Wilhelmina
zu Braunschweig
zur Erlangung des Grades einer
Doktorin der Naturwissenschaften
(Dr.rer.nat.)
genehmigte
D i s s e r t a t i o n

von Patricia Nikodem
aus Frankfurt am Main

1. Referentin oder Referent: PD Dr. Dietmar Pieper
2. Referentin oder Referent: Prof. Dr. Norbert Käufer
eingereicht am: 08.12.2003
mündliche Prüfung (Disputation) am: 10.02.2004

2004

Table of contents

Preface

This thesis is presented to obtain the Ph.D. degree from the Technical University of Braunschweig. The work was performed at the Gesellschaft für Biotechnologische Forschung mbH (GBF), Braunschweig, from October 2000 to September 2003 with PD Dr. Dietmar Pieper as supervisor. The Ph.D. stipend was financed by the DFG-European Graduate College 653: „*Pseudomonas*: Biotechnology and Pathogenicity".

I would like to express my great gratitude to my supervisor PD Dr. Dietmar Pieper for his excellent and committed supervision during my Ph.D.. His strong interest in this project and his kindness and gratitude to allow me to go to many inspiring conferences, courses and research stays to collaborators has been precious to me.

I would like to thank Prof. Dr. Norbert Käufer and Prof. Dr. Dieter Jahn for participating in my Ph.D. commission.

I would like to thank Iris Plumeier for technical assistance and her great efforts to make the lab run and her caring about all lab members. Thanks to all other members and guests of the Biodegradation group for their great concern and cooperation. I also would like to thank Daniela Regenhardt, Holger Heuer, Manolo Ferrer and all other people of the microbiology department at GBF for their support when ever help was needed.

Special thanks to Dr. Volker Hecht for excellent collaboration and modeling of enzyme kinetics, as well as critical evaluation of experimental data and many fruitful discussions.

Thanks to Dr. Victor Wray for NMR analysis and help in interpretation of the data.

I also want to address my sincere thanks to Associate Prof. Tim Tolker-Nielsen, Associate Prof. Michael Givskov and Prof. Søren Molin from the Molecular Microbial Ecology group at the Technical University of Denmark (DTU) for great hospitality, where the genetic part of this work was performed. I want to thank them and all members of the group for their helpfulness and for enthusiastic, inspiring and fruitful discussions on scientific questions. Thanks as well for all the smaller and larger social gatherings that contribute to an excellent atmosphere in the group.

I would also like to express my gratitude to all members of the European Graduate College „*Pseudomonas*: Biotechnology and Pathogenicity" at the MHH in Hannover, the GBF in Braunschweig, Rigshospitalet and DTU in Denmark, especially to Prof. Dr. Burkhard Tümmler and Helga Riehn-Kopp for the great effort in organizing many excellent scientific seminars, Ph.D. courses and social gatherings

Once more, thanks to PD Dr. Dietmar Pieper, who has financed my stay at our collaborators in Santiago, Chile by a grant of the "Internationales Büro" sponsored by the BMBF. Thanks to the Prof. Bernardo Gonzalez and the staff of the Molecular Genetics and Microbiology group at the Universidad Cathólica for great hospitality, excellent assistance and support on all matters.

Finally, I want to sincerely thank my friends and family, especially my boyfriend, Dr. Morten Hentzer, who have supported and encouraged me throughout this work.

Frederiksberg, November 2003. Patricia Nikodem

Summary

In the present study a novel metabolic pathway for 4-and 5-chlorosalicylate degradation in *Pseudomonas* sp. strain MT1, a bacterial isolate derived from a four-membered 4-chlorosalicylate degrading community, was elucidated.

4-chlorocatechol, 3-chloromuconate and maleylacetate were identified to be metabolites of the pathway. Transformation of 4- and 5-chlorosalicylate was shown to be catalyzed by a salicylate 1-hydroxy-lase. The reaction product 4-chlorocatechol was subject to intradiol cleavage by a catechol 1,2-dioxygenase with substrate specificity similar to enzymes of the 3-oxoadipate pathway. Thus MT1 is the first strain described to mineralize chloroaromatics without the involvement of a dioxygenase specialized for chloroaromatic ring-cleavage.

Transformation of 3-chloromuconate constitutes the core of the novel pathway and the responsible enzymes were identified and purified. Muconate cycloisomerase (MCI) catalyzed 3-chloromuconate transformation to mainly protoanemonin and minor amounts of *cis*-dienelactone and maleylacetate. Protoanemonin and *cis*-dienelactone are dead-end products of MT1 metabolism. A second muconate cycloisomerase (MCIB), transforms 3-chloromuconate to protoanemonin and *cis*-dienelactone in equal amounts and is assumed to be an evolutionary intermediate between muconate and chloromuconate cycloisomerases. Even though purified *trans*-dienelactone hydrolase (*trans*-DLH) acts neither on 3-chloromuconate, nor on protoanemonin, it was found that simultaneous presence of *trans*-DLH and one of the cycloisomerases yielded considerately less protoanemonin and more maleylacetate than when 3-chloromuconate was transformed by MCI or MCIB alone. As *trans*-DLH converts 4-fluoromuconolactone to maleylacetate, it is suggested that this enzyme hydrolizes 4-chloromuconolactone, the assumed intermediate of 3-chloromuconate cycloisomerization, and thus prevents protoanemonin formation in favor of maleylacetate formation. *cis*-Dienelactone formation was not effected by the presence of *trans*-DLH, indicating that its production does not necessitate the intermediate formation of 4-chloromuconolactone. Maleylacetate is channeled to the 3-oxoadipate pathway by a maleylacetate reductase (MAR).

Detailed analysis of 3-chloromuconate transformation by the concomitant action of purified MCI (or MCIB) and *trans*-DLH revealed that product formation was not only dependent on the ratio of enzymes, but that higher protein concentrations favored maleylacetate formation over protoanemonin formation. Such a behavior can be explained by kinetic models describing the

reaction mechanism with a spontaneous degradation of 4-chloromuconolactone to protoanemonin competing with a *trans*-DLH catalyzed hydrolization of 4-chloromuconolactone to maleylacetate.

MCI was induced to high activity during growth on salicylate and to a much lower extent during growth on chlorosalicylate. This indicates that MCI, despite its extraordinary high activity with 3-chloromuconate is part of the 3-oxoadipate pathway of MT1. In contrast, MCIB and *trans*-DLH were predominantly induced during growth on chlorosalicylate. This suggests that MCI and MCIB belong to independent regulons.

trans-DLH differs from previously described *cis*/*trans*-dienelactone hydrolases not only by substrate specificity, but also by its susceptibility to reducing and chelating agents. Partial protein sequences revealed no homology to previously described proteins. Thus, *trans*-DLH seems to be a member of a previously undescribed protein family.

The MAR encoding gene is not localized in a chlorocatechol gene cluster, as none of the other typical enzymes forming such clusters was coinduced. MAR of MT1 was shown to differ from MAR $TfdF_I$ of JMP134 by its substrate specificity, being capable to transform *cis*-acetylacrylate. This activity could explain the previous observation of *cis*-acetylacrylate being a growth substrate for MT1, which had been misinterpreted as an indication for *cis*-acetylacrylate as a pathway intermediate in an earlier study (106).

Abbreviations

4-ClML	4-chloromuconolactone
bp	Base pairs
CMCI	Chloromuconate cycloiosmerase
DLH	Dienelactone hydrolase
DMSO	Dimethylsulfoxide
DNA	Deoxyribonucleic acid
ε	Extinction coefficient
EDTA	Ethylene diamine tetraacetic acid
FPLC	Fast protein liquid chromatography
HPLC	High pressure liquid chromatography
Hz	Hertz
k_{cat}	Catalytic rate constant
kDa	Kilodalton
K_i	Inhibition constant
K_m	Michaelis-Menten constant
K_{SS}	Substrate inhibition constant
λ	Wavelength
M	Molar
MAR	Maleylacetate reductase
MAR	Maleylacetate reductase
MCI	Muconate cycloisomerase
MCIB	Novel muconate cycloisomerase
MIC	Minimal inhibitory concentration
MS	Mass spectrometry
MW	Molecular weight
NAD^+	Nicotinamide adenine dinucleotide
NCBI	National Center for Biotechnology Information
ND	Not determined
NMR	Nuclear magnetic resonance spectrometry
PCB	Polychlorinated biphenyls
PCN	Polychlorinated naphthalenes
PCR	Polymerase chain reaction
ppm	parts per million
Q-TOF	Quadropole Time of Flight
RNA	Ribonucleic acid
SDS-PAGE	Sodium dodecyl sulphate polyacrylamide gel electrophoresis
U	Unit
UV	Ultraviolet
V_{max}	Maximal velocity

1. Introduction

1.1 Natural and xenobiotic aromatic compounds in the environment

Aromatic compounds form a large class of organic molecules which contain one or more aromatic rings. They can be substituted and combined into large polyaromatic molecules, giving millions of possible different compounds (167). Aromatic compounds play an important role in natural carbon cycles as they are indispensable constituents of proteins and electron transport chains and important plant constituents such as hydroquinones, flavonoids or lignin (53, 156). Though, a wide variety of naturally occurring halogenated aromatics have been identified (5), most haloaromatic compounds present in the environment are products of human activity. The use of chloroaromatic compounds (eg. polychlorinated biphenyls (PCB) or polychlorinated naphthalenes (PCN)) became popular in the beginning of the last century. Due to their high stability they found large application as inflammables, insulators, and preservative additives in coatings, colours, and organic solvents (96, 166). Other chlorinated aromatics such as chlorinated dibenzofurans and dibenzodioxins were formed as by-products during production processes or incineration. Among others, polychlorinated naphthalenes have been identified as priority pollutants by the U.S. Environmental Protection Agency (57). It is the same chemical inertness that made chloroaromatics popular for many modern applications, now responsible for their persistence in the environment. Even though substantial progress has been made to reduce industrial pollution, also by limiting the number of applications, major accidents still occur and a considerable number of polluted sites exist. A prominent example is the industrial waste site near Bitterfeld, Germany, comprising a 25 km^2 area and $2 \cdot 10^8$ m^3 of groundwater contaminated predominantly with chlorobenzene, resulting in significantly increased atmospheric concentrations of chlorobenzenes (11, 87, 117). Some of the contaminated sites are a high risk for contamination of drinking-water supplies and as such a substantial health hazard for current and future generations (160, 179).

1.2 Aerobic degradation of aromatic compounds by bacteria

The degradation of aromatic compounds has been subject to intensive investigations (147). Under aerobic conditions a large variety of upper pathway reactions, which comprise only a few reaction types (121), most importantly mono- and dioxygenations (53), transform aromatics to a small number of central metabolites; dihydroxy derivatives, such as catechols or protocatechuate and gentisate which undergo oxygenolytic cleavage of the aromatic ring (50, 125) (Fig. 1). Gentisate is oxidized by gentisate 1,2-dioxygenases between the carboxyl-substituted carbon and the adjacent hydroxylated carbon to maleylpyruvate (44, 172, 186). Protocatechuate can either be cleaved in an introdiol (*ortho*-cleavage*)* or extradiol (*meta*-cleavage*)* fashion (50) and then be further metabolized to Krebs cycle intermediates (100, 101) (Fig. 1).

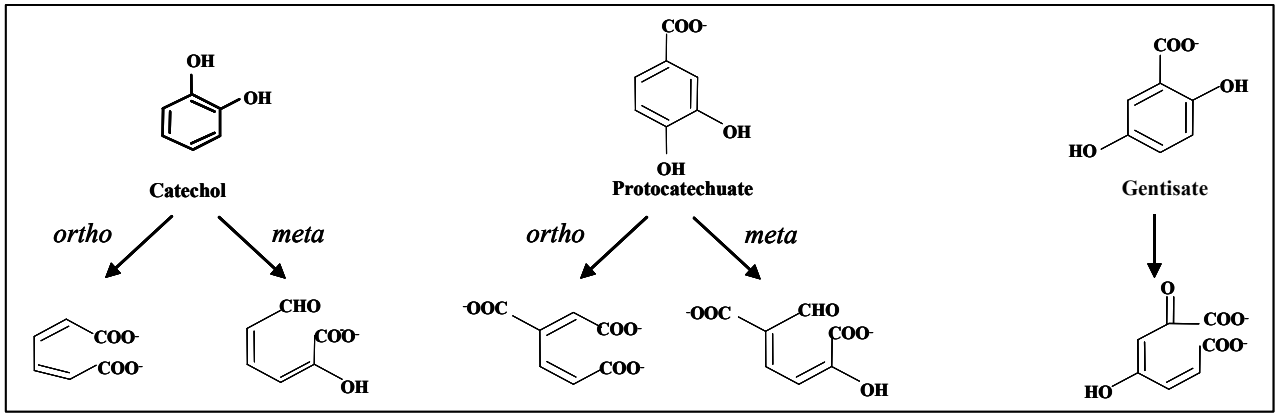

Figure 1: Catechol, protocatechuate and gentisate as central intermediates in aromatic degradative pathways. Modes of ring-cleavage of these intermediates are indicated.

Catechols are the central intermediate of the degradation of aromatic hydrocarbons like benzoates, benzenes or phenols, amino acids and toluenes (50).

Unsubstituted catechol can be readily degraded by the wide-spread catechol branch of the 3-oxoadipate pathway (50, 100) (Fig. 4 A) which proceeds by *ortho*-cleavage of the aromatic ring by catechol 1,2-dioxygenase to *cis*,*cis*-muconate. Muconate is further transformed to muconolactone (4-carboxymethylbut-2-en-4-olide) by muconate cycloisomerase, followed by isomerization to enollactone (4-carboxymethylbut-3-en-4-olide) catalyzed by muconolactone isomerase. Enollactone hydrolase hydrolyzes enollactone to 3-oxoadipate. 3-Oxoadipate is further transformed by 3-oxoadipate:succinyl-CoA transferase and 3-oxoadipyl-CoA thiolase to succinate and acetyl-CoA which can readily be mineralized in the Krebs cycle.

Methylcatechols are generally metabolized via *meta*-cleavage. This reaction is catalyzed by a catechol 2,3-dioxygenase leading to 2-hydroxymuconic semialdehydes (6, 129, 176) which are further converted to the final pathway products, pyruvate and acetylaldehyde or their derivatives (161) (Fig. 2).

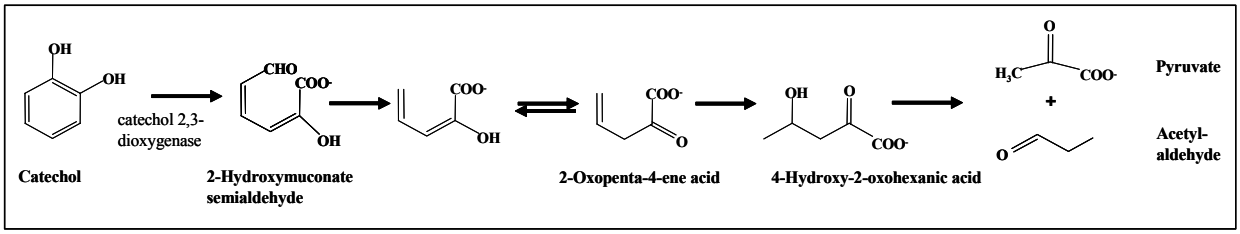

Figure 2: Degradation of catechols by the *meta*-cleavage pathway.

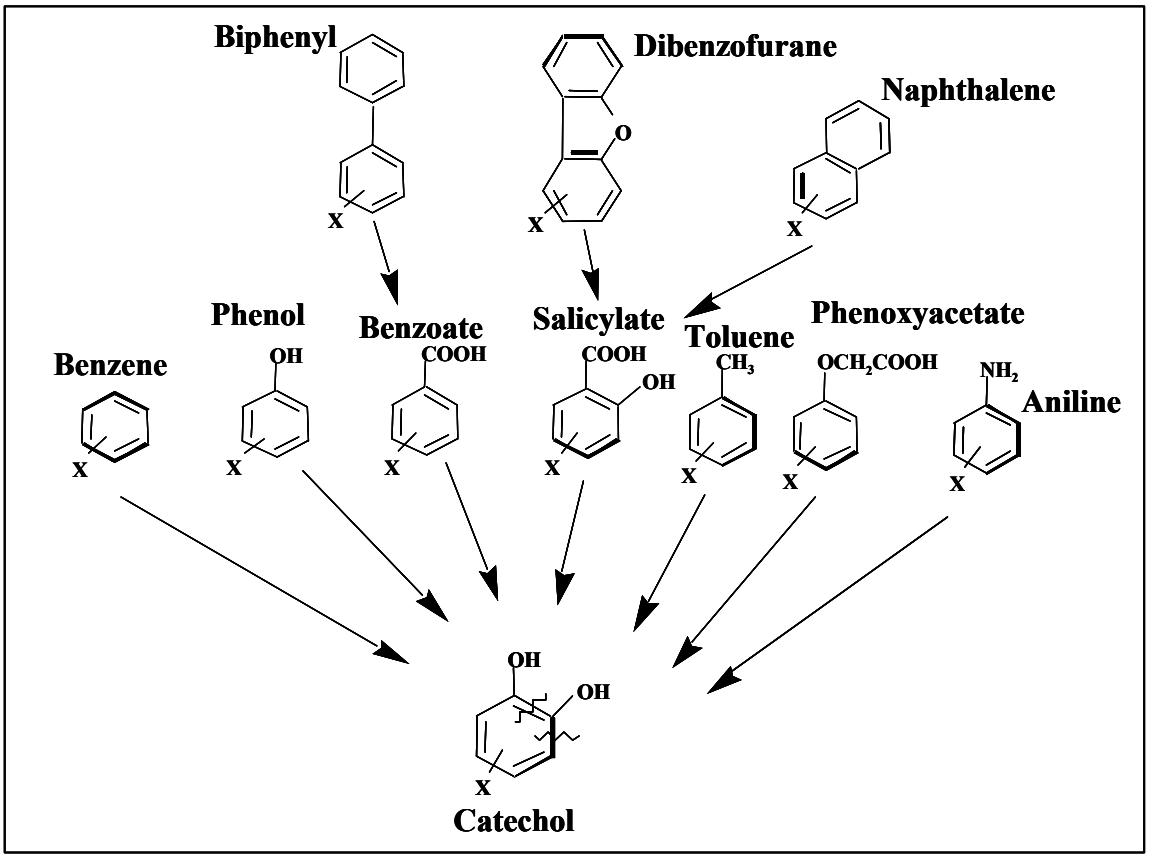

Figure 3: Catechol as central intermediate in the aerobic degradation of aromatic compounds.

Poly- and bicyclic aromatic compounds, such as naphthalenes, dibenzofurans and biphenyls, are transformed by so-called peripheral or "upper pathway" reactions, to central intermediates; naphthalenes and dibenzofurans are degraded via salicylates (32, 37, 182), biphenyls via benzoates

as intermediates (41) (Fig 3). Though direct ring fission of salicylate (59) has been described, the degradation of salicylate involves either transformation by a salicylate 5-hydroxylase to gentisate (40, 47) or by a salicylate 1-hydroxylase yielding catechol (121, 182, 184).

1.3 Degradation of chlorocatechols by the specialized chlorocatechol pathway

Various enzymes involved in the degradation of aromatic compounds such as toluene dioxygenase (43) benzoate dioxygenase (122) or salicylate hydroxylase (82) have been reported to be of relatively broad substrate specificity and to be capable to transform at least some lower chlorinated substrate analogues. Such activities usually result in the formation of chlorosubstituted catechols from chloroaromatics. Chlorocatechols, in most cases reported thus far, are degraded by enzymes of the chlorocatechol pathway, also called the modified *ortho*-cleavage pathway (30, 121, 124, 139). The chlorocatechol pathway (Fig. 4 B) involves *ortho*-cleavage by chlorocatechol 1,2-dioxygenase which is highly active with chlorocatechols (30), a chloromuconate cycloisomerase highly active with chloro-*cis*,*cis*-muconates (139), a dienelactone hydrolase active with *cis*- and *trans*-dienelactone (4-carboxymethylenebut-2-en-4-olide) (139), and a maleylacetate reductase (70) that reduces the hydrolysis product, maleylacetate, to 3-oxoadipate. 3-Oxoadipate conversion into Krebs-cycle intermediates relies on the 3-oxoadipate:succinyl-CoA transferase and 3-oxoadipyl-CoA thiolase of the 3-oxoadipate pathway. However, degradation of chlorocatechols via a *meta*-cleavage pathway has also recently been described (86).

1.4 Comparison of the 3-oxoadipate and the chlorocatechol pathway

1.4.1 Biochemistry of the 3-oxoadipate and the chlorocatechol pathway

The first enzymes of the 3-oxoadipate pathway for catechol degradation and of the chlorocatechol pathway carry out identical reactions. Catechol 1,2-dioxygenase and chlorocatechol 1,2-dioxygenase, respectively, cleave the aromatic ring of (chloro)catechols between the hydroxyl groups (*ortho* position) leading to the respective muconates (Fig. 4). However, these classes of enzymes differ significantly in their substrate specificity. Whereas chlorocatecol 1,2-dioxygenases from proteobacteria exhibit similar activities with catechol and 4- and 3-chlorocatechol activity of catechol 1,2-dioxygenases with 4-chlorocatechol and 3-chlorocatechol is low (10 % and 1 %) compared to its activity with catechol (13, 30, 121).

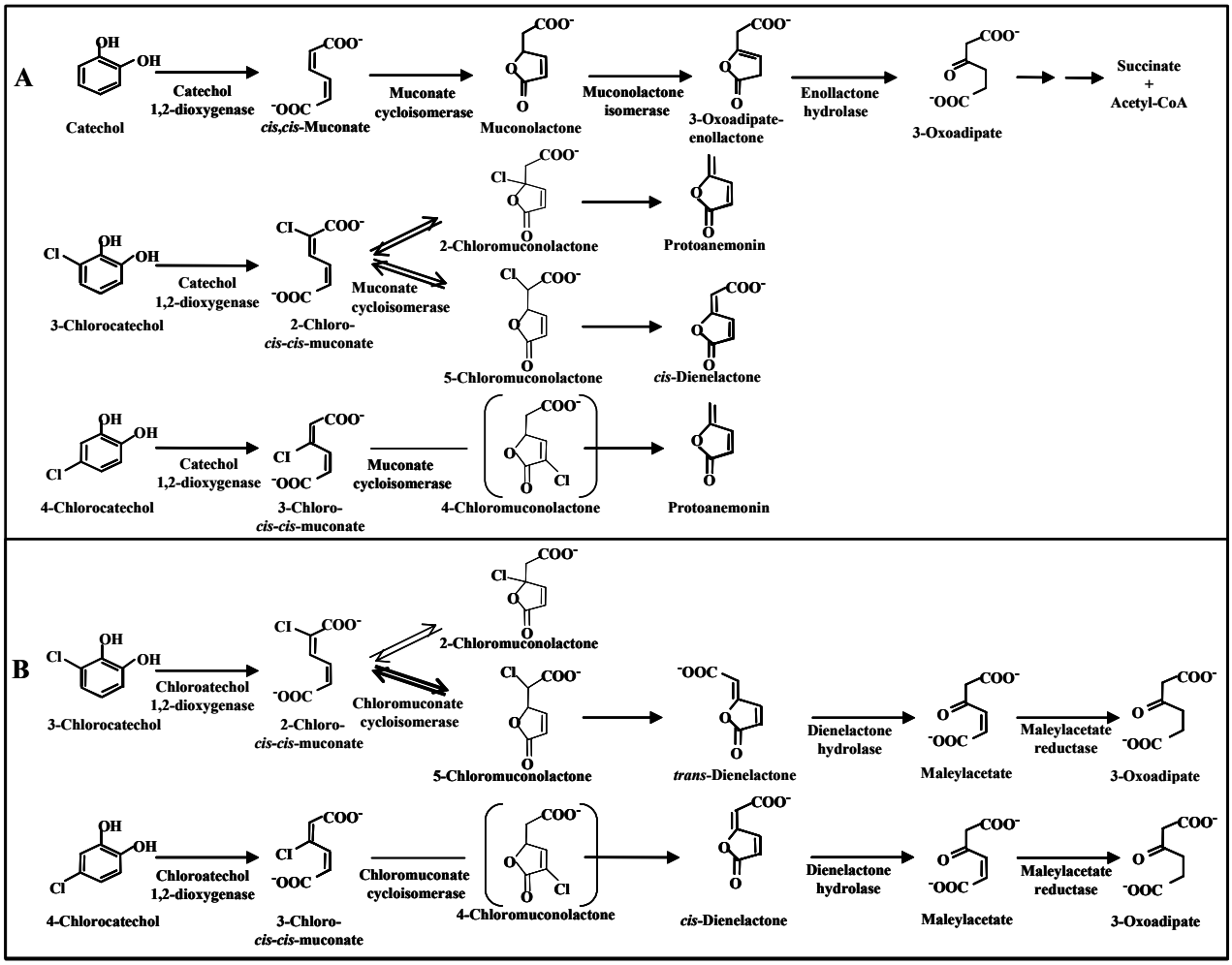

Figure 4: Transformation of catechol, 3-chloro-and 4-chlorocatechol by the proteobacterial 3-oxoadipate pathway **(A)** and chlorocatechol pathway **(B)**. Postulated metabolites of hypothetical presence are embraced in brackets.

Similarly, muconate cyloisomerases involved in the 3-oxoadipate pathway are reported to have a narrow substrate specificity being highly active with unchlorinated muconate, whereas their activity with 2- and 3-chloromuconate is very low (139, 169). In contrast, protobacterial chloromuconate cycloisomerases have a relaxed substrate specificity and thus can transform muconate, 2-chloro- and 3-chloromuconate with high activities (139). Whereas *trans*-dienelactone is the product formed from 2-chloromuconate by chloromuconate cycloisomerases, 3-chloromuconate yields *cis*-dienelactone. However, whereas catechol- and chlorocatechol dioxygenases differ only in substrate specificity, muconate and chloromuconate cycloisomerases differ also in the reaction they catalyze (see 1.5).

Muconolactone, the cycloisomerization product formed during catechol degradation via the 3-oxoadipate pathway, is further transformed by muconolactone isomerase, a reaction which has no

counterpart in the chlorocatechol pathway. The enzyme shifts the double bond of muconolactone to form 3-oxoadipate enollactone (enollactone) and thus prepares the lactone for hydrolysis (103). In contrast, *cis*- or *trans*-dienelactone formed from chlorocatechols have a conjugated double bond adjacent to the lactone bond and can therefore be subject to direct hydrolysis. Hydrolysis of enollactone yields directly 3-oxoadipate, whereas hydrolization of dienelactones by *cis*-/*trans*-dienelactone hydrolase release maleylacetate. It was already in 1980 described that the enollactone hydrolase of the 3-oxoadipate pathway and *cis*-/*trans*-dienelactone hydrolase of the chlorocatechol pathway show no cross-reactivity (132, 139). Reduction of maleylacetate to 3-oxoadipate by maleylacetate reductase in the chlorocatechol pathway has no analogous counterpart in the 3-oxoadipate pathway.

1.4.2 Genetics of the 3-oxoadipate and the chlorocatechol pathway

The 3-oxoadipate pathway has been observed in a broad range of microorganisms. As it plays a key role in the catabolism of a wide variety of aromatic compounds, it is not surprising that this pathway is present in all four *Pseudomonas* species whose genome has been analyzed thus far (62). The two branches of the 3-oxoadipate pathway, i. e. the protocatechuate branch (*pca* genes) and the catechol branch (*cat* genes), converge at 3-oxoadipate enollactone in *Pseudomonas*. One set of enzymes (*pcaDIJF* gene products) complete the conversion of the latter to the Krebs cycle intermediates, succinyl-CoA and acetyl-CoA. In some other bacterial species such as *Acinetobacter* sp. ADP1, the catechol branch and the protocatechuate branch never converge and two independently regulated set of genes encode isofunctional enzymes for the last three steps of the pathway (62, 104). In contrast to the chromosomally encoded 3-oxoadipate pathway, the chlorocatechol pathway is usually encoded on mobile genetic elements, often on plasmids (6, 32, 62, 161, 176) and generally encoded by a single operon.

Due to the biochemical analogies between the pathways, it was assumed that the chlorocatechol pathway had derived from the wide-spread 3-oxoadipate pathway (29). Indeed, proteobacterial catechol 1,2-dioxygenases and chlorocatechol 1,2-dioxygenases share 25 – 35 % amino acid identity, among catechol 1,2-dioxygenases the percentage of identical positions varies from 27 - 58 %, and among chlorocatechol 1,2-dioxygenases from 55 - 66 % (34, 134, 162, 164). Muconate cycloisomerases and chloromuconate cycloisomerases share significant amino acid

identity of 40 - 45 % (133). In contrast, sequence similarities between enollactone and dienelactone hydrolases are not significant (133).

1.5 Muconate and chloromuconate cycloisomerases

Muconate cycloisomerase and chloromuconate cycloisomerase were first distinguished by their substrate specificity (139). Muconate cycloisomerases are active with unsubstituted muconate, but their activity with 2-chloromuconate, 3-chloromuconate and 2,4-dichloromuconate is very low. In contrast, chloromuconate cycloisomerases are highly active with chloromuconates, while their activity with muconate can be decreased (78, 139, 168, 169).

Recent studies have demonstrated that chloromuconate cycloisomerases and muconate cycloisomerases also differ in the reactions they catalyze (8, 168, 171). Proteobacterial chloromuconate cycloisomerases transform 2-chloromuconate predominantly by 3,6-cycloisomerization to 5-chloromuconolactone and by subsequent dehalogenation to *trans*-dienelactone (78, 139, 140, 171) whereas proteobacterial muconate cycloisomerases catalyzes 3,6- and 1,4-cycloisomerization with 2-chloro- and 5-chloromuconolactone as the final products (168) (Fig. 4) (168). 3-Chloromuconate is subject to cycloisomerization and dehalogenation by chloromuconate cycloisomerases with *cis*-dienelactone as product (139) whereas muconate cycloisomerases form toxic protoanemonin as product by an unknown mechanism (8) (Fig. 4).

Chloromuconate cycloisomerases thus differ from muconate cycloisomerases in terms of: (i) increased turnover of 2-chloro-*cis*,*cis*-muconate, (ii) discrimination between the two possible cycloisomerization directions of this substrate, (iii) dehalogenation of (+)-5-chloromuconolactone, (iv) increased conversion of (+)-5-chloromuconolactone, (v) increased conversion of 3-chloromuconate and 2,4-dichloro-*cis*,*cis*-muconate and (vi) avoidance of protoanemonin formation during 3-chloro-*cis*,*cis*-muconate transformation (131, 169). Crystallization and studies of the three-dimensional structure of muconate cycloisomerase of *Pseudomonas putida* PRS2000 (55) and chloromuconate cycloisomerase of *Ralstonia eutropha* JMP134 (49, 76) have provided new insights into substrate binding and catalytic mechanisms. Both muconate cycloisomerase and chloromuconate cycloisomerase consist of eight identical subunits, each containing an essential manganese ion at the active site (55, 76, 131). Comparisons of the reaction mechanisms of muconate cycloisomerase and mandelate racemase lead to postulation of an enol/enolate

intermediate formed during cycloisomerization (42, 55, 131). In the transformation of muconate, a proton is added to this intermediate resulting in the formation of muconolactone.
Site-directed mutagenesis studies (72) showed that both, the formation of muconolactone from muconate or the formation of chloromuconolactones from 2-chloromuconate as well as the formation of protoanemonin from 3-chloromuconate, as carried out by muconate cycloisomerases, requires protonation catalyzed by a lysine residue. In contrast, protonation is not necessary for the formation of *cis*-dienelactone as catalyzed by chloromuconate cycloisomerases (42, 72). Whereas dehalogenation of 3-chloromuconate seems to be a rather simple process, dehalogenation of 2-chloromuconate is more complex. Structural studies on the wild-type and variants muconate cycloisomerase of PRS2000 suggested that dehalogenation necessitates the rotation of the lactone group of intermediary 5-chloromuconolactone, to give *trans*-dienelactone (131).
However, even though site-directed mutagenesis studies had increased our knowledge on the reaction mechanisms of muconate and chloromuconate cycloisomerases, exchanges of specific amino acids at the active site of the muconate cycloisomerase of *Pseudomonas putida* PRS2000 demonstrated that the putative evolution from muconate cycloisomerases to chloromuconate cycloisomerases of gram-negative bacteria cannot be mimicked by a single or double substitutions, but must be the result of a rather complex process (169).

Contrary to information on proteobacterial muconate and chloromuconate cycloisomerases, there is only poor information on the respective enzymes from gram positive organisms. A muconate cycloisomerase and a chloromuconate cycloisomerase had been purified from the gram positive strain *Rhodococcus opacus* 1CP (33, 34). Like proteobacterial muconate cycloisomerases, muconate cycloisomerase of strain 1CP had only poor activity with chloromuconates. However, in contrast, this enzyme converted 2-chloromuconate to 5-chloromuconolactone as only products and was not capable to transform 2-chloromuconolactone. The 1CP derived chloromuconate cycloisomerase differed from the 1CP muconate cycloisomerase mainly by its capability to rapidly transform 3-chloromuconate and was as well neither capable to dehalogenate 2-chloromuconate nor to transform 2-cloromuconolactone (150). Recently, a second chloromuconate cycloisomerase was described from the same strain (90). Even though it exhibited higher turnover numbers with 2-chloromuconate, this enzyme was as well not capable to dehalogenate 2-chloromuconate and 5-chloromuconolactone was the only cycloisomerization product. None of the three protein sequences were highly related to muconate and chloromuconate cycloisomerases of gram negative

strains (34, 91). The metabolic diversity of (chloro)muconate cycloisomerases was further underlined by studies of Plumeier et al. who recently demonstrated that the chloromuconate cycloisomerase $TfdD_{II}$ of the gram-negative bacterium *Ralstonia eutropha* JMP134 is also only distantly related to all other cycloisomerases characterized thus far and is unable to efficiently convert 2-chloro-*cis,cis*-muconate to *trans*-dienelactone (114).

1.6 Enollactone hydrolases and dienelactone hydrolases

Enollactone hydrolase and *cis*-/*trans*-dienelactone hydrolase (*cis*-/*trans*-DLH) catalyze hydrolysis of lactones in the 3-oxoadipate and the chlorocatechol pathway, respectively. The low sequence similarity (<12 % identical amino acid positions) (39, 133, 163) and the lack of cross-reactivity between enollactone hydrolases and *cis*-/*trans*-DLH with each others substrates (85, 95, 133, 139) disproves the hypothesis that *cis*-/*trans*-DLH of the chlorocatechol pathway was recruited from enollactone hydrolase of the 3-oxoadipate pathway (Fig. 4).

Dienelactone hydrolases involved in the chlorocatechol pathway are usually active with both the *cis*- and the *trans*-isomer. Such a specificity is necessary as *cis*-dienelactone is the product formed during degradation of 4-chlorocatechol via 3-chloromuconate, and *trans*-dienelactone is formed during metabolism of 3-chlorocatechol via 2-chloromuconate by enzymes of the chlorocatechol pathway as described above. However, dienelactone hydrolases with more restricted substrate specificity have been described by Schlömann et al. (137). The authors analyzed the degradation of 4-fluorobenzoate by bacterial isolates and showed that various strains can mineralize this substrate without expressing chlorocatechol dioxygenase and chloromuconate cycloisomerase. Obviously enzymes of the 3-oxoadipate pathway capable to transform fluorosubstituted analogues were recruited. However, as described above, the metabolic routes of halocatechol and catechol metabolism diverge after cycloisomerization. It was thus expected, that growth on fluorobenzoate necessitates the induction of a dienelactone hydrolase and a maleylacetate reductase. The work of Schlömann et al. resulted in two new findings. Firstly, the authors observe 4-fluoromuconolactone but not *cis*-dienelactone as cycloisomerization product (135). Secondly, new types of dienelactone hydrolases were shown to be induced during growth on fluorobenzoate. *Ralstonia eutropha* 335, H16 and JMP222 (132, 137) induced a dienelactone hydrolase active only with *trans*-dienelactone. This enzyme was shown to be capable to transform 4-fluoromuconolactone and obviously together with a maleylacetate reductase recruited for 4-fluorobenzoate degradation.

Burkholderia cepacia was shown to harbor a dienelactone hydrolase exclusively active with *cis*-dienelactone but the function of this enzyme in fluorobenzoate degradation was not evident.
Rhodococcus opacus 1CP was recently reported to harbor a DLH with similar substrate specificity active only with *cis*-dienelactone (85) as part of a novel pathway for chlorocatechol degradation (89, 90, 91). This enzyme is obviously involved only in 4-chloro- and 3,5-dichlorocatechol degradation, which both are degraded via *cis*-dienelactones. Based on susceptibility to inhibition by *p*-chloromercuribenzoate, protein sequence comparison (about 20-30 % amino acid identity with proteobacterial *cis*-/*trans*-DLH) (34, 85) *R. opacus* DLH was suggested to be closer related to proteobacterial *cis*-/*trans*-DLH than to *cis*-DLH of *B. cepacia* indicating that substrate specificity is not necessarily a valid property for classification of the DLH (85, 133).
Above mentioned results on *Rhodococcus* raised the question, how 3-chlorocatechol is degraded by this strain, as cycloisomerization gives rise to 5-chloromuconolactone as product, which is not further transformed by the cycloisomerases of this strain. Prucha et al. had shown, that 5-chloromuconolactone can be transformed at high activity by muconolactone isomerases of the 3-oxoadipate pathway (119). In contrast to proteobacterial chloromuconate cycloisomerases, which catalyze the formation of *trans*-dienelactone (as dehalogenation necessitates a rotation of the lactone ring in the active site of the enzyme), muconolactone isomerase catalyze the formation of *cis*-dienelactone (119). Moiseva could show, that *Rhodococcus opacus* recruits a muconolactone for 3-chlorocatechol degradation, thereby forming *cis*-dienelactone rather than *trans*-dienelactone as intermediate of 3-chlorocatechol degradation (89).

1.7 Maleylacetate reductases (MAR)

MAR catalyze the last step of the chlorocatechol pathway, the NADH- dependent reduction of maleylacetate to 3-oxoadipate (Fig. 4). Various substituted maleylacetates have been shown to be substrates for the enzyme. As the enzyme obviously catalyze a hydrid transfer to the C2 carbon, 2-chloromaleylacetate is converted into an instable intermediate, which spontaneously eliminate halide forming maleylacetate, which is subject to a second round of reduction forming 3-oxoadipate (70).
Most MAR encoding genes investigated so far are located in the specialized metabolic gene clusters encoding enzymes involved in aromatic (4, 35, 65, 152), and especially, chlorocatechol degradation (38, 67, 68, 79, 114, 143, 163). MAR is also involved in the degradation of chloroaromatics via

hydroquinones or hydroxyhydroquinones. In *Sphingobium chlorophenolicum*, 2,6-dichloro-hydroquinone as intermediate of pentachlorophenol degradation is directly cleaved by PcpA dioxygenase. Evidence for the formation of 2-chloromaleylacetate was given (99, 180), which should arise after hydrolysis of the direct ring-cleavage product. MAR, as shown for the degradation of chlorocatechols, is assumed to channel 2-chloromaleylacetate into the Krebs cycle, and a MAR encoding gene *pcpE* was localized upstream of *pcpA* (16) but not clustered with other genes of the pathway. Similarly, degradation of 2,4,5-trichlorophenoxyacetate via hydroxyquinol by *B. cepacia* AC1100 or of 2,4,6-trichlorophenol by *Ralstonia eutropha* JMP134 involves maleylacetate reductases and their genes are not clustered with genes of the chlorocatechol pathway. In addition MAR play a crucial role in aerobic bacterial degradation of multiple aromatic compounds, such as resorcinol, 2,4-dihydroxybenoate (21) or nitro- or sulfoaromatics (35, 65, 152). Maleylacetate reductases thus fulfill functions in various different aromatic degradative pathways.

1.8 Misrouting of aromatic compounds to toxic protoanemonin as dead-end product

It is generally accepted that metabolites formed during transformation of aromatic compounds can be more toxic than the original substrate (52, 83, 128, 148). Consequently mineralization rather than incomplete biotransformation is important for bioremediation. Yet, the majority of microorganisms capable to transform substituted aromatics by unspecific peripheric reactions often does not harbor the appropriate enzymes for a lower metabolic pathway – leading to metabolic misrouting and accumulation of dead-end products. Therefore it is not surprising that during metabolism of chloroaromatics, chlorocatechols often accumulate (48, 124) or are further transformed by enzymes of the wide-spread 3-oxoadipate pathway (8, 146), which leads to unproductive misrouting (Fig. 4). Blasco et. al described that catechol 1,2-dioxygenase transforms 4-chlorocatechol to 3-chloro-*cis*,*cis*-muconate in analogy to the reaction catalyzed by chlorocatechol 1,2-dioxygenase. A toxic compound with antimicrobial activity, protoanemonin, is the product of 3-chloromuconate transformation by muconate cycloisomerase (8). Protoanemonin formation in turn was assumed to be the reason for the poor survival of PCB cometabolizing organisms in soil microcosms. Though the indigenous soil microflora was demonstrated to metabolize protoanemonin (7), no defined reaction or defined enzyme activity capable to transform protoanemonin has been characterized so far. As the only exception, protoanemonin has been observed to be a substrate, though a very poor

one, for *cis*-/*trans*-DLH of the chlorocatechol pathways (14) - no significant activity with protoanemonin has been detected for other DLHs.

Protoanemonin formation has been shown to occur not only by misrouting of 4-chlorocatechol into the 3-oxoadipate pathway but also by misrouting of 3-chlorocatechol (146). As described above, muconate cycloisomerases catalyze cycloisomerization of 2-chloromuconate to form 2-chloro- and 5-chloromuconolactone, which are both substrates for muconolactone isomerase. Whereas 5-chloromuconolactone is transformed into *cis*-dienelactone, protoanemonin was shown to be formed from 2-chloromuconolactone, probably by elimination of CO_2 and chloride from chlorosubstituted enollactone. Kinetic investigations of the reaction have shown high amounts of protoanemonin to be produced from 2-chloromuconate. Thus protoanemonin accumulation seems to be a general problem when organisms harboring a 3-oxoadipate pathway are confronted with chloroaromatics.

1.9 Microbial communities

The pioneering work by Louis Pasteur and the germ theory of disease presented by Robert Koch in 1881 and 1884 describing the ability of pure cultures of microorganisms to cause disease, basically conceptualized the microbial research and until recently, most studies have been focused on pure cultures. However, in nature, microorganisms live in communities (18) and, even pure cultures grown for a considerable period of time tend to diversify (120). Despite competition with other species, there are several advantages for bacteria to reside in multispecies communities (145). Some of the benefits could be improved access to resources and niches that are not available for isolated cells. Problems resulting from accumulation of dead-end metabolites of a pathway of a single organism can be avoided in bacterial communities. Bacteria can interact metabolically by transformation of "dead" metabolites of one strain by another strain (24, 51, 97, 106, 177). Thus, the metabolic potential of a community corresponds to the sum (or even more) of the metabolisms of the single cells in the system (145) and laboratory studies document increased biodegradation by mixed cultures (36).

Enrichment culture techniques have traditionally been used to isolate single bacterial strains capable of metabolizing certain compounds, but recently the technique has been applied to isolate bacterial communities with special metabolic properties (6, 28, 45, 47, 77, 106, 137, 177). For example enrichment strategies by continuous culture techniques have allowed enrichment of a defined

bacterial community able to degrade 4-chlorosalicylate at GBF, Braunschweig, Germany, in a chemostat feed with 4-chlorosalicylate as only source of carbon and energy. The chemostat was inoculated with sediment from the aerobic zone of the creek Spittelwasser which flows into the river Elbe, sampled close to Bitterfeld, Germany, a site famous for its history of pollution by chemical industry (11, 87, 117, 179). A bacterial four strain community was enriched and the members *Pseudomonas* sp. MT1 , *Empedobacter* sp. MT2, *Alcaligenes* sp. MT3 and *Pseudomonas* sp. MT4 are present in stable relative amounts (84 ± 5% MT1, 8± 4% MT3 and MT4 and 1 % MT2) (106). Inoculation of new chemostats with the four strains resulted reproducibly in reestablishment of the community with all four strains in the above described relative amounts. Though MT1 can grow in absence of the other strains on 4-chlorosalicylate as only carbon source, it never out-competes the others in the mixed culture indicating that their presence must be of benefit to MT1. For efficient substrate degradation via 4-chlorocatechol, as assumed for MT1 (106), metabolic fluxes must be well balanced to avoid accumulation of 4-chlorocatechol, which can be toxic to bacteria (108). The other strains might feed on misrouted and accumulated metabolites of MT1 and thus, enhance and stabilize growth of MT1. Supporting this view, it was demonstrated that the community could grow at higher dilution rates than MT1 as a monoculture (106).

1.10 Strains of investigations

1.10.1 *Pseudomonas* sp. strain MT1

Pseudomonas sp. strain MT1 is the most abundant strain of the above mentioned 4-membered bacterial community (106). In addition, MT1 can grow on 4-chlorosalicylate, 5-chlorosalicylate, and non-substituted salicylate, but not on 3-chlorosalicylate in monoculture. As small amounts of 4-chlorocatechol can be detected in the culture medium, 4-chlorosalicylate is assumed to be metabolized via the central intermediate 4-chlorocatechol (106). As only *ortho*-cleavage activity against catechol and 4-chlorocatechol, but no *meta*-cleavage activity has been described in MT1 cell extracts (106) and as transformation of catechol was more efficient than of 4-chlorocatechol, it was assumed that metabolism proceeds via the 3-oxoadipate pathway. Neither chlorocatechol 1,2-dioxygenase nor maleylacetate reducing activity which are typical for the chlorocatechol pathway have been detected in cell extracts of MT1 (106). Blasco et al. have demonstrated earlier, (see 1.8, Fig. 4) that action of homogeneous catechol 1,2-dioxygenase and muconate cycloisomerase of the 3-oxoadipate pathway leads to quantitative transformation of

4-chlorocatechol to protoanemonin (8). Consequently Pelz et al. hypothesized that MT1 harbors a novel pathway of 4-chlorocatechol degradation including reactions of the 3-oxoadipate pathway via protoanemonin as intermediate (106). Earlier Brückmann et al. had described the capability of a *cis*-/*trans*-DLH of the chlorocatechol pathway to convert protoanemonin to *cis*-acetylacrylate. In contrast, *cis*-DLH and *trans*-DLH were shown not to be active with protoanemonin (14). The fact that MT1 was able to grow on *cis*-acetylacrylate was claimed to support the hypothesis of protoanemonin as central intermediate of a new pathway which is hydrolyzed to *cis*-acetylacrylate. Unfortunately, Pelz et al. did not test for any dienelactone hydrolase activity, nor could they demonstrate any protoanemonin transforming activity in cell extracts. Neither was the fate of *cis*-acetylacrylate investigated. Therefore, the metabolic pathway of chlorosalicylate degradation by MT1 remained highly speculative (106). However, the ability of MT1 to mineralize 4-chlorocatechol without accumulation of bacterial-toxic protoanemonin, though it expresses enzymes of the 3-oxoadipate pathway, demands studying its novel metabolic properties. In addition, elucidation of the metabolic pathway of 4-chlorosalicylate degradation in MT1 will contribute essentially to understanding the metabolic network in the bacterial community MT1 was isolated from.

The fact that MT1 is a *Pseudomonas* strain makes it an even more interesting study object.
Pseudomonas is a very diverse genus belonging to the γ-subgroup of proteobacteria. *Pseudomonas* are rod shaped, gram negative bacteria which are found in large numbers in all major natural environments, in association with plants and animal, as well as human pathogens (154). Due to their remarkable physiological diversity (155) which are reflected at the genetic level (154), many *Pseudomonas* strains are able to metabolize or co-metabolize recalcitrant chemicals that are dangerous environmental pollutants or precursors to valuable products. Consequently, *Pseudomonas* is of outstanding interest for bioremediation or fine-chemical producing industry (31, 138, 160, 173) and investigation of its metabolic potential and metabolic flux will lead to deeper understanding of bacterial metabolisms and novel applications.

1.10.2 *Pseudomonas* sp. strain RW10

Similarly to *Pseudomonas* sp. strain MT1, *Pseudomonas* sp. strain RW10 is a member of a bacterial community, a two-strain consortium, which was enriched for growth on 3-chlorodibenzofuran from aerobic sediment samples of the Elbe river downstream of Hamburg harbor, Germany (177). Neither of the strains of the consortium can grow in pure culture on 3-chlorodibenzofuran. However, *Pseudomonas* sp. strain RW10 grows on 4-chloro and 5-chlorosalicylate, metabolites of chlorodibenzofurans degradation as well as on salicylate, as only source of carbon and energy, evidencing that the second strain, *Sphingomonas* sp. RW16, transforms 3-chlorodibenzofuran to 4-chlorosalicylate which is used as growth substrate for RW10. Similar to cell extracts of MT1, RW10 cell extracts transform 4-chloro- and 5-chlorosalicylate in high yield (>70 %) to protoanemonin (8) and harbor activities of enzymes of the 3-oxoadipate pathway (catechol 1,2-dioxygenase) (177), whereas degradative routes of (chloro)salicylate via catechol *meta*-cleavage, chlorocatechol or the gentisate pathway have been excluded (177). In analogy to the hypothesized metabolic route in *Pseudomonas* sp. strain MT1 (106), Wittich et al. (177) hypothesized that RW10 mineralizes 4-chlorocatechol via protoanemonin as intermediate. During growth on chlorosalicylate, MT1 expresses a *trans*-dienelactone hydrolyzing activity at levels higher than those observed during growth on salicylate, indicative of its involvement in chlorosalicylate degradation. However, the authors could not detect any significant protoanemonin transforming activity in cell extracts. Moreover, purified *trans*-DLH of this strain had previously been shown not to exhibit any significant protoanemonin transforming activity (14). Despite this fact and due to the observation that *cis*-acetylacrylate serves as carbon source for growth of MT1 and RW10 it was speculated that protoanemonin might be transformed in RW10 and in MT1 by a hydrolase to *cis*-acetylacrylate (106). As *trans*-DLH evidently cannot fulfill this function it could be argued that the postulated protoanemonin transforming enzyme of RW10 is not active under *in-vitro* assay conditions or becomes inactive by cell disruption and therefore has not been determined. Elucidation of the putative novel metabolic pathway in *Pseudomonas* sp. strain RW10 or MT1 will broaden our current knowledge on aerobic 4-chlorocatechol degradation.

1.11 State of the art and outline of the project

Pseudomonas sp. strain MT1 and RW10 were assumed to both harbor a novel pathway of 4-chlorocatechol degradation involving protoanemonin and *cis*-acetylacrylate as intermediates.

Metabolic properties of the two strains were to be re-evaluated properly through analysis of metabolites and enzyme activities. As both strains contain a similar metabolic route, MT1 was chosen as type strain for more detailed analysis. It was observed that the pathway in MT1 is indeed novel, but that protoanemonin is rather a minor side-product and not a major metabolite of the pathway.

The key enzymes of this metabolic route, two muconate cycloisomerases (MCI and MCIB) and a *trans*-dienelactone hydrolase (*trans*-DLH) were characterized in detail and the metabolism of 4-chlorocatechol to 3-oxoadipate clarified.

Maleylacetate reductase, which has its function in the new metabolic route by converting maleylacetate into 3-oxoadipate was observed to be active on *cis*-acetylacrylate forming laevulinate as side activity, explaining previous misinterpretations of *cis*-acetylacrylate degradation as indication for its involvement in the pathway.

Genetic analysis of the novel pathway was approached using degenerated primers deduced from the obtained protein sequences of the three key enzymes. A fragment of MT1 MCI was successfully cloned, sequenced and compared with other MCI and CMCI encoding genes.

2. Materials and Methods

2.1 Bacterial strains

The 5- and 4-chlorosalicylate degrading organism *Pseudomonas* sp. strain MT1 was isolated by continuous culture enrichment on 4-chlorosalicylate from sediment of the Elbe river (Germany) (106). Strain MT1 is the most abundant strain in a stable 4-membered community.

Pseudomonas sp. strain RW10 (DSM 12647) and *Sphingomonas* sp. strain RW16 were enriched from aerobic sediment sample of the river Elbe downstream of Hamburg harbor (177, 178) based on their capability to degrade, as a two membered culture, 3-chlorodibenzofuran. Whereas RW16 transforms 3-chlorodibenzofuran into 4-chloro and 5-chlorosalicylate as well as traces of salicylate, RW10, like MT1, can grow on salicylate, 4- and 5-chlorosalicylate as only source of carbon and energy.

E. coli DH5ά containing the expression vector pTP20 (118) (for overexpression of chlorocatechol 1,2-dioxygenase of RW71) and *Ralstonia eutropha* JMP222 containing pBBR1M-I (comprising the chlorocatechol gene module I of *R. eutropha* JMP134) (107) were used for partial purification of auxiliary enzymes.

BL21-Gold(DE3)pLysS strain (Stratagene, La Jolla, CA, USA) was used for expression of wild-type and mutant muconate cycloisomerases from *P. putida* PRS2000 which had been cloned into pET-11a*, a derivative of pET-11a vector containing Apr and PT7lac (157), by Vollmer et al. (169).

E. coli JM109 was used for cloning of PCR fragments during the molecular part of this thesis (98).

2.2 Culture conditions and preparation of cell extracts

Liquid cultures of *Pseudomonas sp.* strain MT1 were grown in LB-medium (130) or in mineral salts medium (22, 28) using 50 mM phosphate buffer (pH 7.5). The medium was supplemented with the indicated carbon source, usually at 2.5 mM for chlorinated and 5 mM for unchlorinated carbon sources (salicylate or succinate). For growth curves, cultures were inoculated to an OD_{600} of 0.01-0.015 with cells growing exponentially on the respective substrate. Cells were grown in fluted Erlenmeyer flasks, incubated at 30 ^{O}C on a rotary shaker at 150 rpm. Growth was monitored spectrophotometrically at 600 nm. Cells were harvested during late exponential growth by centrifugation with 9000 x g and resuspended in Tris/HCl buffer (50 mM, pH 7.5) supplemented with 2 mM $MnCl_2$, and after addition of a trace of DNase I disrupted by passing twice through a

French press (Aminco, Silver Spring, MD, USA). Cell debris was removed by 30 minutes ultracentrifugation with 100,000 x *g* at 4 °C.

2.3 Biochemical methods

2.3.1 Enzyme assays

All enzymatic assays were performed in 50 mM Tris/HCl, pH 7.5, 2 mM $MnCl_2$ by following photometrical absorption changes upon enzyme addition if not stated otherwise. Assays were performed in a total volume of 1 ml (in 1 ml cuvettes) or 300 µl (in 500 µl cuvettes) in order to economize ingredients.

Catechol 1,2-dioxygenase (EC 1.13.11.1) and **chlorocatechol 1,2-dioxygenase** (EC 1.13.11.1) were measured by determining the formation of muconic acid from catechol (ε_{260} = 16,800 l M^{-1} cm^{-1}), 2-chloromuconic acid from 3-chlorocatechol (ε_{260} = 17,100 l M^{-1} cm^{-1}) and 3-chloromuconic acid from 4-chlorocatechol (ε_{260} = 12,400 M^{-1} cm^{-1}), respectively (29). Here, 50 mM Tris/HCl, pH 7.5 was used as buffer supplemented with 1 mM EDTA in order to deplete all present Mn^{2+} and thus preventing cycloisomerase activity. Substrates were supplied at 0.2 mM initial concentrations.

Catechol 2,3-dioxygenase (EC 1.13.11.2) was measured by determining formation of 2-hydroxymuconic semiladehyde from catechol (0.1 mM) (ε_{375} = 36,000 M^{-1} cm^{-1}) (86) in 50 mM phosphate buffer, pH 8.0.

Muconate and chloromuconate cycloisomerizing activities (EC 5.5.1.1)(EC 5.5.1.7) Activities in cell extracts were determined by measuring the depletion of muconate or 2-chloromuconate which were added at 0.1 mM initial concentration with ε_{260} = 16,800 M^{-1} cm^{-1} and ε_{260} = 17,100 M^{-1} cm^{-1}, respectively (29).

When both 3-chloromuconate cycloisomerasing enzymes of *Pseudomonas* sp. strain MT1 were separated by FPLC, activity of partially purified MCIB could be detected photometrically by the formation rate of *cis*-dienelactone from 0.1 mM 3-chloromuconate. $\varepsilon_{278\ nm}$= 1505 M^{-1} cm^{-1} was calculated to be the reaction coefficient.

Low activities of muconate cycloisomerases and MCIB with 2-chloro- and 2,4-dichloromuconate were determined by following incubation over up to 40 minutes with the photometer at 260 nm and HPLC analysis for substrate depletion.

Dienelactone hydrolase (DLH) (EC 3.1.1.45) activity was determined by depletion of 0.05 mM *cis*- or *trans*-dienelactone (ε_{280}= 17,000 (139) and $\varepsilon_{280\ nm}$= 15,625 M^{-1} cm^{-1}, respectively) (137). In order to be capable to compare activities of different key enzymes in single and multi-enzyme assays (i), and as *trans*-DLH of MT1 was subject to a rapid inhibition during turnover in 10 mM histidine/HCl, pH 6.5 buffer (137) (ii), activity was determined in 50 mM Tris/HCl, pH 7.5, 2 mM $MnCl_2$.

Activities of *trans*-DLH with 3-chloromuconate (160 µM) or protoanemonin (100 µM) were determined by HPLC (Methanol-H_2O (30:70)) using up to 80 U/ml (measured with *trans*-dienelactone) of purified *trans*-DLH.

3-oxoadipate enol-lactone hydrolase (**Enollactone hydrolase)**, (EC 3.1.1.24) was assayed in 50 mM Tris/HCl, pH 8.0 or 7.5 with 0.3 mM muconolactone and non-limiting excess of partially purified muconolactone isomerase (see below).

Muconolactone isomerase (EC 5.3.3.4) activity in cell extracts or partially purified was determined in 50 mM Tris/HCl, pH 7.5 with 0.2 mM 5-chloro-3-methylmuconolactone as substrate following the formation of the respective dienelactone $\varepsilon_{280\ nm}$= 17,000 M^{-1} cm^{-1} (100). Combined activity of muconolactone isomerase and enollactone hydrolase in cell extracts was determined by incubation in 50 mM Tris/HCl, pH 8 with 300 µM muconolactone and $\varepsilon_{230\ nm}$= 1,400 M^{-1} cm^{-1}.

Salicylate 1-hydroxylase (EC 1.14.13.1) (10, 185) was determined in 50 mMTris/HCl, pH 8.0 supplemented with 1 mM EDTA and substrate concentrations of 0.2 mM salicylate, 4-chloro- and 5-chlorosalicylate and NADH. Activities were measured by following the oxidation of NADH with $\varepsilon_{340\ nm}$= 6,220 M^{-1} cm^{-1}. The background activity of the cell extracts with NADH in the absence of substrate was determined and subtracted from the activity measured when substrate was present.

Maleylacetate reductase (MAR) (EC 1.3.1.32) was measured in cell extracts or partially purified enzyme preparations in 50 mM Tris/HCl, pH 7.5 according to Seibert et al. (143), using 0.05 mM maleylacetate freshly prepared by alkaline hydrolysis of *cis*-dienelactone and 0.2 mM NADH. Activity was calculated from NADH oxidation was followed with $\varepsilon_{340\ nm}$= 6,220 M^{-1} cm^{-1}. Assays without addition maleylacetate served as reference.

Activities against *cis*-acetylacrylate or *trans*-acetylacrylate, respectively, were measured respectively using 0.05 mM *cis*-acetylacrylate and 0.1 mM NADH. Decrease of *cis*-acetylacrylate was also followed over time by HPLC analysis with Methanol-H_2O (18:82).

Specific activities are expressed as μmol of substrate converted or product formed per minute per gram protein at 25 ^{O}C.

2.3.2 Protein concentration

Protein concentrations were determined by the Bradford procedure using the Bio-Rad (Hercules, CA, USA). Protein assay with bovine serum albumin as protein standard (12). Protein content of whole cells of MT1 grown on salicylate or 5-chlorosalicylate was estimated to be 0.13 ± 0.03 g protein/l at an OD_{600} = 1 (this study).

2.3.3 Resting cell assays

Cells pre-grown on 5-chlorosalicylate were washed twice in phosphate buffer (50 mM, pH 7.4) and resuspended in 10 ml of the same buffer to give an OD_{600} = 1. After addition of substrate (1 mM), cells were incubated at 30 ^{O}C and 120 rpm for up to 5 hours. Samples of the supernatants were taken at different time points, cells were spinned down immediately in a Microcentrifuge (13000 rpm) and the supernatants were analyzed by HPLC.

2.3.4 Transformation by cell extracts

4-Chlorocatechol (200 μM) or 3-chloromuconate (0.055 – 0.43 mM) were incubated at room temperature in Tris/HCl buffer (50 mM, 2 mM $MnCl_2$, pH 7.5) with extracts of 5-chlorosalicylate-grown MT1 cells corresponding to final protein contents of 60 or 360 μg protein/ml. Transformation of 4- or 5-chlorosalicylate was followed in the presence of NADH (400 μM). Samples of the assays were taken over time and directly injected into an HPLC for identification and quantification of metabolites.

2.3.5 *In-situ* transformation of 3-chloromuconate by partially purified enzymes of MT1

Fractions eluted from chromatographic columns during partially protein purification were assayed for 3-chloromuconate transforming activity by HPLC analysis of assays containing 0.1 mM

3-chloromuconate and 1-5 µl of enzyme fraction in a total volume of 0.1 ml Tris/HCl (50 mM, 2 mM $MnCl_2$, pH 7.5).

2.3.6 *In-situ* transformation of 3-chloromuconate by the combined action of a cycloisomerase and *trans*-DLH of MT1

Product formation from 3-chloromuconate by purified MCI or MCIB in the presence of purified *trans*-DLH was analyzed by HPLC in assays performed at room temperature in 150 µl Tris/HCl (50 mM, 2 mM $MnCl_2$, pH 7.5) with 40-300 µM 3-chloromuconate as substrate. In experiments with combined action of two enzymes, MCI was added to give an activity (determined by the transformation of 0.1 mM *cis,cis*-muconate) of 0.18 – 2.7 mU MCI/ml (determined with 0.1 mM *cis*,*cis*-muconate) and corresponding to 0.45 - 6.75 nM, whereas *trans*-DLH was added to those assays with increasing amounts ranging from 0.608 – 2523 mU *trans*-DLH (determined by the transformation of 0.05 mM *trans*-dienelactone) and corresponding to 0.041 – 168 nM.

MCIB was added to 0.2 mM 3-chloromuconate to give an activity of 53 mU/ml (determined with 0.1 mM 3-chloromuconate) (corresponding to 8.8 nM MCIB) throughout one set of mixing experiments, whereas the amount of simultaneously added *trans*-DLH varied from 1.3 - 1302 mU/ml (determined with 0.05 mM *trans*-dienelactone and corresponding to 0.087 - 86.6 nM, respectively). In a second experiment 72 mU MCIB/ml (12 nM) and 0.66 – 1980 mU *trans*-DLH/ml (0.044 nM - 132 nM) were concomitantly added.

0.1 mM 3-chloromuconate was incubated with MCI of *Pseudomonas putida* PRS2000 and *trans*-DLH of strain MT1 or with MCIB of strain MT1 and *cis*-/*trans*-DLH ($TfdE_I$) of *Ralstonia eutropha* JMP134 and products were quantified by HPLC analysis. Concentrations of the respective enzymes are given in the result's part.

2.3.7 Influence of enzyme inhibitors on *trans*-DLH activity

5 mU/ml *trans*-DLH were incubated in the presence of EDTA (1 or 10 mM), *o*-phenanthroline (1 mM), $HgCl_2$ (1 mM), $ZnCl_2$ (1mM), $CuCl_2$ (1 mM), or 4-chloromercurybenzoate (0.02 or 2 mM) in Tris/HCl (50 mM, pH 7.5). Samples of the incubation mixtures were tested for enzyme activity

with the standard photometrical assay as described above at various time points up to 24 hours. Specific inactivation was assessed by comparison of the remaining activity in those assays to a control incubated without inhibitor. For dissolving of *p*-chloromercuribenzoic acid (also named 4-chloromercuribenzoate) in distilled water (20 mM), the pH was adjusted to pH 11. Before the experiments, it was confirmed that the pH of the Tris-buffer remained constant at 7.5 when *p*-chloromercuribenzoic acid solution was added to give a final concentration of 0.2 or 2 mM.

2.3.8 HPLC-analysis

Metabolites were analyzed by injection of 10 µl samples into a Shimadzu (Kyoto, Japan) HPLC system (LC-10AD liquid chromatograph, DGU-3A degasser, SPD-M10A diode array detector and FCV-10AL solvent mixer) equipped with a Lichrospher SC 100 RP8 reversed phase column (125 by 4.6 mm, Bischoff, Leonberg, Germany). Methanol-H_2O containing 0.1 % (vol/vol) H_3PO_4 was used as eluent at a flow rate of 1 ml/min. The column effluent was monitored simultaneously at 210, 260, and 280 nm by the diode array detector.

Table 1. Peak areas of 1 mM standards recorded at the given wavelengths.

Compound	Wavelength (nm)	Peak area
salicylate	210	1130×10^4
5-chlorosalicylate	210	1550×10^4
4-chlorosalicylate	210	1510×10^4
3-chlorosalicylate	210	1540×10^4
4-chlorocatechol	210	730×10^4
3-chlorocatechol	210	1140×10^4
4-fluorocatechol	210	207×10^4
cis-,*cis*-muconate	260	1360×10^4
3-chloro *cis*-, *cis*-muconate	260	320×10^4
2-chloro *cis*-, *cis*-muconate	270	918×10^4
4-fluoromuconolatone	210	155×10^4
protoanemonin	260	590×10^4
cis-dienelactone	280	880×10^4
trans-dienelactone	280	980×10^4
maleylacetate	210	315×10^4
cis-acetylacrylate	205	370×10^4
trans-acetylacrylate	205	350×10^4

Typical retention volumes were as follows: Methanol-H_2O (18:82): 3-chloro-*cis*,*cis*-muconate, 9.6 ml; *cis*-dienelactone, 5.2 ml; *trans*-dienelactone, 1.9 ml; protoanemonin, 4.9 ml; maleylacetate, 0.7 ml; *cis*-acetylacrylate, 2.3 ml; *trans*-acetylacrylate, 2.9 ml. Methanol-H_2O (30:70): 2-chloro-*cis*-dienelactone, 9.4 ml; 2,4-dichloromuconate, 5.0 ml; 4-fluorocatechol, 4.4 ml; 3-chloro-*cis*-*cis*-muconate, 4.3 ml; *cis*-dienelactone, 2.6 ml; protoanemonin, 2.3 ml; 3-fluoro-*cis*-*cis*-muconate, 1.8 ml; 4-fluoromuconolactone, 1.6 ml; *trans*-dienelactone, 1 ml. Methanol-H_2O (66:34): 5-chlorosalicylate, 3.2 ml; 4-chlorosalicylate, 3.6 ml; salicylate, 1.6 ml; 4-chlorocatechol, 1.0 ml; 2-chloro-*cis*-*cis*-muconate, 0.5 ml.

2.3.9 *In-situ* NMR-analysis

One-dimensional ^{1}H-NMR spectra were recorded at 300°K on a Bruker AVANCE DMX 600 NMR spectrometer (Bruker, Rheinstetten, Germany) locked to the deuterium resonance of D_2O in the solution. Spectra were recorded using the standard Bruker 1D NOESY suppression sequence with 280 scans each with a 1.8 s acquisition time and 1.3 s relaxation delay. The center of the suppressed water signal was used as internal reference (δ 4.80 ppm). ^{1}H-NMR spectra are preferably taken with inorganic buffer systems such as phosphate or borate buffer systems (112, 116), as the protons of the often complex organic molecules of organic buffer systems are feared to overlap with the peaks of the compounds of interest. As MAR of *Pseudomonas* sp. MT1 was substantially inhibited in phosphate buffer, we performed *in-situ* ^{1}H-NMR in a 5 mM Tris/HCl, pH 7.5 buffer system (TRIZMA®BASE, Sigma-Aldrich, St. Louis, MO, USA). It was important to re-adjust the pH for compound identification after completion of the reaction.

^{1}H-NMR spectra of the substrates *cis*-acetylacrylate and NADH, as well as its products, laevulinic acid and NAD at 1 mM concentrations, were recorded individually in 5 mM Tris/HCl, pH 7.5 and 20 % (vol/vol) D_2O to serve as standards for identification of all peaks. For *in-situ* NMR the spectrum of 1mM *cis*-acetylacrylate in 5 mM Tris/HCl, pH 7.5 and 20 % (vol/vol) D_2O was recorded before and directly after addition of partially purified MAR to be able to exclude any artifacts by the introduction of the proteins. Substrate transformation and product formation was followed over time.

2.4 Enzyme purification and characterization

2.4.1 Enzyme purification

Proteins were purified using a Fast Protein Liquid Chromatography (FPLC) system (Amersham Biosciences, Uppsala, Sweden) from *Pseudomonas* sp. strain MT1. Cells were harvested during late exponential growth with 5-chlorosalicylate. Cell disruption and all protein elutions were performed in Tris/HCl (50 mM, pH 7.5, 2 mM $MnCl_2$) and 0.5 ml fractions were collected if not stated otherwise.

For partial purification, the cell extract (usually containing between 8 and 20 mg of protein per ml) was applied directly to a MonoQ HR5/5 (anionic exchange) column (Amersham Pharmacia Biotech) or mixed with 2 M $(NH_4)_2SO_4$ to give a final concentration of 0.8 M $(NH_4)_2SO_4$ and, after centrifugation, applied to a SOURCE 15PHE PE 4.6/100 (hydrophobic interaction) column (Amersham Pharmacia Biotech). At least three independent experiments were performed. Proteins were eluted from the MonoQ HR5/5 column by a linear gradient of 0 – 0.4 M NaCl over 25 ml with a flow of 0.2 ml/min (MCI, 0.23 ± 0.03 M; MCIB, 0.32 ± 0.01 M and *trans*-DLH, 0.19 ± 0.01 M NaCl). Proteins were eluted from the SOURCE column by a linear gradient of $(NH_4)_2SO_4$ (0.8 M – 0 M) over 25 ml with a flow of 0.25 ml/min. Hydrophobic interaction chromatography separated MCI (0.06 ± 0.04 M), a novel type of cycloisomerase MCIB (0.25 ± 0.04 M), MAR (0 mM) and *trans*-DLH (0.8 M $(NH_4)_2SO_4$)) thus excluding interference between their activities.

For purification of MCI, MCIB and *trans*-DLH up to 400 mg of protein were applied onto the MonoQ HR 10/10 (Amersham Pharmacia Biotech). A stepwise gradient of 0 – 60 mM NaCl over 40 ml, 60 – 380 mM over 120 ml and 380 – 2000 mM NaCl over 40 ml was applied. The flow rate was 0.3 ml/min. The eluate was collected in fractions of 5 ml volume. All fractions eluting at NaCl concentrations of 90 – 330 mM (a total of 90 ml) containing the enzymes of interest were pooled and concentrated to a final volume of 4.25 ml using ultrafiltration by Centriprep YM-50 (Millipore, Billerica, Mass. USA) according to the protocol of the manufacturer. The protein solution was supplemented with 4 M $(NH_4)_2SO_4$ solution to give a final concentration of 0.8 M $(NH_4)_2SO_4$ and centrifuged directly before application of the soluble proteins to the SOURCE column. Aliquots comprising 40 mg of protein were separated as described for partial purification: MCI (0.06 ± 0.04 M), MCIB (0.25 ± 0.04 M) and *trans*-DLH (0.8 M $(NH_4)_2SO_4$)). Fractions containing MCI, MCIB or *trans*-DLH were combined separately and concentrated by Centricon YM-50 (Millipore). Further purification was achieved by gelfiltration using a Superose 12 HR10/10 column (Amersham Pharmacia Biotech). Proteins were eluted with Tris/HCl (50 mM, 2 mM $MnCl_2$

pH 7.5) over 15 ml (flow rate 0.2 ml/min, fraction volume 0.5 ml). The fractions containing MCI (eluting at 11-12 ml), MCIB (eluting at 10.5 – 11.5 ml) or *trans*-DLH (eluting at 13-14 ml) were applied separately onto a MonoQ HR5/5 column, and eluted using a gradient described above. While MCI and MCIB were homogenous as judged by SDS-PAGE, the *trans*-DLH containing fractions still contained significant amounts of contaminating proteins. Thus, these fractions were desalted by gelfiltration, supplemented with 4 M $(NH_4)_2SO_4$ to give a final concentration of 1.85 M $(NH_4)_2SO_4$ and again applied onto a SOURCE 15PHE PE 4.6/100 column. Proteins were eluted with a stepwise gradient of 1.85 – 0.93 M over 5 ml and 0.93 – 0 M $(NH_4)_2SO_4$ over 20 ml in Tris/HCl (50 mM, 2 mM $MnCl_2$, pH 7.5). *trans*-DLH eluted at ammoniumsulfate concentrations of 0.42 – 0.47 M. Homogeneity was verified by SDS-PAGE.

Muconolactone isomerase was partially purified from cell extract of salicylate grown MT1 by hydrophobic chromatography with a SOURCE 15PHE PE 4.6/100 column. For elution a two-step gradient (1.85 – 1.48 M$(NH_4)_2SO_4$over 25 ml and (1.48 – 0 M $(NH_4)_2SO_4$ over 3 ml) was applied. MLI eluted at 0 M ammoniumsulfate After heat treatment of the fractions containing the enzyme for 20 min at 70 °C and separation from the precipitated proteins by centrifugation in a microcentrifuge, modified as described in (139). Muconolactone isomerase was stored at – 20 °C.

Maleylacetate reductase (MAR) was partially purified from *Pseudomonas* sp. MT1 grown on 5-chlorosalicylate, washed in 50 mM phosphate buffer, pH 7.5 prior to making cell extracts in that buffer. About 6 – 8 mg of proteins were loaded on a MonoQ HR5/5 column and eluted at 0.2 ± 0.01 M NaCl by a linear gradient of 0 – 0.4 M NaCl in phosphate buffer over 25 ml with a flow of 0.2 ml/min. For preparation of MAR to be used in *in-situ*-NMR assays 10 mM Tris/HCl, pH 7.5 buffer instead of phosphate buffer was used throughout the experiment. Similarly, MAR was eluted at 0.2 ± 0.01 M NaCl with a linear gradient of 0 – 2.5 M NaCl over 25 ml, here.

Recombinant TetC (chlorocatechol 1,2-dioxygenase of *P. chlororaphis* RW71) was partially purified by a DEAE Sepharose column as described by Potrawfke et al. (118).

***cis*-/*trans*-DLH** ($TfdD_I$) and MAR ($TfdF_I$) of *R. eutropha* JMP134 were available from previous partial purification by anion exchange chromatography from *R. eutropha* JMP222 containing expression vector pBBR1M-I as described by Plumeier et al. (114).

2.4.2 Determination of molecular mass

The molecular mass of MCI, MCIB and *trans*-DLH were determined by gelfiltration using a Superose 12 column as described above. The column was calibrated for molecular mass determinations with ovalbumin (43 kDa), aldolase (158 kDa), catalase (232 kDa) and Ferritin (440 kDa) (Bio-Rad) as reference proteins.

2.4.3 Protein electrophoresis

10 % SDS-polyacrylamide gel electrophoresis (SDS-PAGE) was performed on a Bio-Rad Miniprotein II essentially as previously described (80). The acrylamide (rotiphorese Gel 30, ROTH, Germany) concentration was 10 % (wt/vol). The proteins were stained with Coomassie brilliant blue (Serva, Heidelberg, Germany). Prestained low range protein marker from Bio-Rad and peqGOLD Protein MW Marker from Peqlab, Germany were used.

2.4.4 Amino acid sequencing

Highly purified protein fractions were separated from low amounts of contaminating proteins by SDS-PAGE and electroblotted onto a PVDF membrane (Millipore) which was stained with Coomassie brilliant blue R250 0.1 % in a methanol (40 % vol/vol), acetic acid (10 % vol/vol), H_2O (50 % vol/vol) solution for 15-30 minutes. The membrane was destained in the solution without Coomassie and dried over night on Whatman paper. The protein bands were excised and N-terminal amino acid sequencing was performed with an Applied Biosystem model 494A Procise HT sequencer by Rita Getzlaff at the GBF.

For internal MS/MS sequencing the gel after SDS-PAGE was stained with Coomassie brilliant blue G250 and bands containing the protein of interest were cut out, neutralized in fresh 10 mM ammoniumbicarbonate (15 min) and destained in acetonitril (50 % vol/vol) / 10 mM ammoniumbicarbonate (50 % vol/vol) prior to drying in a speed vac. Gelpieces were soaked with 5 – 10 µl of trypsine solution (2 µg/ml) for 30 minutes and the same amount of 50 mM ammoniumcarbonate was added. The digests were incubated at 37 °C over night. The peptides were extracted by addition of 50 µl of a fresh solution of 50 mM ammoniumbicarbonate and twice with 100 µl of a solution consisting of acetonitril (60 % vol/vol), formic acid (0.5 % vol/vol) H_2O (49.5 % vol/vol) solution. Extracts were combined and concentrated in a speed vac at 4 °C over

several hours. The dried peptides could be stored at -20 °C. Prior to sequencing, peptides were re-dissolved in approx. 10 µl 5 % vol/vol formic acid and cleaned with Zip Tips (Millipore) according to the manufactures protocol in order to eliminate salts and detergents (54). Sequencing was performed by the structural department of GBF with a Quadropole Time Of Flight (Q-TOF) mass spectrometer.

Obtained sequences were compared with GeneBank (USA), Protein database (PDB, USA), protein informative resource (PIR), reference sequence collection (RefSeq, NCBI, USA), protein research foundation (PRF, Japan) and SwissProt using FastA and tblastn (BLASTP 2.25 (Nov-16-2002)).

2.4.5 Analysis of kinetic data

Kinetic data of muconate cycloisomerase, MCIB and *trans*-DLH were determined with homogeneous proteins in 50 mM Tris/HCl, pH 7.5, 2 mM $MnCl_2$. As the enzymes had to be stored until the performance of experiments, their actual activities were determined using the respective standard tests (see 2.3.1) and all given activities were normalized to the activity of the enzyme right after purification. At least two independent experiments were performed for each value. K_m and V_{max} were calculated by nonlinear regression to the Michaelis-Menten equation, using the Curve Fit feature of Sigma-Plot 2000, if not stated otherwise. Turnover numbers (k_{cat} values) were calculated assuming a subunit molecular mass of 40 ± 2 kDa for MCI and of 39 ± 4 kDa for *trans*-DLH.

***K_m* and *k_{cat}* of muconate cycloisomerase (MCI)** for muconate were determined spectrophotometrically at substrate concentrations up to 1.3 mM. Muconate depletion was followed at λ=260 nm (**ε** = 16,800 M^{-1} cm^{-1} (30) substrate concentrations of 50 – 130 µM), λ=285 nm (**ε** = 3,800 M^{-1} cm^{-1}, substrate concentrations of 130 – 350 µM) or λ=295 nm (ε = 1,100 M^{-1} cm^{-1} substrate concentrations of 350 – 1300 µM).

Transformation of 3-chloromuconate by MCI was followed by HPLC analysis at substrate concentrations of 75 µM – 1500 µM using 5 mU/ml (measured with 100 µM *cis,cis*-muconate initial concentration) of purified MCI. Samples were taken during the reaction and protoanemonin formation was directly analyzed by HPLC. Kinetic constants were calculated based on protoanemonin formation rates.

***K_m* and *k_{cat}* of MCIB** for 3-chloromuconate transformation was determined spectrophotometrically in the presence of an excess of partially purified *cis*-/*trans*-DLH from *R. eutropha* JMP134 ($TfdD_I$). As confirmed by HPLC analysis, independent of the substrate concentration, MCIB catalyzed the

transformation of 3-chloromuconate into 48 ± 5 % *cis*-dienelactone and protoanemonin, respectively in a 1:1 ratio. Addition of *cis*-/*trans*-DLH resulted in the prevention of any significant *cis*-dienelactone accumulation by transforming it into maleylacetate, thus resulting in a decrease in absorption at 260 nm. The extinction coefficient of the reaction was determined by comparison of photometrical spectra and HPLC analysis of the same assay over time to be $\varepsilon_{260\ nm}$= 2,000 M^{-1} cm^{-1}.

***K_i* of MCIB** for 4-methylmuconolactone resulting in a 50 % inhibition was calculated with the following equation describing the effects of inhibitor and substrate concentrations on competitive inhibition:

$$[I]_{0.5} = \left(1 + \frac{[S]}{K_m}\right) K_i$$

; with [I] = 1 mM (4-methylmuconolactone inhibitor concentration)

[S] = 0.1 (3-chloromuconate as substrate concentration)

K_m = 0.105 mM (K_m-value of MCIB with 3-chloromuconate)

Kinetic data of *trans*-dienelactone hydrolase (*trans*-DLH) with *trans*-dienelactone as substrate were determined spectrophotometrically at substrate concentrations up to 0.5 mM and followed at λ=280 nm (substrate concentrations up to 130 µM) or λ=305 nm (ε = 4380 M^{-1} cm^{-1} substrate concentrations of 130 – 520 µM).

The turnover of 4-fluoromuconolactone by *trans*-DLH was analyzed spectrophotometrically at λ=240 nm using a reaction coefficient of 4200 M^{-1} cm^{-1} ($\varepsilon_{maleylacetate}$ = 4700 M^{-1} cm^{-1}, $\varepsilon_{4\text{-fluoromuconolactone}}$= 500 M^{-1} cm^{-1})(123).

***K_m* of maleylacetate reductase (MAR)** for maleylacetate and *cis*-acetylacrylate were determined by following NADH reduction photometrically as described above with initial substrate concentrations of 0.02 – 0.2 mM maleylacetate and 0.025 – 0.6 mM *cis*-acetylacrylate, respectively.

Equations describing enzyme activities versus substrate concentrations.

Michaelis-Menten equation $v = V_{\max} \frac{[S]}{[S] + K_m}$

Polynomial expression describing substrate inhibition $[S]/v = \frac{K_m}{V_{\max}} + (1/V_{\max})[S] + (1/K_{SS} \bullet V_{\max})[S^2]$ (2, 56).

2.5 Chemicals

Chemicals were purchased from Riedel de Haen (Seelze, Germany), Baker (Philipsburg, NJ, USA), Sigma-Aldrich (St. Louis, MO, USA), Fluka AG (St. Gallen, Switzerland) and Merck AG (Darmstadt, Germany). 4-Chlorocatechol was obtained from Helix Biotech (USA).

3-Chloro-*cis,cis*-muconate and 3-fluoro-*cis,cis*-muconate were freshly prepared from 4-chlorocatechol or 4-fluorocatechol in Tris/HCl (50 mM, pH 7.5, 2 mM $MnCl_2$) using partially purified chlorocatechol 1,2-dioxygenase TetC of *P. chlororaphis* RW71 overexpressed in *E. coli* (118). Completed substrate transformation was confirmed by HPLC analysis.

4-Fluoromuconolactone was prepared *in-situ* from 3-fluoro-*cis*,*cis*-muconate by purified MCI. Complete substrate conversion was again verified by HPLC. Enzymes were removed from the preparation by filtration with Centricon YM-10 (Millipore).

Maleylacetate was freshly prepared by alkaline hydrolysis of *cis*-dienelactone (143).

***cis*-Dienelactone and 4-fluorocatechol** were kindly provided by Walter Reineke (Bergische Universität – Gesamthochschule Wuppertal, Germany) and Stefan Kaschabeck (TU Bergakademie Freiberg, Germany).

***trans*-Dienelactone and protoanemonin** were prepared as described earlier (8, 123). Protoanemonin was also formed by addition of partially purified MCI to 3-chloromuconate preparation.

***cis*-Acetylacrylate** was obtained by isomerization of 5 mM *trans*-acetylacrylate (Lancaster Synthesis, Morecambe, UK) over night under UV irradiation (λ = 254 nm) (132). Efficiency of isomerization was checked by HPLC analysis.

2.6 Molecular techniques

2.6.1 Genomic DNA extraction

Genomic DNA of *Pseudomonas sp*. strain MT1 was obtained by a modified protocol of Grimberg et al. (46). 25 ml of cells grown in LB OD_{600}=1 were harvested and washed with TNE buffer (10 mM Tris/HCl, 10 mM NaCl, 10 mM EDTA, pH 8.0). The pellets could be stored thereafter at –20 °C. The pellet was resuspended in 5 ml TNEX-buffer (TNE buffer supplemented with 1 % Triton-X 100) and 270 µl fractions transferred in 2 ml tubes. To each tube 30 µl of lysozyme (10 mg/ml) and 7.5 µl of freshly prepared Proteinase K (20 mg/ml) were added. The tubes were incubated for 2 h at 37 °C, followed by incubation for 2-3 h at 65 °C. The DNA was precipitated by

addition of 15 µl of 5 M NaCl, gentle inverting the tubes and gentle addition of cold 96 % ethanol. After 2-3 minutes the tubes were gently inverted again prior to spinning down the DNA for 10 min with 15000 rpm at 4 °C. The supernatant was discharged and the pellet washed with 1 ml cold 96 % ethanol. The pellet was dried at 37 °C and resuspended in 100 µl MilliQ water over night at 4 °C.
For preparation of the genomic walker libraries (Stratagene, La Jolla, CA, USA) DNA was restricted with *Sma*I, *Eco*RV, *Pvu*II and *Stu*I. DraI was found not to restrict genomic DNA of MT1 under standard conditions. The digests were further purified by QIAprep Spins for Minipreps (QIAGEN, Hilden, Germany). In contrast to the protocol, solution P1, P2 and N3 were mixed prior to addition to the digest. Thereby large fragments of DNA were not precipitated and could be eluted from the column.

2.6.2 PCR assays

PCR reactions were performed with Taq polymerase (Amersham or Invitrogen (Carlsbad, CA, USA) in 1 x Taq-buffer of the respective supplier. The effect of the addition of different concentrations of DMSO (0, 1, 5, 10 %) or Q-solution (QIAGEN) to the PCR assays was tested, as those agents modify the melting temperature of DNA and thereby often facilitate amplification of GC rich templates, as present in *Pseudomonas* genomes. The addition of 5 % dimethylsufoxide (DSMO) was shown to be optimal. $MgCl_2$ (1.5 mM) was added when using Invitrogen polymerase. 5 µl of 10 µM primers were added to 25 µl assay volume. The concentration of genomic DNA used in the assays seemed to be very crucial. If not stated otherwise 0.2 µl of an approximately 100 ng/µl genomic DNA preparation were added to the assays. PCR was performed in a Biometra Thermocycler T3 at a total volume of 25 µl with: 5 min initial denaturation at 95 °C followed by 30 cycles of 30 seconds at 95 °C, 30 seconds at 40 °C and 90 seconds of 72 °C. After the last cycle elongation was prolonged for 10 more minutes and the samples were cooled at 4 °C until analysis.

2.6.3 TA Cloning, electroporation

PCR fragments were purified by electrophoresis on a 0.8 % agarose gel followed by extraction using the GFX PCR DNA and Gel Band Purification Kit (Amersham Biosciences). The purified fragment was cloned into the pCR®4-TOPO vector, provided linearized and topoisomerase I-activated with 3'-T overhangs, with the TOPO TA Cloning® Kit for Sequencing (Invitrogen)

according to the manufacturer protocol. The vector has a minimized multiple cloning site and M13-priming sites notably close to the product insertion site for efficient sequencing. Immediately after ligation the plasmid was transferred into *E. coli* JM105 by electroporation (400 OHMs, 2.5 kVolt). The transformants were incubated at 30 °C for 1 – 1.5 hours in LB without selective agent, before plated onto LB Amp^{100} agar and incubation over night at 37 °C.

2.6.4 Preparation of electrocompetent cells

Exponentially grown *E. coli* JM105 were made electrocompetent by washing them twice with sterile MilliQ water (130). Competent cells were stored in 10 % glycerol at –80 °C.

2.6.5 Plasmid preparation

Plasmids were extracted with the QIAprep® Miniprep Kit (Qiagen, Hilden, Germany) according to the protocol for Qiaprep Spin Minipreps and eluted in MilliQ water.

2.6.6 Southern Blot

Aliquots of genomic DNA of *Pseudomonas sp*. MT1 were restricted separately with four distinct 6-basepair cutters *Sma*I, *Eco*RV, *Pvu*II and *Stu*I. The digests (1 µg) were loaded on a 0.7 % agarose gel and eletrophoresed The DNA fragments from the digest were fractionized to smaller pieces by incubating the gel for 10 min in 0.37 % (v/v) HCl. Subsequently the DNA was denatured by incubation in 0.5 M NaOH, 1.5 M NaCl denaturation-buffer for 40 min, neutralized in 0.5 M Tris, 3 M NaCl, pH 7.2 for at least 60 min and rinsed with water. The DNA was blotted onto a Nylon membrane (Nytran N, Schleicher & Schuell, Germany) which was presoaked in 6x SSC buffer for 10 sec just prior to placing it onto the gel. 10x SSC (1.5 M NaCl, 0.15 M sodiumcitrate, pH 7.0) was run by capillary forces passing from below the gel upwards through the membrane and ensured the transfer of DNA over night. The membrane was rinsed with 6x SSC placed between Whatman paper and dried at 80 °C for 2 hours.

The membrane was prehybridized by being gently shaken in hybridization buffer (5x SSC, 1 % (w/v) blocking reagent (Boehringer Mannheim, Mannheim, Germany), 0.1 % (w/v) lauroylsarcosine, 0.02 % (w/v) SDS) at 60 °C for 1 hour. The probes were denatured by boiling for

5 min and shocking on ice water to avoid re-annealing. The prehybridization buffer was discarded and preheated hybridization buffer (including 600 ng DIG labeled probe) was added in amounts sufficient to cover the membrane. Hybridization was performed at 60 °C over night in a closed box to prevent evaporation. The hybridizing buffer including the probe was decanted and stored for later experiments at 4 °C. Rinsing and detection of hybridized bands was performed according the protocol of DIG DNA Labeling and Detection Kit from Boehringer Mannheim.

2.6.7 Expression of wild-type and mutant muconate cycloisomerase from *P. putida* PRS2000

Plasmids pCATB1, pCATB51 and pCATB54 carrying the wild type and the mutant muconate cycloisomerases I54V-CatB and A271S-CatB of *Pseudomonas putida* PRS2000, respectively, were kindly provided by Schlömann (169). The plasmids were transferred into BL21-Gold-derived competent cells designed for high-level protein expression using T7 RNA polymerase-based expression systems. The BL21-Gold(DE3)pLysS competent cells which provide tight control for expression of toxic proteins, were transformed according to the protocol of chemocompetent cells. Clones harbouring the plasmid were selected on LB Amp^{100} plates and grown and induced in LB-medium Amp^{100} (130), as described by Vollmer et al. (169).

2.6.8 Alignment and phylogenetic tree of (chloro)muconate cycloisomerases

Sequences for the alignment were obtained from the NCBI database detected by tblastn search with the available 159 amino acid long protein sequence of *Pseudomonas* sp. strain MT1 (this study). Well studied and putative muconate and chloromuconate cycloisomerases, as well as some reliable sequences from genome projects and other approaches were selected. Protein accession numbers are given in the figure of the alignment. The alignment was performed using CLUSTAL W (159) using default values and a 159 amino acid block containing the full sequence of muconate cycloisomerase of *Pseudomonas* sp. strain MT1 was cut out. A phylogenetic tree was generated using the neighbour joining method option of CLUSTAL W with 1000 bootstraps.

3. RESULTS

3.1 Growth of *Pseudomonas sp*. strain MT1 and RW10 on chlorosalicylates

Pseudomonas sp. strain MT1 can grow on 4-chloro- and 5-chlorosalicylate and on salicylate as only source of energy and carbon with growth rates of 0.05 h^{-1} (2.5 mM 4-chlorosalicylate as carbon source), 0.16 h^{-1} (2.5 mM 5-chlorosalicylate) and 0.38 h^{-1} (5 mM salicylate), respectively. The maximal OD_{600} obtained during growth were 0.2, 0.3 and 0.9, corresponding to yields of 10, 15.5 and 23 mg protein per mmole substrate, respectively. MT1 was not able to use 3-chlorosalicylate as only source of carbon and energy.

During growth on 2 mM 5-chlorosalicylate MT1 excreted *cis*-dienelactone and minor amounts of protoanemonin corresponding to 17 and 4 % of the initial substrate concentration, respectively.

Pseudomonas sp. strain RW10 showed similar growth rates of 0.10 h^{-1} (2.5 mM 4-chlorosalicylate), 0.12 h^{-1} (2.5 mM 5-chlorosalicylate) and 0.35 h^{-1} (5 mM salicylate) and grew to maximal OD_{600} of 0.2, 0.3 and 1.0, respectively.

3.2 Enzyme activities in cell extracts

Cell extracts of MT1 grown on 5-chlorosalicylate (Table 2) exhibited a significant catechol 1,2-dioxygenase activity, but neither catechol 2,3-dioxygenase nor gentisate dioxygenase activity, indicating a metabolism via salicylate 1-hydroxylase and chlorocatechol *ortho*-cleavage. This fact was supported by the observation of a NADH dependent salicylate and chlorosalicylate transforming activity in cell extracts. All mono-chlorinated salicylates were transformed at rates 25 - 50 % that of salicylate, resembling substrate specificities of salicylate 1-hydroxylase encoded by the *nahG* gene (82). Transformation rates of 4-chlorocatechol by both salicylate and 5-chlorosalicylate-grown cells were 13 – 21 % those of catechol, whereas activities with 3-chlorocatechol were negligible (< 2 % that of catechol). Such a substrate specificity is indicative for the induction of a catechol 1,2-dioxygenase rather than a chlorocatechol 1,2-dioxygenase, which usually is highly active against 3-chlorocatechol (30, 121). In accordance with an induction of enzymes of the 3-oxoadipate pathway was the observation of a muconate transforming activity, whilst activity against 2-chloromuconate was absent (< 5 U/g), indicating expression of muconate cycloisomerase (MCI) (139).

Table 2. Specific activities in cell extracts of *Pseudomonas* sp. strain MT1 grown on 5-chlorosalicylate, salicylate and succinate. Activities are given in U/g protein. ND = not determined.

		Growth substrate		
Enzyme	**Substrate**	**5-chlorosalicylate**	**salicylate**	**succinate**
Salicylate 1-hydroxylase	salicylate	460	120	< 5
	3-chlorosalicylate	120	ND	ND
	4-chlorosalicylate	240	ND	ND
	5-chlorosalicylate	190	ND	ND
Catechol 2,3-dioxygenase	catechol	< 1	< 1	ND
	dihydroxybiphenyl	< 1	< 1	ND
Catechol 1,2-dioxygenase	catechol	740	390	< 10
	3-chlorocatechol	14	< 1	ND
	4-chlorocatechol	160	50	ND
Cycloisomerase	muconic acid	25	350	< 5
Muconolactone isomerase	5-chloro-3-methylmuconolactone	< 2	10	ND
MLI + enollactone hydrolase	muconolactone	< 70	400	ND
Dienelactone hydrolase	*cis*-dienelactone	< 5	< 5	ND
	trans-dienelactone	600	100	< 5
	protoanemonin	< 5	< 5	ND
Maleylacetate reductase	maleylacetate	1120	510	ND
	cis- acetylacrylate	60	20	ND
	trans-acetylacrylate	< 5	< 5	< 5

Muconolactone was transformed with an activity of approximately 400 U/g protein by cell extracts of salicylate grown MT1, indicating the combined presence of muconolactone isomerase and enol-lactone hydrolase. In contrast, muconolactone depletion by cell extracts of 5-chlorosalicylate grown cells was lower and never exceeded 20 % the rate observed in salicylate grown cells. Transformation of 5-chloro-3-methylmuconolactone, as a measure for muconolactone isomerase activity, by cell extracts of salicylate grown cells was much lower than it had been described for muconolactone isomerase activity of *Ralstonia eutropha* JMP134 cell extracts (307 U/g) (119). This might indicate that 5-chloro-3-methylmuconolactone was not a good substrate for the muconolactone isomerase of MT1 in contrast to the one of JMP134. Nevertheless, muconolactone isomerase activity with 5-chloro-3-methylmuconolactone in extracts of salicylate-grown cells was about 5 to 10 fold higher compared to extracts of 5-chlorosalicylate grown cells, similar to the expression pattern of muconate cycloisomerase (MCI). Both cell extracts exhibited a high activity with *trans*-dienelactone, but not with *cis*-dienelactone. As previously described, dienelactone hydrolases (DLH) involved in the chlorocatechol pathway are active with both, *cis*- and *trans*-dienelactone (133, 137, 139) or only the *cis*-isomer (85). However, hydrolases only transforming

the *trans*-isomer (133, 136) have previously also been reported in *Ralstonia* strains capable to grow on 4-fluorobenzoate (137) and in *Pseudomonas* sp. strain RW10 growing on chlorosalicylate (177). As in *Pseudomonas* sp. strain RW10, *trans*-DLH activity in MT1 was higher in 5-chlorosalicylate-grown compared to salicylate-grown cells. Activity with maleylacetate was remarkably high and unexpected, because maleylacetate reductase (MAR) is usually expressed together with other enzymes of the chlorocatechol pathway and there was almost no activity reported in MT1 by Pelz et al. (106).

Enzyme activities observed in cell extracts of 5-chlorosalicylate or salicylate grown cells of strain RW10 were highly similar to those observed in MT1. Catechol 1,2-dioxygenase, MCI, *trans*-DLH and MAR were induced, but no catechol 2,3-dioxygenase (Table 3). Like in MT1 MCI activity was higher in salicylate grown cells, whereas the other enzyme activities were higher in 5-chlorosalicylate grown cells.

Table 3. Specific activities in cell extracts of *Pseudomonas* sp. strain RW10 grown on 5-chlorosalicylate and salicylate. Activities are given in U/g protein.

		Growth substrate	
Enzyme	**Substrate**	**5-chlorosalicylate**	**salicylate**
Catechol 2,3-dioxygenase	catechol	< 1	< 1
	dihydroxybiphenyl	< 1	< 1
Catechol 1,2-dioxygenase	catechol	500	200
	3-chlorocatechol	< 1	< 1
	4-chlorocatechol	120	30
Cycloisomerase	muconic acid	10	450
Dienelactone hydrolase*	*cis*-dienelactone	< 5	< 5
	trans-dienelactone	600	100
	protoanemonin	< 5	< 5
Maleylacetate reductase	maleylacetate	500	100
	cis- acetylacrylate	130	10
	trans-acetylacrylate	90	< 5

* in Histidine buffer

Despite of previous propositions that MT1 and RW10 harbor a new metabolic route for chlorosalicylate degradation with protoanemonin as a central intermediate (106, 177) formed from 4-chlorocatechol by the successive action of catechol 1,2-dioxygenase and MCI (8) (Fig. 4 B), in none of these organisms significant protoanemonin transforming activities could be observed. Wittich et al. had postulated that protoanemonin could be hydrolyzed to give *cis*-acetylacrylate, possibly by the action of *trans*-DLH (177). However, as shown for the *trans*-DLH of RW10 (14), the activity of purified *trans*-DLH of MT1 with protoanemonin was < 1 % that with *trans*-

dienelactone (see 3.4.3) raising doubts on the hypothesis of protoanemonin as intermediate. Nevertheless, there was a significant NADH dependent *cis*-acetylacrylate transforming activity in MT1. This activity was later shown to be due to a side activity of MAR (see 3.7.1).

Cell extracts of succinate-grown MT1 did not exhibit salicylate 1-hydroxylase, catechol 1,2-dioxygenase, MCI, DLH or MAR activities. Thus, all those activities are inducible and not constitutively expressed.

3.3. Metabolites in the degradation of chlorosalicylates by *Pseudomonas* sp. strain MT1

3.3.1. Metabolites formed during transformation of chlorosalicylates and 4-chlorocatechol by resting cells of *Pseudomonas sp.* strain MT1

The enzymatic activities detected in cell extracts of MT1 (see 3.2) did not account for a continuous route of degradation. However, despite the absence of any protoanemonin transformation in cell extracts, such an activity can be missed by the assay conditions. To further analyze the metabolic route of chlorosalicylate degradation in MT1, the different chlorosalicylates as well as the probable pathway intermediate 4-chlorocatechol were transformed by 5-chlorosalicylate grown resting cells (Fig. 5). During transformation of 4- and 5-chlorosalicylate, 4-chlorocatechol and 3-chloromuconate were excreted transiently in small amounts (< 10 % of applied substrate), indicating them to be intermediates of the metabolic pathway. Protoanemonin and *cis*-dienelactone accumulated in amounts corresponding to approximately 7 ± 3 % and 10 ± 5 % of the initial substrate concentration, respectively (Fig. 5 A, B). Further transformation of 4-chlorocatechol and 3-chloromuconate was rapid compared to the minor decrease in *cis*-dienelactone concentration. In contrast 3-chlorosalicylate transformation lead to transient excretion of 3-chlorocatechol (< 50 %) which was further transformed into 2-chloromuconate as a dead-end product (Fig. 5 C). When resting cells were incubated with 4-chlorocatechol, the same metabolites were identified as for 4- and 5-chlorosalicylate incubation, though higher concentrations of 3-chloromuconate (up to 15 % of initial substrate concentration) were excreted (data not shown).

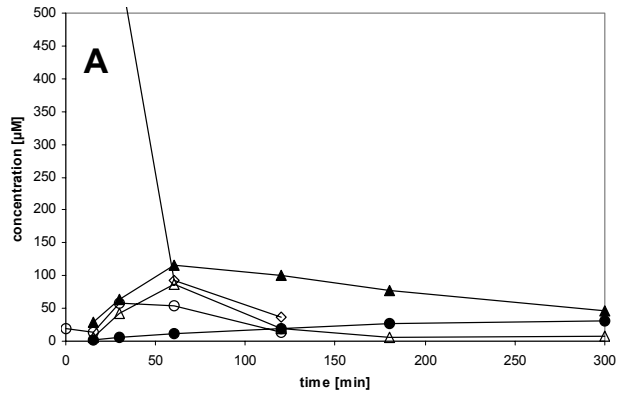

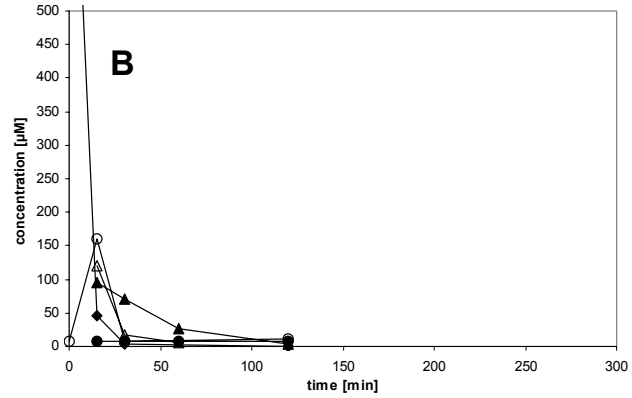

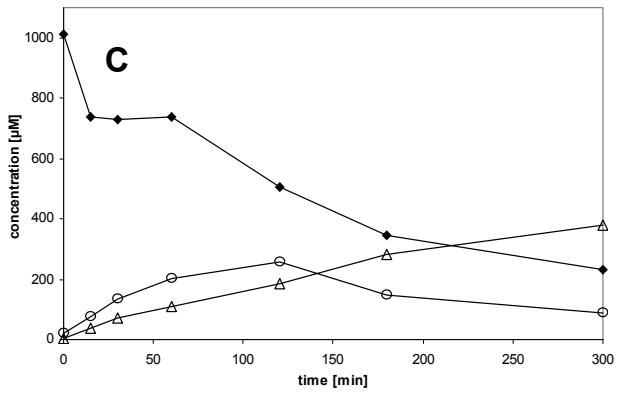

Figure 5. Transformation of (1 mM) 4-chlorosalicylate (**A**), 5-chlorosalicylate (**B**) and 3-chlorosalicylate (**C**) by 5-chlorosalicylate grown resting cells of *Pseudomonas sp*. strain MT1 of an OD_{600}=1 (**A**; **C**) or OD_{600}=5 (**B**).
◊ 4- chlorosalicylate; ♦ 5- and 3-chlorosalicylate; ○ 4- and 3-chlorocatechol; Δ 3-and 2-chloromuconate; ▲*cis*-dienelactone; ● protoanemonin.

3.3.2. Metabolites formed during transformation of 4-chlorocatechol or 3-chloromuconate by cell extracts of *Pseudomonas* sp. strain MT1

When 4-chlorocatechol was transformed by cell extracts of 5-chlorosalicylate-grown cells (corresponding to 60 µg of protein per ml), a fast depletion occurred with concomitant formation of 3-chloromuconate. 3-Chloromuconate was only a transient intermediate, and both *cis*-dienelactone and protoanemonin were observed as transformation products (Fig. 6). Even though 40 ± 10 % of the substrate applied accumulated as protoanemonin (30 ± 5 %) and *cis*-dienelactone (10 ± 5 %), the transformation was not stoichiometric. In fact, the formation of a third product was observed, which, by HPLC analysis, was shown to co-elute with authentic maleylacetate and which exhibited an identical absorption spectrum. Assuming its identity with maleylacetate, this compound comprised 55 ± 10 % of the initial substrate concentration. It was further transformed when NADH was added to the reaction mixture.

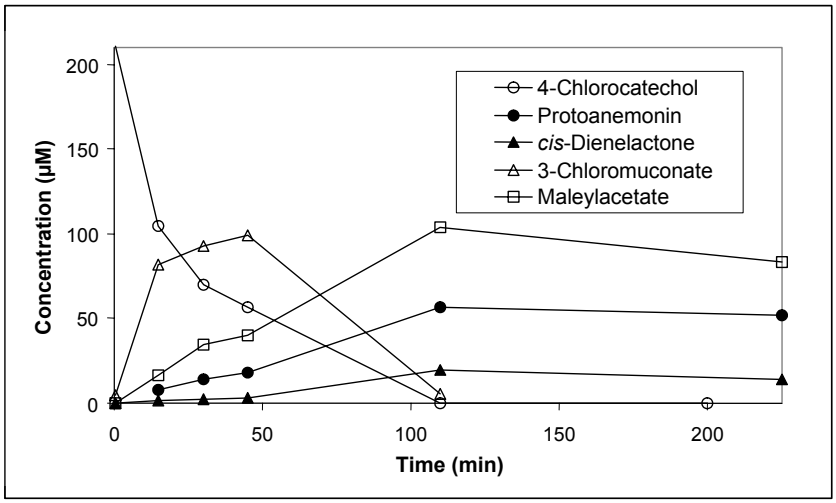

Figure 6: Transformation of 4-chlorocatechol by cell extract (60 µg of protein/ml) of 5-chlorosalicylate grown *Pseudomonas* sp. strain MT1. ○ 4-chlorocatechol; Δ 3-chloromuconate; ▲*cis*-dienelactone; ● protoanemonin, □ maleylacetate.

Similarly, all three products were produced (protoanemonin: 35 ± 20 %; *cis*-dienelactone: 20 ± 5 %; maleylacetate: 45 ± 20 %) when 3-chloromuconate was transformed by cell extracts (60 to 360 µg protein/ml). Transformation of both *cis*-dienelactone and protoanemonin was negligible in all experiments performed.

Interestingly, the product ratios were only reproducible, if assays were repeated with a defined protein concentration. Increasing the concentration of cell extract resulted in a decrease in protoanemonin and an increase in maleylacetate formation (Table 4). *cis*-Dienelactone production was not affected. Assays performed with varying 3-chloromuconate concentrations, demonstrated that the ratio of products was independent of the initial substrate concentration.

Table 4. Products formed from 4-chlorocatechol and 3-chloromuconate by cell extracts of 5-chlorosalicylate grown *Pseudomonas* sp. strain MT1 in dependence of protein and substrate concentrations.

Substrate	**Initial concentration [µM]**	**Cell extract [µg/ml]**	**Proto-anemonin [%]**	***cis*-Diene-lactone [%]**	**Maleyl-acetate [%]**	**recovery [%]**	**Maleylacetate: protoanemonin (ratio)**
4-chloro-catechol	200	60	30 ± 10	10 ± 5	55 ± 10	95	1.8
3-chloro-muconate	110	60	56 ± 2	22 ± 3	33 ± 3	101	0.6
	55	360	10 ± 5	27 ± 5	52 ± 8	90	5.2
	110	360	15 ± 5	23 ± 5	65 ± 5	93	4.3
	430	360	15 ± 5	22 ± 5	52 ± 8	87	5

3.3.3. Metabolites formed during transformation of 3-chloromuconate by partially purified enzymes

Experiments with cell extracts had shown that protoanemonin and *cis*-dienelactone were only formed as side products. The major metabolite in the degradative pathway of 4- and 5-chlorosalicylate had been identified as maleylacetate. The catabolic pathway of chlorosalicylate degradation in MT1 thus seems to comprise salicylate 1-hydroxylase and catechol 1,2-dioxygenase, forming 4-chlorocatechol and 3-chloromuconate as reaction products, respectively (Fig. 7). The fate of 3-chloromuconate, however, remained unclear. Incubation of 3-chloromuconate with cell extracts had demonstrated the formation of maleylacetate, beside protoanemonin and *cis*-dienelactone. This, however, can not be explained with current knowledge.

3-Chloromuconate, by MCI and chloromuconate cycloisomerases (CMCI) reported thus far, is transformed into protoanemonin (8) and *cis*-dienelactone (139), respectively. No *cis*-dienelactone or protoanemonin transforming activity was detected in cell extracts. The conversion of 3-chloromuconate to *trans*-dienelactone has never been observed, but a *trans*-DLH converting *trans*-dienelactone to maleylacetate was detected in MT1 cell extracts (Fig. 8).

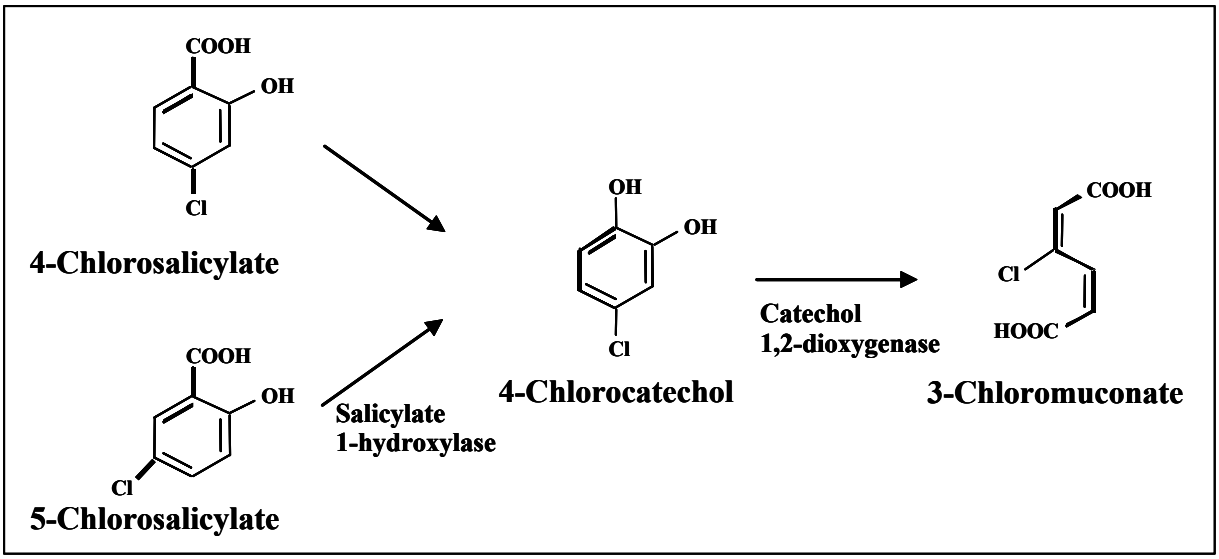

Figure 7: Pathway of 4-chloro and 5-chlorosalicylate degradation by *Pseudomonas* sp. strain MT1.

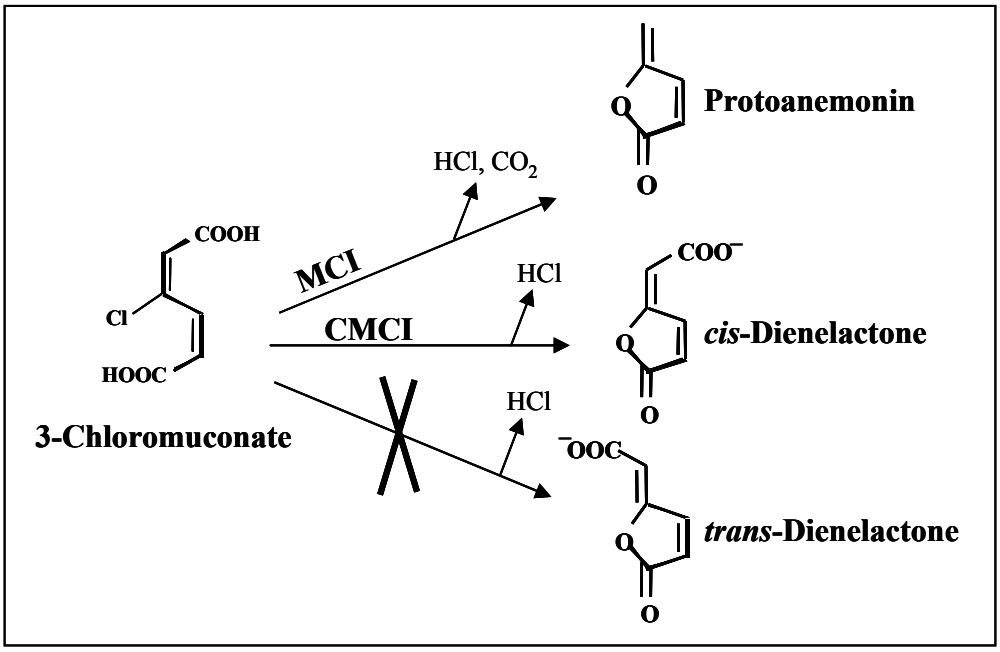

Figure 8: Transformation of 3-chloromuconate by MCI, (muconate cycloisomerase); CMCI, (chloromuconate cycloisomerase) and so far not observed transformation (X).

In order to characterize enzymes involved in the formation of maleylacetate from 3-chloromuconate, extracts of 5-chlorosalicylate-grown cells were fractioned by FPLC and fractions tested for 3-chloromuconate transforming activity by HPLC analysis (Fig. 9).

Astonishingly, two distinct 3-chloromuconate transforming activities were observed after hydrophobic interaction chromatography. Fractions eluting at 0.05 ± 0.04 M $(NH_4)_2SO_4$ converted 3-chloromuconate dominantly into protoanemonin (80 ± 5 %) with minor amounts of maleylacetate being formed. The respective enzyme thus resembles a MCI and was later on used for detailed analysis. Fractions eluting at 0.25 ± 0.04 M $(NH_4)_2SO_4$ formed approximately equal amounts of protoanemonin (48 ± 3 %) and *cis*-dienelactone (48 ± 5 %) and thus displayed a product spectrum intermediate to those of MCI and CMCI (Fig. 9 A,B). The respective enzyme is termed MCIB thereafter.

None of the 3-chloromuconate transforming enzymes formed any detectable amount of *trans*-dienelactone, and both observed dominating reaction products, protoanemonin and *cis*-dienelactone, were dead-end metabolites for MT1 (see 3.3.1 and 3.3.2). In contrast to transformation by cell extracts, only negligible amounts of maleylacetate were observed. Thus, it was speculated, that in the cell extract another enzyme might convert an intermediate product of 3-chloromuconate conversion into maleylacetate.

To evaluate this possibility, cell extracts were fractioned by a different method, anion-exchange chromatography. Again two distinct activities against 3-chloromuconate were determined. Enzymes eluting at 0.3 ± 0.02 M NaCl converted 3-chloromuconate to an approximately equal mixture of protoanemonin and *cis*-dienelactone as described above. However, 3-chloromuconate was transformed into maleylacetate and protoanemonin by fractions eluting at 0.25 ± 0.04 M NaCl, demonstrating that those fractions contained all necessary proteins for maleylacetate formation (Fig. 9 D).

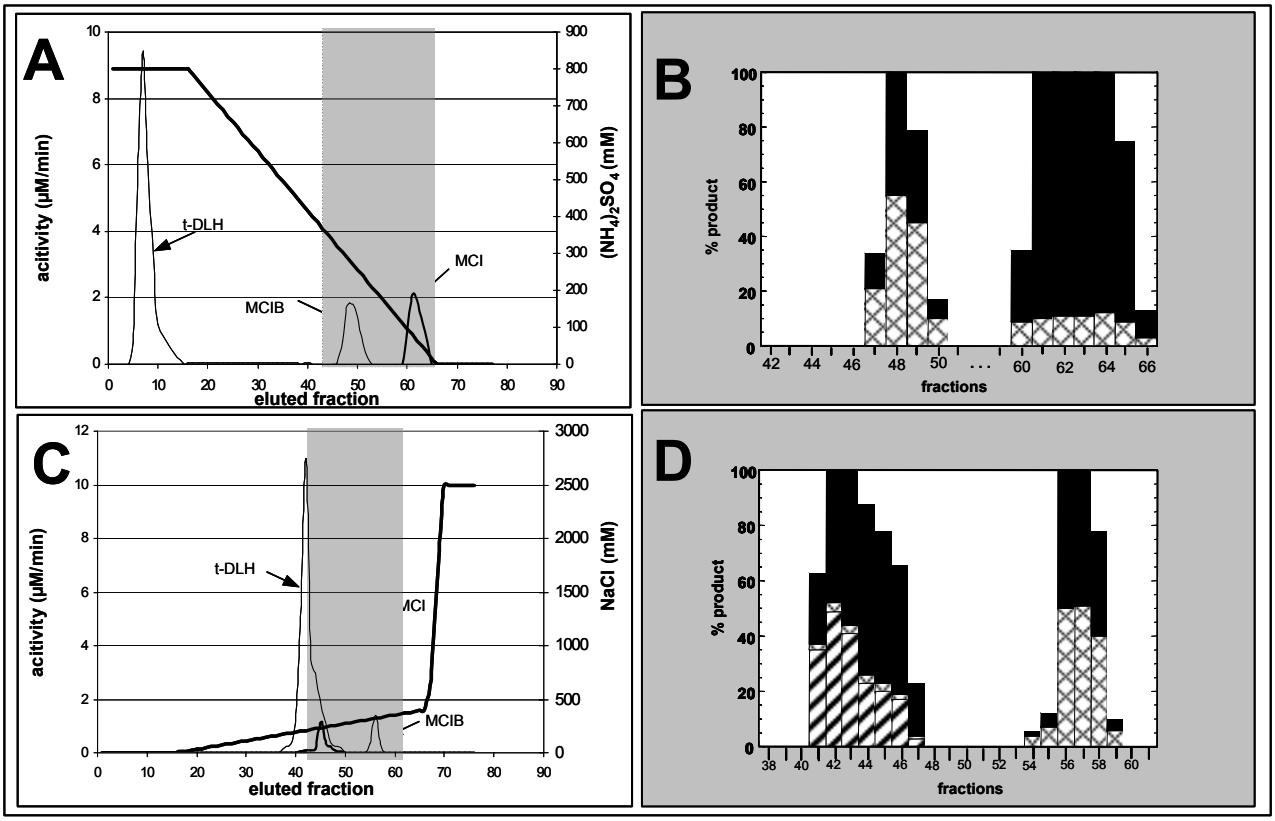

Figure 9: Separation of proteins from cell extracts of 5-chlorosalicylate grown *Pseudomonas* sp. strain MT1 by means of hydrophobic-interaction with a SOURCE 15PHE PE column (**A**) or anion-exchange with a MonoQ HR5/5 column (**B**). Cell extracts were either directly applied (**B**) or applied after addition of ammonium sulfate (final concentration of 0.8 M) (**A**), and proteins were eluted with a linear gradient of $(NH_4)_2SO_4$ (0.8 to 0 M) or NaCl (0 to 0.4 M). The eluted fractions (0.5 ml) were analyzed for activities with 0.1 mM muconate, 0.1 mM 3-chloromuconate and 0.05 mM *trans*-dienelactone. Activities of MCIB and *trans*-DLH are given in µmole/min per fraction, activities of MCI in (µmole * 10)/min per fraction (A, C). Products and substrates after incubation of 0.1 mM 3-chloromuconate with 1 - 5 µl of the respective fraction for 10 - 30 min were quantified by HPLC. For in **A** and **C** shaded fractions the relative amount of products and substrate are given as stacked columns in **B** and **C**, respectively: ☐ 3-chloromuconate; ■ protoanemonin; ▩ *cis*-dienelactone; ▨ maleylacetate.

It has previously been assumed that conversion of 3-chloromuconate to protoanemonin should proceed via 4-chloromuconolactone as reaction intermediate (8) (Fig. 10) and it could be postulated that hydrolysis of 4-chloromuconolactone would lead to maleylacetate. 4-Fluoromuconolactone has previously been described as a rather stable product of 3-fluoromuconate cycloisomerization by MCI of *Ralstonia eutropha* 335, *Burkholderia cepacia* and *R. eutropha* JMP134 (135). Furthermore, Schlömann showed, that 4-fluoromuconolactone is converted by *trans*- and *cis*-/*trans*-DLH of *R. eutropha* 335 and *R. eutropha* JMP134 ($TfdE_I$) to maleylacetate (133) (Fig. 10 B). Thus, it could be speculated that *trans*-DLH of MT1 acts on 4-chloromuconolactone transiently formed during cycloisomerization of 3-chloromuconate, producing maleylacetate. In fact, analysis of the elution profiles demonstrated that *trans*-DLH and MCI co-eluted during anionic exchange chromatography (*trans*-DLH 0.19 ± 0.01 M NaCl) (Fig. 9 C) but not during hydrophobic interaction chromatography (*trans*-DLH 0.8 M $(NH_4)_2SO_4$) (Fig. 9 A).

In order to substantiate that formation of maleylacetate was actually due to the activity of *trans*-DLH and not to any other undefined protein co-eluting with MCI, partially purified *trans*-DLH obtained by hydrophobic interaction chromatography was used in combination with the respective partially purified MCI or MCIB . The respective *trans*-DLH containing fractions turned over neither 3-chloromuconate, nor protoanemonin or *cis*-dienelactone. However, the addition of *trans*-DLH containing fractions to reactions containing partially purified MCI resulted in the formation of significantly increased amounts of maleylacetate from 3-chloromuconate. Similarly, maleylacetate was formed in high amounts when 3-chloromuconate was incubated with a combination of *trans*-DLH and MCIB. This indicated that *trans*-DLH interacts with both cycloisomerizing activities and is responsible for the increased maleylacetate formation. Consequently *trans*-DLH, MCI and MCIB were defined as the key enzymes of a new metabolic pathway in MT1.

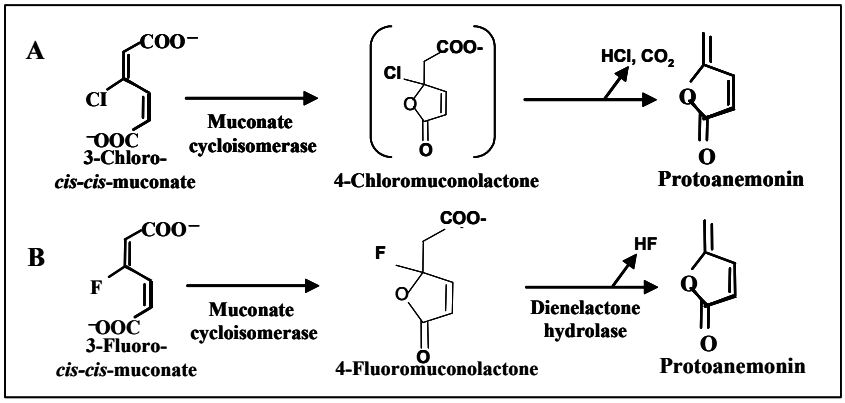

Figure 10: Transformation of 3-chloromuconate to protoanemonin catalyzed by muconate cycloisomerase (MCI) (8). Postulated reaction intermediate given in brackets **(A)**. Transformation of 3-fluromuconate by MCI to 4-fluoromuconolacton which can be hydrolized by different dienelactone hydrolases to maleylacetate (133) **(B)**.

3.4. Characterization of key enzymes of the novel pathway

3.4.1. Characterization of homogeneous muconate cycloisomerase (MCI)

MCI of MT1 was purified to homogeneity. The molecular mass of the native MCI was estimated by gelfiltration to be 255 ± 20 kDa and by SDS-PAGE a single band of 40 ± 2 kDa was observed (Table 5). It can thus be assumed, that this enzyme, like MCI of *P. putida* PRS2000 (55) or CMCI from *R. eutropha* JMP 134 ($TfdD_I$) (60) is a homo-octamer.

The N-terminal sequence of MCI from MT1 (TQAKIESIETILVDLPTVRPHKLAM) showed a significant similarity to the CatB protein (accession number Q43931) of *Acinetobacter calcoaceticus* (14 identical amino acids) and to CatB from *Pseudomonas putida* PRS2015 (accession number P08310, 10 identical amino acids) which also shares significant similarity (amino acid 213 to 231) to an internal sequence of the MT1 MCI (**AC**K**VLGDNG**L**DL**L**EKP**L**SR**) (identical amino acids are marked in bold).

Table 5. Molecular characterization of MCI, MCIB and *trans*-DLH of *Pseudomonas* sp. strain MT1.

Enzyme	Molecular mass [kDa]	Subunit mass [kDa]	N-terminal amino acid sequence	Inner protein sequences
MCI	255 ± 20	40 ± 2	TQAKIESIETILVDL PTVRPHKLAM	
				is_d: DLAEAEHFLDVR
				is_c: ACKVLGDNGLDLLEKPLSR
MCIB	350 ± 20	43 ± 3	SQGFVIGRVLAQR LDIPFSQPIRMSFGT LD	
				is_b: FGSGDPDAELLR
				is_c: TLSTGSEGGDLAEGER
				is_d: MLFQENGGLEG
trans-DLH	85 ± 30	39 ± 4	TDTSKSLPTYKQLL ERKDAPPGSSWGL FGK	
				is_c: VSQGVTLEPGDAVLLR
				is_d: AFSLDLLATSLYALLAGPSL
				is_e: KLDLDAGASGKALSAKVLEAAR
				is_f: VDVNGAYSVDEAQALR

The substrate spectrum and kinetic parameters of MCI at a glance, were only partially similar to those of previously described proteobacterial MCIs. As expected, both, 2-chloromuconate and 2,4-dichloromuconate were only poor substrates for the enzyme (Table 6). However, both muconate and 3-chloromuconate were transformed at relatively high rates, in contrast to previous information

obtained during analysis of other MCIs (139, 169), which indicated a poor activity of these enzymes with 3-chloromuconate. The K_m-value for muconate (1.73 ± 0.35 mM) was significantly higher than those previously reported for MCI of *P. putida* PRS2000 (0.04 mM) (169), *Acinetobacter calcoaceticus* ADP1 (0.13 mM) (169) or *Pseudomonas* sp. strain B13 (0.056 mM) (139). However, maximal turnover numbers were in the same order of magnitude (169). Surprisingly, a comparison of k_{cat}/K_m values indicated 3-chloromuconate to be preferred over muconate as a substrate by MCI of MT1. At substrate concentrations of 0.1 mM the enzyme transformed 3-chloromuconate about 3.5 times faster compared to muconate (Table 6). Activities slightly approaching the values reported here have only be given for two site-directed mutants of *P. putida* PRS2000 MCI (see 3.8.1.3) by Vollmer et al. (169).

Purified MCI of MT1 transformed 3-chloromuconate into protoanemonin as dominant product, and HPLC analysis revealed, that *cis*-dienelactone and maleylacetate were formed as side products corresponding to 8 ± 4 % and 8 ± 5 %, respectively, of the initial substrate concentration.

Besides muconate and 3-chloromuconate, MCI of MT1 was able to transform 3-fluoromuconate. The formation of a single product was observed which, as determined by HPLC analysis, exhibited only negligible absorbance at wavelengths > 240 nm. Similarly, under physiological conditions the product exhibited only an absorption maximum at 208 nm (Fig. 11). This absorption behavior is characteristic for 4-fluoromuconolactone which was identified as the product formed during cycloisomerization of 3-fluoromuconate by MCI of *Ralstonia eutropha* 335 and JMP134 (135). The identity of the product formed from 3-fluoromuconate by MCI of MT1 as 4-fluoromuconolactone was further confirmed by its transformation into maleylacetate by *trans*-DLH (see 3.4.3) (Fig. 10 B).

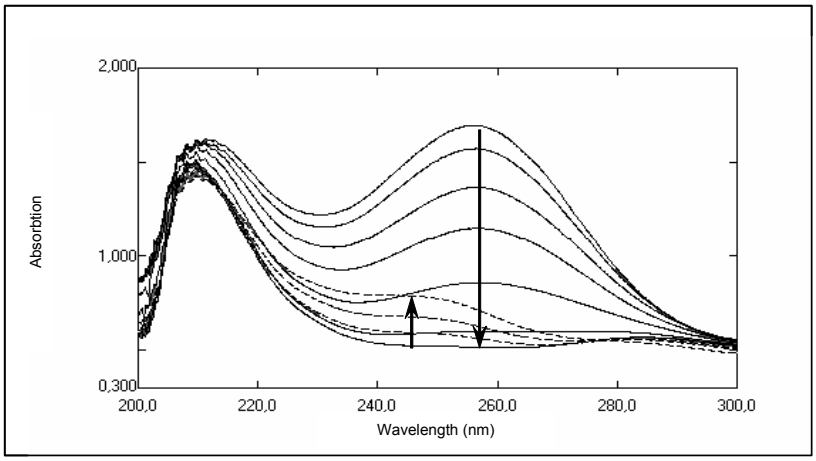

Figure 11: Overlay spectra during transformation of 3-fluoromunate to 4-fluromuconolactone by partially purified MCI and of 4-fluoromuconolactone to maleyl-acetate by purified *trans*-DLH. Spectral changes during incubation with MCI are indicated by ↓, those during transformation by *trans*-DLH by ↑.

Table 6. Substrate specificities of MCI and MCIB of *Pseudomonas* sp. strain MT1in comparison to CMCI and MCI from different sources.

Strain	Enzyme	Substrate	Activity at 0.1 mM substrate (U/mg)[a]	K_m (µM)[b]	k_{cat} (min^{-1})[b]	k_{cat}/K_m (min^{-1} $µM^{-1}$)[b]
Pseudomonas sp. strain MT1	MCI	muconate	9.9 ± 1.2	1730 ± 350	7500± 350	4.3
		3-chloromuconate	35 ± 6	410 ± 75	7200 ± 520	17.6
		2-chloromuconate	0.09 ± 0.02	ND[c]	ND	ND
		2,4-dichloromuconate	< 0.001	ND	ND	ND
Pseudomonas sp. strain MT1	MCIB	muconate	< 0.001	ND	ND	ND
		3-chloromuconate	140 ± 10	105 ± 15	6670 ± 470	63
		2-chloromuconate	< 0.003	ND	ND	ND
		2,4-dichloromuconate	0.47 ± 0.05	ND	ND	ND
Ralstonia eutropha JMP 134	CMCI (= $TfdD_I$)	muconate	1.6	996 ± 35	700 ± 10	0.71
		3-chloromuconate	48	98 ± 3	3770 ± 70	38
		2-chloromuconate	3	79 ± 3	215 ± 5	2.7
		2,4-dichloromuconate	57.5	23 ± 1	2810 ± 40	120
Pseudomonas sp. strain B13	CMCI (ClcB)	muconate	3.3	270 ± 55	480 ± 70	1.8
		3-chloromuconate	21.7	160 ± 55	2240 ± 480	14
		2-chloromuconate	8.5	42 ± 6	480 ± 30	11
		2,4-dichloromuconate	7.9	26 ± 2	390 ± 10	15
Pseudomonas putida PRS2000	MCI (CatB)	muconate	223	40 ± 4	12600 ± 400	310
		3-chloromuconate	0.38	320 ± 200	64 ± 30	0.20
		2-chloromuconate	0.76	59 ± 5	49 ± 2	0.83
		2,4-dichloromuconate	0.06	26 ± 3	3.3 ± 0.1	0.13
P. putida PRS2000 I54V	MCI I54V	muconate	31.9	96 ± 8	2500 ± 100	26
		3-chloromuconate	3.45	45 ± 8	200 ± 10	4.4
P. putida PRS2000 A271S	MCI A271S	muconate	131.5	35 ± 3	7100 ± 200	200
		3-chloromuconate	8.57	180 ± 20	960 ± 60	5.4

[a] The data for strains JMP134, B13 and PRS2000 were calculated from references (149, 170 and 169).
[b] The data for strains JMP134, B13 and PRS2000 are from references (149, 170 and 169).
[c] ND, not determined

Muconate and chloromuconate cycloisomerases were demonstrated to catalyze the formation of an equilibrium between 2-chloromuconolactone, 5-chloromuconolactone and 2-chloromuconate when transforming 2-chloromuconate (168, 171).Thus muconolactones are known to be substrates to those enzymes (116), however, some, like 4-methylmuconolactone (111) are not transformed. In order to try to accumulate the hypothesized reaction intermediate, the structural analogue 4-methylmuconolactone was incubated with MCI and it was tested, if it can be recognized as an inhibitor. HPLC analysis showed that the substrate analogue 4-methylmuconolactone (1 mM) was not transformed by MCI (data not shown) and that its inhibition on 3-chloromuconate (0.1 mM) transformation or protoanemonin formation by MCI (0.8 mU/ml determined with 0.1 mM muconate; 0.2 nM MCI) was less than 4 %. Assuming competitive inhibition to take place, it can be calculated that the *Ki* value for 4-methylmuconolactone is less than 19 mM.

3.4.2. Characterization of homogenous MCIB

Various reports analyzed the kinetic differences between muconate and chloromuconate cyloisomerases and their evolutionary relationships. However, attempts to identify amino acid residues responsible for the formation of different products from 3-chloromuconate failed thus far (72). As CMCI produces nearly exclusively *cis*-dienelactone, and MCI protoanemonin, MCIB can be regarded as a probably evolutionary intermediate between these two types of enzymes.

Purified MCIB transformed 3-chloromuconate stoichiometrically to equal amounts of protoanemonin and *cis*-dienelactone (48 ± 5 % respectively). Only very minor amounts of maleylacetate could be detected (5 ± 3 %). Following 3-chloromuconate transformation over time showed that both major products were formed in a constant ratio, indicating that the reaction mechanism was independent of the substrate concentration.

The native molecular mass of MCIB was estimated by gelfiltration to be 350 ± 20 kDa and a single band of 43 ± 3 kDa was observed on SDS-gels. Thus MCIB might be a homooctamer, just like MCI of *P. putida* PRS2000 (55) or CMCI from *R. eutropha* JMP134 (49) or as assumed for MCI of *Pseudomonas* sp. strain MT1. No significant similarity of neither the N-terminal nor inner protein sequences was observed when these sequences were compared to sequences of cycloisomerases available in databases (Table 5).

Out of the substrates tested, only 3-chloromuconate was transformed with high activity by this enzyme. Thus the absence of a significant activity with muconate distinguishes MCIB from MCI reported thus far, and the absence of a significant activity against 2-chloromuconate distinguishes it from most proteobacterial CMCI (78, 168, 169, 170). However, MCIB resembles the CMCI of *R. eutropha* JMP134 ($TfdD_{II}$) which also exhibits negligible activity with muconate (114) and the CMCI of the gram-positive *Rhodococcus opacus* 1CP (ClcB) also having negligible activity with muconate and 2-chloromuconate, but in contrast to MCIB of MT1 exhibits significant activity with 2,4-dichloromuconate (151).

Like MCI, MCIB of MT1 (1.9 mU/ml; 0.3 nM MCIB) was not able to transform 4-methylmuconolactone (data not shown). 4-Methylmuconolactone (1 mM), however, inhibited significantly 3-chloromuconate (0.1 mM) transformation and protoanemonin formation by 50 %. Thus, 4-methylmuconolactone was recognized as inhibitor, but not converted by MCIB. Assuming competitive inhibition to take place a K_i value for 4-methylmuconolactone of 0.5 mM can be calculated. No accumulation of the hypothesized cycloisomerization intermediate could be detected – the sum of substrate (3-chloromuconate) and products (protoanemonin, *cis*-dienelactone and maleylacetate) remained constant throughout the experiment**.**

3.4.3. Characterization of homogeneous *trans*-dienelactone hydrolase (*trans*-DLH)

Dienelactone hydrolases (DLH) have been divided into three classes according to their substrate specificities by Schlömann. Type I DLH transform *trans*-dienelactone much more efficient than *cis*-dienelactone, type II DLH have an inverse substrate preference and type III transform both isomers with similar efficiencies (132).

The molecular mass of native *trans*-DLH was determined to be 85 ± 30 kDa by gelfiltration. As a single band at 39 ± 4 kDa was visible on SDS-PAGE it can be assumed that *trans*-DLH of *Pseudomonas* sp. strain MT1 is a monomeric or dimeric enzyme (Table 5). In comparison, DLH involved in the chlorocatechol pathway and active with both *cis*- and *trans*-dienelactone, such as *cis*-/*trans*-DLH of *Pseudomonas* sp. strain B13 (105), *P. putida* strain 87 (149) and *Rhodococcus opacus* 1CP (85) as well as *cis*-DLH of *Burkholderia cepacia* (136) had been shown to be monomeric proteins. Similarly, *trans*-DLH of *Ralstonia eutropha* 335 was assumed to be a monomeric enzyme (132). Partial *trans*-DLH protein sequences (Table 5) were compared with

databases, but no significant similarity was obtained. Also no significant similarity was found when 21 selected DLH protein sequences from SwissProt and the unpublished N-terminal sequence of *trans*-DLH of *Ralstonia eutropha* 335 (58) were compared with the N-terminal sequence of MT1 *trans*-DLH. The activity of *trans*-DLH in 10 mM Histidine /HCl, pH 6.5 (137) was characterized by a rapid initial reaction followed by a drastic decrease in rate when 10 – 15 % of the substrates was converted, indicating that the enzyme was not acting as a typical catalyst, but that it was inhibited during transformation as previously observed for catechol 2,3-dioxygenase (69). However, when transformation was performed in 50 mM Tris/HCl, pH 7.5 no inactivation was observed.

Table 7: *trans*-Dienelactone hydrolase (*trans*-DLH) of *Pseudomonas* sp. strain MT1 in comparison to other DLH.

Strain	**Enzyme**	**Substrate**	**Activity at 0.1 mM substrate (U/mg)**	K_m **(min^{-1})**	k_{cat} **(min^{-1})**	k_{cat}/K_m **(min^{-1} µM^{-1})**
Pseudomonas sp. strain MT1	*trans*-DLH	*cis*-dienelactone	< 1			
		trans-dienelactone	710 ± 37	480 ± 20	159000 ± 8500	330
		4-fluoromuconolactone	190 ± 4	1200 ± 20	98000 ± 2200	82
		enollactone	20 ± 10			
Alcaligenes eutrophus 335	*trans*-DLH	*cis*-dienelactone	-			
		trans-dienelactone	+			
		4-fluoromuconolactone	+			
		enollactone	+			
Alcaligenes eutrophus JMP 222	*trans*-DLH	*cis*-dienelactone	-			
		trans-dienelactone	+			
		4-fluoromuconolactone	(+)			
		enollactone	(+)			
Pseudomonas sp. strain B13	*cis*-/*trans*-DLH	*cis*-dienelactone	+	400		
		trans-dienelactone	+	15		
		4-fluoromuconolactone	+			
		enollactone	-			
Alcaligenes eutrophus JMP 134	*cis*-/*trans*-DLH	*cis*-dienelactone	+	140 *		
		trans-dienelactone	+	110 *		
		4-fluoromuconolactone	+			
		enollactone	-			
Rhodococcus erythropolos 1CP	*cis*-DLH	*cis*-dienelactone	24	28	923	33
		trans-dienelactone	< 0.2			
		4-fluoromuconolactone	< 0.5			
		enollactone	-			
Burkholderia cepacia	*cis*-DLH	*cis*-dienelactone	220 ± 75	590 ± 240	49000 ± 17000	83
		trans-dienelactone	< 0.9			
		4-fluoromuconolactone	< 0.5			
		enollactone	< 4.5			

(*) determined in cell extracts. Data taken from following references: *Alcaligenes eutrophus* 335 (133, 132); *A. eutrophus* JMP222, (133); *Pseudomonas* sp. strain B13 (133); *A. eutrophus* JMP134 (133, 132); *Rhodococcus erythropolis* 1CP (133, 85); *Burkholderia cepacia* (136, 132).

The K_m for *trans*-dienelactone (480 μM) (Table 7) was higher than those reported for *cis*-/*trans*-DLH of the chlorocatechol pathway (133, 139) for this substrate. *trans*-DLH also exhibited significantly higher turnover numbers than *cis*-/*trans*-DLH of *Pseudomonas sp.* strain B13 (1800 min^{-1}, (95)) and even a higher turnover number compared to *cis*-DLH of *B. cepacia* with *cis*-dienelactone (49.000 min^{-1} (136)). Activities of *trans*-DLH with 3-chloromuconate, protoanemonin and *cis*-dienelactone were negligible (< 0.1 % of the activity with 0.1 mM *trans*-dienelactone). Thus, while *trans*-DLH obviously interferes with the reaction catalyzed by MCI and MCIB, presumably preventing the formation of protoanemonin and supporting the formation of maleylacetate (see 3.5), the enzyme neither acts on the substrate (3-chloromuconate) nor on the product (protoanemonin) of this reaction.

As, 4-chloromuconolactone, the postulated intermediate of 3-chloromuconate cycloisomerization (8, 72) was not available, transformation of the rather stable analogue 4-fluoromuconolactone (135) by *trans*-DLH was tested. HPLC revealed the quantitative transformation of 4-fluromuconolactone into a single product with a retention behavior and absorption spectrum identical to that of maleylacetate. Spectrophotometric analysis showed the product to exhibit an absorption maximum under physiological conditions of 243 nm, in accordance with its identity as maleylacetate (112, 143) (Fig. 11). According to the k_{cat}/K_m-values, *trans*-dienelactone was the preferred substrate, being transformed approximately 4 times more efficiently than 4-fluoromuconolactone (Table 7). Similarly, *trans*-DLH of *Ralstonia eutropha* 335 and JMP222, as well as *cis*-/*trans*-DLH of *Pseudomonas* sp. B13 induced during growth on 4-fluorobenzoate (137) were reported to convert 4--fluoromuconolactone. Only *cis*-DLH of *Burkholderia cepacia* did not transform 4-fluoromuconolactone (133).

Like the *trans*-DLH of *Ralstonia eutropha* 335 and JMP222, also the *trans*-DLH of *Pseudomonas* sp. strain MT1 exhibit a reasonable activity with enollactone. However, this activity, at a substrate concentration of 0.1 mM corresponds to only 4 ± 2 % the activity with *trans*-dienelactone, whereas activity of *trans*-DLH of *R. eutropha* 335 with enollactone was 40 ± 10 % the activity with *trans*-dienelactone (132). Nevertheless, *trans*-DLHs seem to differ from *cis*-DLH and *cis*-/*trans*-DLH, which have no detectable activity with enollactone (133, 137).

Organic mercurial substances like 4-chloromercurybenzoate have a high affinity for sulfhydryl groups in proteins and can be used for binding and inactivation studies. *trans*-DLH of MT1 was not inhibited by 4-chloromercurybenzoate, a characteristic shared with *cis*-DLH of *B. cepacia* (136). In

contrast, all *cis*-/*trans* DLH and even *trans*-DLH of JMP222 and 335 were reported to be inactivated by 4-chloromercurybenzoate (85, 95, 132). However, heavy metals had strong effects on *trans*-DLH activity (Table 8).

Table 8. Effects of inhibitors on *trans*-dienelactone hydrolase (*trans*-DLH) activity of *Pseudomonas* sp. strain MT1.

Enzyme inhibitor	**Concentration (mM)**	**Relative enzyme activity (%)[a] after incubation for**		
		5 min	60 min	240 min
EDTA	1	27 ± 3	17 ± 3	ND[b]
	10	13 ± 3	7 ± 3	ND
o-Phenanthroline	1	55 ± 4	18 ± 3	ND
4-Chloromercuribenzoate	0.02	> 90	> 90	> 90
	2	> 90	> 90	> 90
$HgCl_2$	1	6 ± 3	ND	ND
$ZnCl_2$	1	< 5	ND	ND
$CuCl_2$	1	34 ± 5	26 ± 4	ND

[a] Activity of purified *trans*-DLH is given compared to a control incubated without inhibitor.
[b] ND, not determined

Schlömann stated that *trans*-DLHs need Mn^{2+} for efficient activity in contrast to *cis*- and *cis*-/*trans*-DLH (132, 133). In order to test whether ions were necessary for catalysis, *trans*-DLH was incubated with the chelating agents EDTA and *o*-phenanthroline. Both agents significantly inhibited *trans*-DLH of MT1 (Table 8). Thus, with respect to inhibition by EDTA, *trans*-DLH of MT1 resembles *trans*-DLH of JMP222 and 335, and contrasts *cis*-/*trans*-DLH of *Ralstonia eutropha* JMP134 (133) and *cis*-DLH of *P. cepacia* (78) which were not susceptible to EDTA.

3.5. *In-situ* transformation of 3-chloromuconate by purified enzymes

3.5.1 *In-situ* transformation of 3-chloromuconate by combined action of MCI and *trans*-DLH of MT1

When purified MCI of MT1 was incubated with 3-chloromuconate, protoanemonin was the major reaction product (>75 %) and only minor amounts of *cis*-dienelactone (8 ± 4 %) and maleylacetate (8 ± 5 %) were detected as side products (Fig. 12 A). However, when *trans*-DLH of MT1 was added simultaneously to the reaction mixture, higher amounts of maleylacetate and less protoanemonin were detected. Formation of *cis*-dienelactone was not effected by the addition of *trans*-DLH (Fig. 12 B - C). Following the transformation of 3-chloromuconate over time with different enzyme ratios showed, that all the products were continuously formed and that 3-chloromuconate was transformed quantitatively into protoanemonin, *cis*-dienelactone and maleylacetate. No other compounds were accumulating during the reaction.

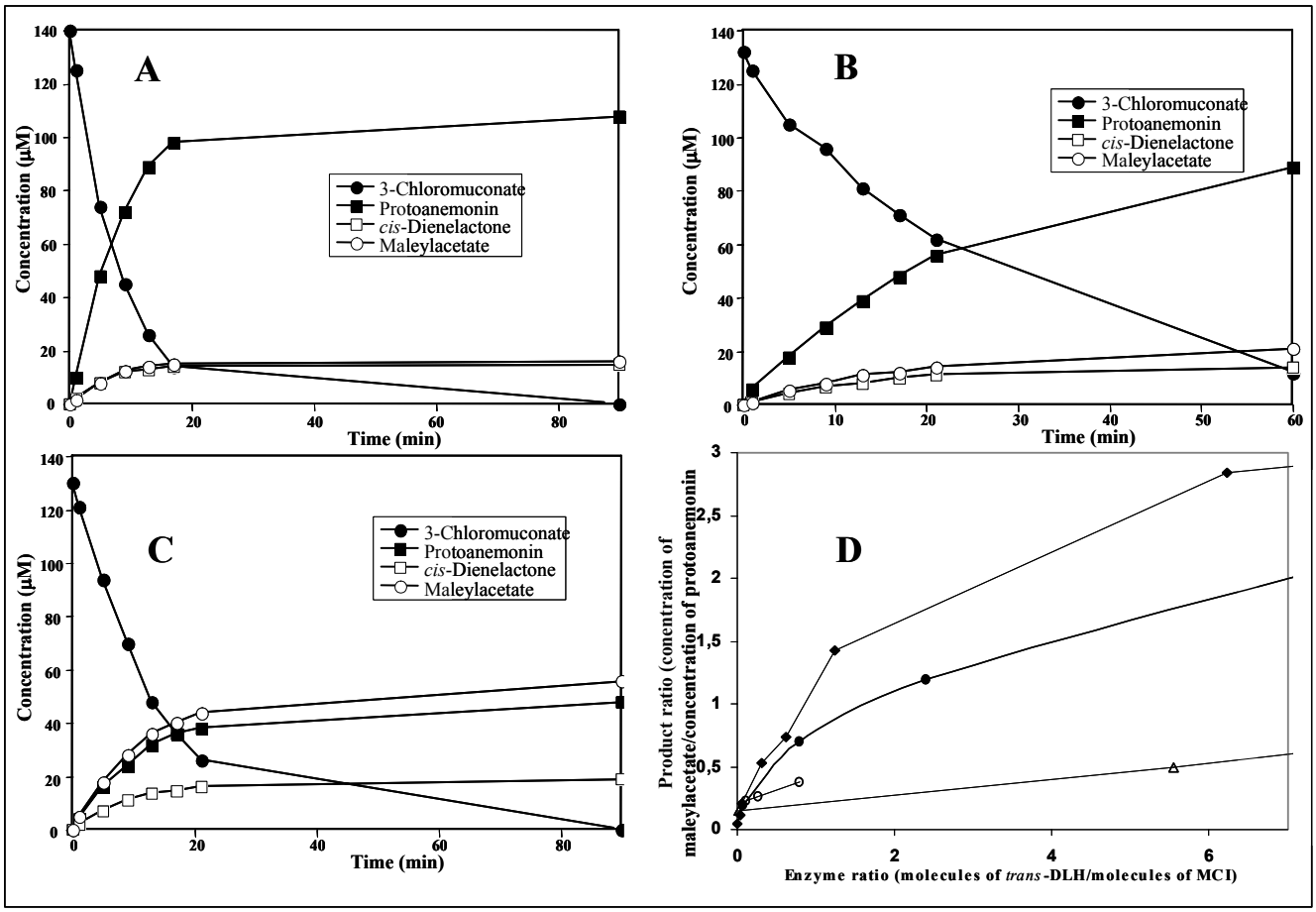

Figure 12: Transformation of 3-chloromuconate by purified MCI or MCI and *trans*-DLH. (**A**) Transformation by MCI (0.9 mU/ml, 2.25 nM; (**B**) Transformation by MCI (0.3 mU/ml, 0.75 nM) and *trans*-DLH (2.7 mU/ml, 0.18 nM); (**C**) Transformation by MCI (0.9 mU/ml, 2.25 nM) and *trans*-DLH (81 mU/ml, 5.4 nM); (**D**) Distribution of products in dependence to the applied enzyme ratio. MCI was added in fixed concentrations of 6.75 nM (♦); 2.25 nM (●); 0.75 nM (○) or 0.45 nM (Δ) .

It could be demonstrated, that the product ratio was independent of the initial substrate concentration (Fig. 13). When different concentrations of 3-chloromuconate (43 µM, 130 µM and 290 µM) were incubated with 2.25 nM MCI (0.9 mU/ml) and 5.4 nM *trans*-DLH (81 mU/ml), maleylacetate and protoanemonin were produced in approx. equal amounts throughout the whole transformation process. In all those assays 42 ± 2 % of the substrate was transformed into maleylacetate, 42 ± 5 % into protoanemonin and 12 ± 3 % into *cis*-dienelactone.

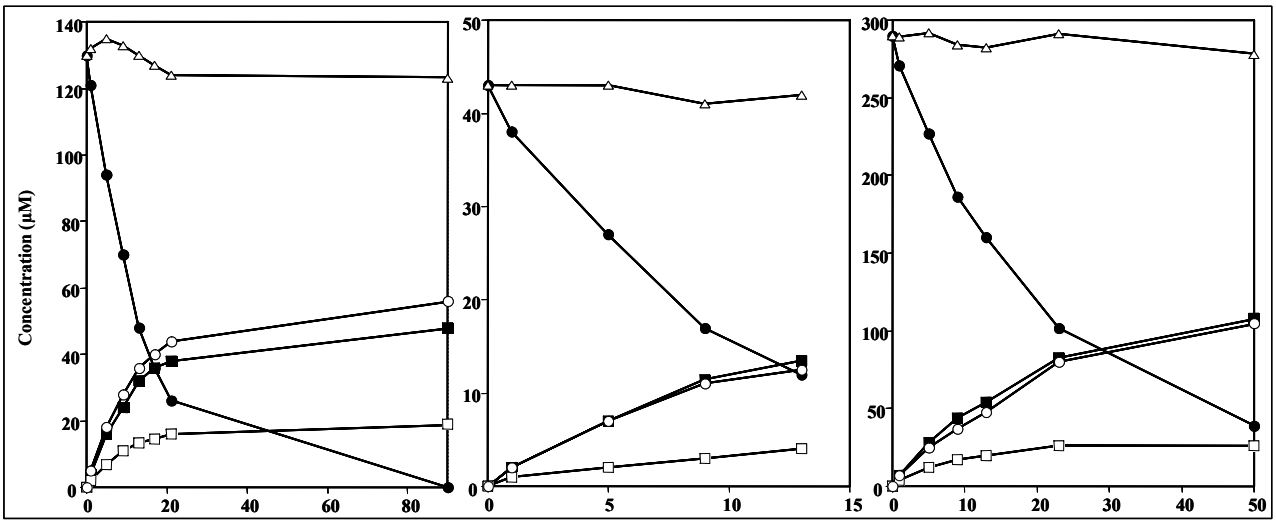

Figure 13: Transformation of different concentrations of 3-chloromuconate by a constant ratio of MCI (2.25 nM) and *trans*-DLH (5.4 nM). Δ recovery (concentration of substrate plus concentration of products), ○ maleylacetate, ● 3-chloromuconate, □ *cis*-dienelactone, ■ protoanemonin.

Increasing the amount of *trans*-DLH at a fixed concentration of MCI resulted in an increase in maleylacetate formation. Different kinetic models were analyzed by Volker Hecht (GBF), if they could explain the observed enzyme kinetics and product shifts upon addition of enzyme mixtures. MCI was assumed to directly form *cis*-dienelactone without involving the intermediate formation of 4-chloromuconolactone, whereas protoanemonin and maleylacetate formation was assumed to necessitate the intermediate formation of this compound. However, a simple competition between MCI catalyzing the formation of protoanemonin, and *trans*-DLH, catalyzing the formation of maleylacetate from 4-chloromuconolactone, could not explain the observed reaction kinetics. The kinetic data, however, could be explained by a rather improbable formation of a second reaction intermediate (I2) by *trans*-DLH, which spontaneously rearrange to form maleylacetate and a minor amount of protoanemonin (model 1), or by the enzymatic formation of both, maleylacetate and minor amounts of protoanemonin from 4-chloromuconolactone by *trans*-DLH (model 2) (Fig. 14 A).

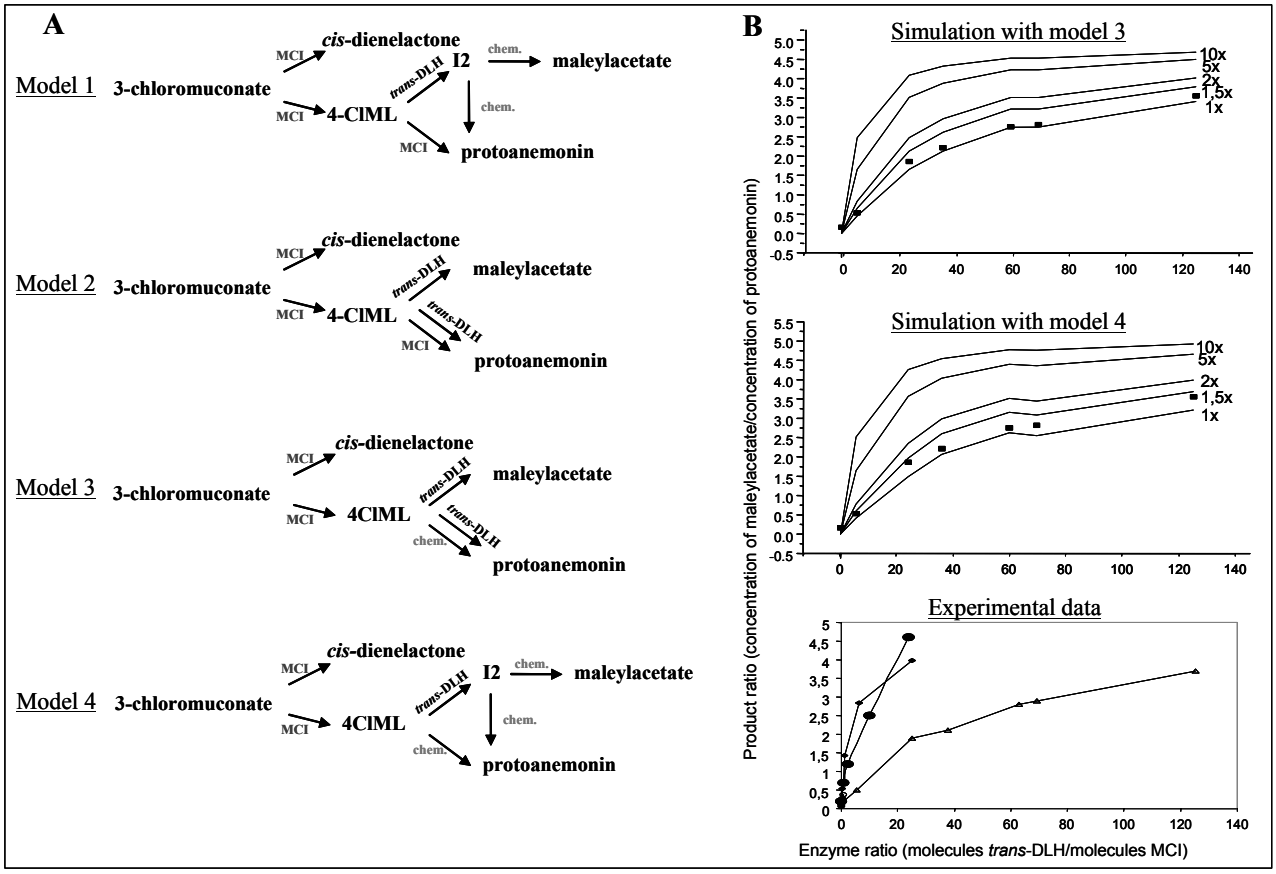

Figure 14: (A) Kinetical models describing the formation of *cis*-dienelactone, protoanemonin and maleylacetate as products from 3-chloromuconate by MCI and *trans*-DLH catalyzed reactions or by spontaneous chemical reaction (chem.). Hypothesized intermediate 4-chloromuconolactone (4-ClML); hypothesized second reaction intermediate (I2). **(B)** Dependency of product ratio on the enzyme ratio and on the concentration of total proteins. Experimental data from data set with 0.45 nM with various concentrations of *trans*-DLH are indicated by symbols. Simulation of the composition of the formed product ratio using model 3 and model 4 with increasing total protein concentration (1.5, 2, 5 and 10 fold). (**B** bottom) Product formation versus enzyme ratio with ♦ 2.7 mU/ml, 6.75 nM MCI; ● 0.9 mU/ml, 2.25 nM MCI; ◦ 0.3 mU/ml, 0.75 nM; Δ 0.18 mU/ml, 0.45 nM MCI with various concentrations *trans*-DLH as in Fig. 12 D.

Both models were able to fit single data sets quite well. However, kinetic results from different data sets, where MCI was added in different fixed amounts (Fig. 12 D), could not be fitted by models 1 and 2. As shown in Fig. 12 D the ratio of products formed was not only dependant on the ratio of *trans*-DLH/MCI. Experiments performed at constant concentrations of MCI of 0.45 nM, 0.75 nM, 2.25 nM and 6.75 nM (corresponding to 0.18 mU MCI/ml, 0.3 mU MCI/ml, 0.9 mU MCI/ml and 2,7 mU MCI/ml with 0.1 mM muconate, respectively) and increasing concentrations of *trans*-DLH showed, that at a constant ratio of *trans*-DLH/MCI, the formation of maleylacetate was favored by a high protein concentration.

The dependence of the product composition on the total protein concentration cannot be explained by the mechanisms used in models 1 and 2. It can, however, be explained if a spontaneous reaction competed with an enzyme catalyzed reaction. Both models were therefore modified assuming chemical formation of protoanemonin from 4-chloromuconolactone.

The two modified models (model 3 and model 4) were fitted to an experimental data set describing 3-chloromuconate transformation in the presence of 0.45 nM MCI (0.18 mU MCI/ml) with various amounts of *trans*-DLH. Good agreement between model and experimental data were obtained for both models. The models were then used to simulate product formation using 1.5, 2.5, 5 and 10 fold total enzyme concentrations (Fig. 14 B). Even though both models not perfectly describe the increase in maleylacetate formation by increasing protein concentration, both models are in reasonably good agreement with the measured data. It should be noted, that measurements performed here, are highly dependent on the accuracy of protein activity determinations, determination of substrate and product formation, such that deviations to the model can easily be explained by experimental errors.

Thus, the assumption that protoanemonin formation is a spontaneous reaction competing with an enzyme catalyzed transformation into maleylacetate is in accordance with the experimental data and explains the increase in maleylacetate formation upon increasing enzyme concentrations.

In contrast to model 3, model 4 predicts accumulation of 4-chloromuconolactone at high total protein concentrations (5 – 20 fold). Experimentally we have never detected any misbalance of substrate and product concentrations, even when 3-chloromuconate (0.3 mM) was incubated with 50 times MCI (22.5 nM, 9 mU MCI/ml). In addition there is no necessity to assume a second intermediate in model 3, so that model 3 obviously best describes the experimental findings.

3.5.2. *In-situ* transformation of 3-chloromuconate by the combined action of MCIB and *trans*-DLH of MT1

Purified MCIB transformed 3-chloromuconate into protoanemonin (48 ± 5 %) and *cis*-dienelactone (48 ± 5 %) in equal amounts. As observed during 3-chloromuconate transformation by MCI, only very minor amounts of maleylacetate (5 ± 3 %) were detected. To analyze, if the product composition, as shown above for MCI, can be influenced by co-incubation with *trans*-DLH, 3-chloromuconate (0.1 mM) was transformed by enzyme mixtures. MCIB was added in activities corresponding to 53 mU/ml and 72 mU/ml (determined with 0.1 mM 3-chloromuconate,

(corresponding to 8.8 nM and 12 nM MCIB, respectively), whereas *trans*-DLH was applied with amounts ranging from 0.66 mU/ml – 1980 mU/ml (with 0.05 mM *trans*-dienelactone, corresponding to 0.044 nM – 132 nM *trans*-DLH), respectively. Addition of *trans*-DLH to the reaction mixture resulted in an increased formation of maleylacetate and decreased formation of protoanemonin, whereas the amount of *cis*-dienelactone produced remained constant (Fig. 15). As observed for the combined action of MCI and *trans*-DLH, the product composition (maleylacetate/protoanemonin ratio) was also dependent on the concentration of enzymes in the assays, whereas the amount of *cis*-dienelactone formed was independent of the presence of *trans*-DLH and did not vary upon addition of different protein concentrations.

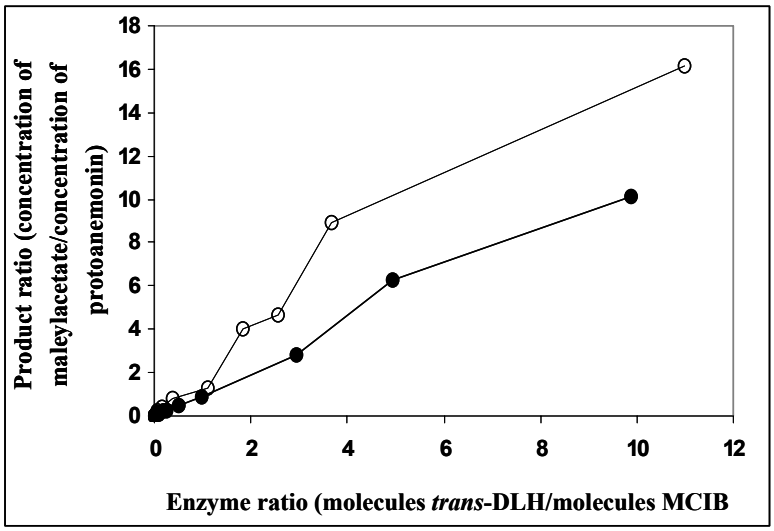

Figure 15: Transformation of 3-chloromuconate by ● 8.8 nM MCIB, 53 mU/ml; ◦ 12 nM MCIB, 72 mU/ml in the presence of increasing concentrations of *trans*-DLH.

3.5.3. *In-situ* transformation of 3-chloromuconate by combined action of MCI of *Pseudomonas putida* PRS2000 and *trans*-dienelactone hydrolase of *Pseudomonas* sp. strain MT1

In order to test whether intermediate 4-chloromuconolactone formation from 3-chloromuconate is a general capability of MCIs, and thus if protoanemonin formation can be generally prevented if a *trans*-DLH activity is present concomitantly, the archetype muconate cycloisomerase of *Pseudomonas putida* PRS2000 (CatB) was analyzed. This enzyme was previously reported by Vollmer to exhibit an only faint activity with 3-chloromuconate. According to Vollmer, the enzyme, when activities at substrate concentrations of 0.1 mM are compared, transforms muconate 590 times more rapidly than 3-chloromuconate and muconate was reported to be the by far preferred substrate with a K_{cat}/K_m value more than 1000-fold that of 3-chloromuconate (Table 6). In the following

CatB was overexpressed from plasmid pCATB1 (kindly provided from Schlömann and Kaschabeck) containing *catB* of PRS2000, in a *E. coli* BL21 derivative. Transformation of 3-chloromuconate and formation of products were evaluated by HPLC analysis. The reported k_{cat} of 12,600 min^{-1} mM^{-1} was used to calculate the concentration of protein molecules applied in the enzymatic tests. Activities were determined in at least 3 independent experiments. We observed, that 3-chloromuconate was a much better substrate to the CatB than Vollmer et. al had described (Table 12). In contrast to the 590 fold preference for muconate versus 3-chloromuconate (169), we determined an only 30 fold preference for muconate. Vollmer et al. have used a photometrical method to determine 3-chloromuconate transformation based on an initial decrease in absorption during 3-chloromuconate turnover (169). Such a method introduces not only a high error into the determined kinetic data (Table 6). Furthermore, it can be reasoned, that the decrease in absorption during the initial turnover is not due to transformation of 3-chloromuconate into protoanemonin, but due to the intermediate formation of 4-chloromuconolactone. Similarly, a slight decrease in absorption was also observed during transformation of 3-chloromuconate by MCI of MT1, however, 4-chloromuconolactone formation could never be observed by HPLC, and the initial decrease was too insensitive to base an enzymatic test on it. The common opinion, that MCI transform 3-chloromuconate with only a minor side-activity has therefore to be reconsidered.

Similar to MCI of MT1, CatB transformed 3-chloromuconate to mainly protoanemonin (70 ± 8 %) and *cis*-dienelactone (17 ± 5 %). Again, all products were consistently formed over time .
When 3-chloromuconate (0.15 mM) was incubated with 15.6 mU/ml of PRS2000 derived CatB (determined with 0.1 mM muconate and corresponding to 1.24 nM CatB) and an excess of 190 mU/ml of *trans*-DLH of MT1 (determined with 0.05 mM *trans*-DLH, corresponding to 12.6 nM *trans*-DLH). 22 ± 4 % of the substrate were transformed to protoanemonin, 22 ± 2 % to *cis*-dienelactone and the rest (55 ± 5 %) to maleylacetate.
This experiment demonstrated successfully that the product formation from 3-chloromuconate transformation by a proteobacterial MCI is influenced by the concomitant action of MT1 *trans*-DLH. Thus, it can be assumed to be a general phenomenon that the presence of *trans*-DLH can shift the product formation from toxic protoanemonin to maleylacetate for any proteobacterial MCI.

3.5.4. *In-situ* transformation of 3-chloromuconate by combined action of MCIB of MT1 and *cis*-/*trans*-DLH of *Ralstonia eutropha* JMP134

Prevention of protoanemonin formation from 3-chloromuconate during muconate cycloisomerase catalyzed cycloisomerization by concomitant action of a *trans*-DLH, which is assumed to hydrolyze 4-chloromuconolactone to maleylacetate, has not been observed previously. However, Schlömann analyzed the transformation of 4-fluoromuconolactone as an intermediate in the degradation of 4-fluorobenzoate, and observed that both, *trans*-DLHs of *Ralstonia* strains, as well as *cis*-/*trans*-DLHs of the chlorocatechol pathway are capable to transform 4-fluoromuconolactone (133). Therefore it was investigated, whether *cis*-/*trans*-DLH of the chlorocatechol pathway, like *trans*-DLH of MT1, could act on 4-chloromuconolactone as the reaction intermediate of 3-chloromuconate transformation and prevent protoanemonin production. $TfdE_{I,}$ a *cis*-/*trans*-DLH which was partially purified from *R. eutropha* JMP222 (pBBR1MI) (107) was used for this purpose. Thus, 3-chloromuconate (0.1 mM) was incubated with MCIB (21 mU/ml determined with 0.1 mM 3-chloromuconate, corresponding to 3.5 nM MCIB) and $TfdE_I$ (62 mU/ml, determined with 0.1 mM *cis*-dienelactone which corresponds to about 90 mU/ml DLH determined with 0.1 mM *trans*-DL (137)). Substrate conversion was monitored over time by HPLC analysis and spectrophotometrical analysis.

In contrast to the previous experiment (see 3.5.2) where transformation of 3-chloromuconate by MCIB (53 mU/ml) and *trans*-DLH (65 mU/ml) resulted in the formation of significant amounts of maleylacetate (maleylacetate : protoanemonin = 0.45 : 1) addition of *cis*-/*trans*-DLH only lead to formation of maleylacetate resulting from cis-dienelactone transformation. Protoanemonin formation was not reduced. Therefore it can be assumed that the ability of *cis*-/*trans*-DLH $TfdE_I$ to transform the cycloisomerization intermediate 4-chloromuconolactone is at least not as pronounced as that of *trans*-DLH of MT1.

Brückmann et al. have shown that *cis*-/*trans*-DLH of *Pseudomonas* sp. B13 transforms protoanemonin to *cis*-acetylacrylate with 0.8 % of its activity with *cis*-dienelactone (14). Thus we determined whether $TfdE_I$ is also capable to transform protoanemonin. However, we could not detect any significant decrease in protoanemonin concentration and therefore can state that activity of $TfdE_I$ with 0.05 mM protoanemonin is < 0.10 % of its activity with 0.1 mM *cis*-dienelactone.

3.6. Quantification of the expression of MCI and MCIB during growth of *Pseudomonas* sp. strain MT1 on 5-chlorosalicylate and salicylate

Based on the observation that MCIB does not exhibit any significant activity against muconate (Table 6), it is evident, that activities against muconate observed in cell extracts are exclusively due to induction of MCI. In contrast, activities against 3-chloromuconate can be due to both, induction of MCI or MCIB.

In order to determine the activity of MCIB in cell extracts, both, the total activity against 0.1 mM 3-chloromuconate as well as the activity against 0.1 mM muconate were determined. The activities with muconate were 25 U/g and 350 U/g, respectively, in extracts of 5-chlorosalicylate or salicylate grown cells, respectively, showing a significant higher induction of MCI in salicylate grown cells. As the activity of MCI with 0.1 mM 3-chloromuconate is 3.5 fold that with 0.1 mM (see 3.4.1), it can be estimated that the 3-chloromuconate transforming activity of MCI in 5-chlorosalicylate and salicylate grown cells should account for 85 and 1200 U/g, respectively. As the experimentally determined activity with 3-chloromuconate in salicylate-grown cells (1080 U/g) does not exceed above the calculated value (1200 U/g) it can be assumed, that MCIB activity is negligible under these conditions. In contrast, a high activity of 350 U/g observed in chlorosalicylate grown cells cannot be explained by induction of MCI only, but suggest 265 U/g to be due to MCIB induction (Table 9). Thus it can be assumed that MCIB is of minor importance for 3-chloromuconate transformation in salicylate grown cells and that MCIB is induced during growth on 5-chlorosalicylate. When an extract of salicylate grown cells was applied to hydrophobic interaction chromatography, a method separating MCI and MCIB, only negligible activities of MCIB were observed, further evidencing, that this enzyme is specifically induced during growth on 5-chlorosalicylate.

Table 9. Specific activities of MCI and MCIB in cell extracts of *Pseudomonas* sp. strain MT1 grown on salicylate and 5-chlorosalicylate.

Growth substrate	Test substrate	Total activity measured (U/g)	Activity of MCI (U/g)	Activity of MCIB (U/g)
Salicylate	muconate	370	350	-
	3-chloromuconate	1080	1225	-
5-Chlorosalicylate	muconate	25	25	-
	3-chloromuconate	350	80	270

3.7. Maleylacetate reductase (MAR) of *Pseudomonas* sp. strain MT1

3.7.1 MAR and its side activity with *cis*-acetylacrylate

In cell extracts of MT1 grown on 5-chlorosalicylate or salicylate high activities against maleylacetate were detected, as well as significantly lower activities against *cis*-acetylacrylate. In both extracts the activity against *cis*-acetylacrylate corresponds to 4 – 5 % the activity with maleylacetate (at 0.05 mM concentration of the respective substrate). The capability to transform *cis*-acetylacrylate, the hydrolysis product of protoanemonin (14) was previously assumed to be an indication for a metabolic pathway of 4-chlorosalicylate degradation via protoanemonin (177). To analyze, if the activity against *cis*-acetylacrylate was due to cross-reactivity of MAR, an extract of 5-chlorosalicylate grown cell was fractioned by ion exchange chromatography. In fact, both activities co-eluted, and the activity against *cis*-acetylacrylate in the partially purified fractions remained 4 % of the activity with maleylacetate. (Table 10). Thus, it can be assumed that MAR was responsible for transformation of both compounds. This assumption was feasible, as *cis*-acetylacrylate resembles maleylacetate structurally apart from the missing carboxyl group (Fig. 16 A). In contrast to MAR of MT1, $TfdF_I$ MAR from *R. eutropha* JMP134 showed only negligible activity with *cis*-acetylacrylate (Table 10).

Table 10. Activities in cell extracts and of partially purified maleylacetate reductases against maleylacetate, *cis*- and *trans*-acetylacrylate.

Substrate	**Cell extract**		**Partially purified maleylacetate reductase**	
	MT1 salicylate grown	**MT1 5-chlorosalicylate grown**	**MT1 5-chlorosalicylate grown**	**$TfdF_I$**
maleylacetate	100 %	100 %	100 %	100 %
cis-acetylacrylate	4 ± 1 %	3 ± 1 %	4 ± 1 %	0.3 ± %
trans-acetylacrylate	< 1 %	< 1 %	< 1 %	< 1 %

[a] From *Ralstonia eutropha* JMP 222 (pBBR1MI) 3-chlorobenzoate grown.

The applied photometrical test for determining MAR activity is based on measuring NADH oxidation over time. White-Stevens et al. had shown for salicylate hydroxylases that certain substrate analogues uncouple NADH oxidation from substrate reduction (174, 175). In order to exclude such an uncoupling to occur during incubation with *cis*-acetylacrylate, and to proof *cis*-acetylacrylate to be a substrate for MAR, transformations were followed in parallel by HPLC and photometrical analysis. It could be demonstrated that the decrease of *cis*-acetylacrylate was stoichiometric to NADH oxidation and uncoupling was negligible.

As MAR of MT1 seemed to be special in terms of *cis*-acetylacrylate transformation, the kinetic parameters of transformation of both *cis*-acetylacrylate and maleylacetate were determined. Transformation of *cis*-acetylacrylate followed typical Michaelis-Menten kinetics and a K_m of 640 ± 135 µM was calculated.

In contrast, maleylacetate transformation did not follow typical Michaelis-Menten kinetics. The curve could be fitted to a polynomial expression, earlier used for describing enzyme kinetics affected by substrate inhibition (2, 56). A K_m value of 22 ± 5 µM and a K_{SS} value (substrate inhibition constant) of 290 ± 110 µM were determined.

As MAR was not purified to homogeneity, k_{cat} values for maleylacetate or *cis*-acetylacrylate transformation could not be compared. However, comparison of V_{max} values of partially purified MAR showed maximal turnover rates of *cis*-acetylacrylate to be 38 % those of maleylacetate.

3.7.2. *In-situ* NMR-analysis of *cis*-acetylacrylate transformation

In analogy to maleylacetate reduction by MAR, the product of *cis*-acetylacrylate transformation by MAR was assumed to be laevulinate. For identification of the product, transformation of *cis*-acetylacrylate (1 mM) was followed in the presence of 1 mM NADH by ^{1}H-NMR. *cis*-Acetylacrylate exhibited signals at δ=2.35 ppm (methylfunction), δ=6.17 ppm and δ=6.52 ppm (olefinic protons) (Fig. 10 A).

Upon addition of MAR (5 U/ml, determined with 0.05 mM *cis*-acetylacrylate) transformation of *cis*-acetylacrylate was monitored over time (Fig. 16 A, B, C). Samples of NADH and NAD^+ were measured under identical conditions as references, such that the signals of all substrates and products of the reaction could be identified. A buffer concentration of 5 mM was chosen in order to keep the signals of the organic buffer (TRIZMA®BASE, Sigma (Tris[hydroxymethyl]-aminomethane)) low. However, during the reaction, the pH decreased from 7.5 to 3.6. Chemical shifts of signals not arising from NADH or NAD and thus due to the reduction product formed from *cis*-acetylacrylate were detected at δ=2.27 ppm, δ=2.64 ppm (^3J=17.2 Hz) and δ=2.92 ppm (^3J=17.2 Hz), respectively. The chemical shifts and the high coupling constants were indicative for the formation of a product with one methyl and two neighbored methylene groups (Fig. 16 F). Identical signals were observed when laevulinate was measured at pH 3.6 (Fig. 16 E). When the pH was readjusted to neutral conditions (pH 7.0), the signals of the two methylene groups of the reaction product shifted to δ=2.48 ppm (coupling constant ^3J=13.8 Hz) and δ=2.82 ppm (^3J=13.8 Hz).

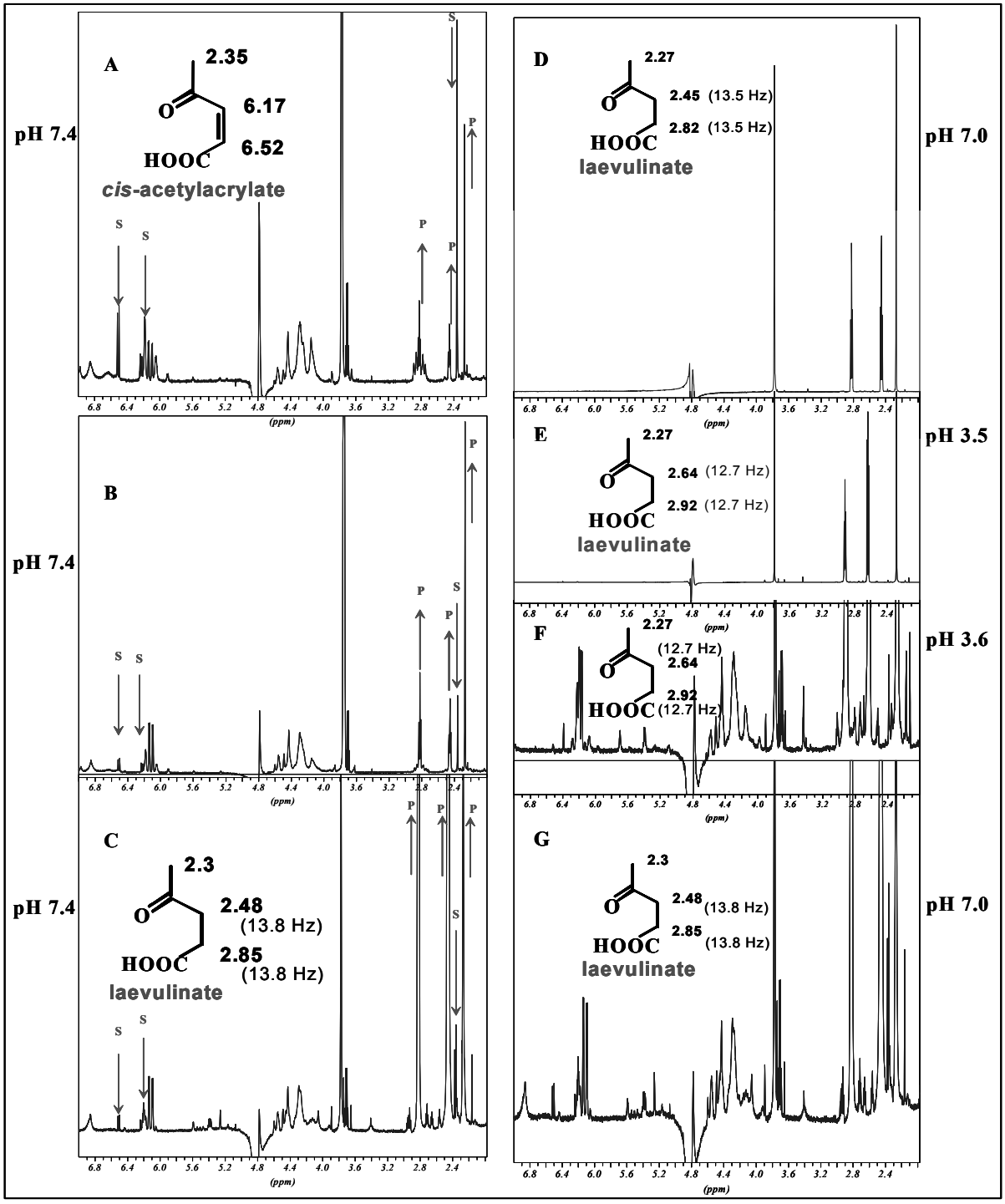

Figure 16: Transformation of *cis*-acetylacrylate by partially purified MAR of *Pseudomonas* sp. strain MT1. *cis*-Acetylacrylate (1 mM) was incubated in the presence of maleylacetate reductase (5 U/ml) and NADH (1 mM). Transformation was monitored over time (**A**: 3 h; **B**: 5.3 h; **C**: 20 h). If necessary the pH was manually adjusted to pH 7.4. Arrows pointing downwards indicate peaks of the substrate (S), *cis*-acetylacrylate; arrows pointing upwards indicate peaks arising due to product (P) formed. All other signals were due to the presence of NAD, NADH or D_2O. Standards of laevulinic acid were measured at pH 7.0 (**D**) and pH 3.5 (**E**). *cis*-Acetylacrylate after incubation with maleylacetate reductase and NADH for ca. 20 h at pH 3.6 (**F**) and after re-adjusting the pH to 7.0 (**G**). Chemical shifts of protons are given in ppm, coupling constants in brackets in Hz.

(Fig. 16 C and G), respectively. The resonance line of the methylfunction was not influenced by the pH. Similarly, the pH influenced the chemical shifts of the methylene groups of a laevulinate standard. At pH 7.0 (Fig. 16 D) signals at δ=2.27 ppm, δ=2.45 ppm (^3J=13.5 Hz) and δ=2.82 ppm (^3J=13.5 Hz) were observed. Thus, the product formed from *cis*-acetylacrylate and laevulinate showed identical NMR spectra and the product of *cis*-acetylacrylate reduction by MAR was identified as laevulinate.

3.8. Genetic approach to identify gene sequences encoding key enzymes of the novel pathway

The novel pathway for 4-chlorocatechol degradation by MT1 comprises enzymes known to be involved in the degradation of natural occurring aromatic compounds. However, the pathway specifically contains two distinct cycloisomerases and a *trans*-DLH. One cycloisomerase (MCI), from the product spectrum, is obviously highly related to proteobacterial MCIs, of the classical 3-oxoadiate pathway for degradation of aromatics. The second cycloisomerase (MCIB), according to its product spectrum, seems to be intermediary to muconate and chloromuconate cycloisomerases. The *trans*-DLH resembles catalytical enzymes previously described in cell extracts of 4-fluorobenzoate degrading *Ralstonia* strains (137). Concomitant action of *trans*-DLH with one or the other cycloisomerase prevents the formation of the metabolic dead-end product protoanemonin which is formed when microorganisms harboring the wide-spread 3-oxoadipate pathway are confronted with 4-chlorocatechol. In order to clarify if the novel pathway is a physiological patchwork of enzymes encoded by genes in different operons or if it constitutes a novel genetic unit, part of this thesis project was aimed at the genetic description of the novel pathway. The genes encoding the three above mentioned key enzymes were attempted to be identified by PCR with degenerated primers derived from N-terminal and inner protein sequences and then to be localized.

3.8.1 Gene encoding muconate cycloisomerase (MCI)

3.8.1.1 Sequencing of MCI

PCR with primers N-term2 and Is D1 (Table 11) and DNA of MT1 as template amplified a 480 bp fragment which was visualized as dominant band on agarose gels (Fig. 17).

Table 11. Amino acid sequences of the N-terminal and an internal tryptic peptide of *Pseudomonas* sp. strain MT1 muconate cycloisomerase (MCI) used for the development of degenerated primers. Peptide sequences underlined were used for the primer design.

Peptide	Amino acid sequence	Name and sequence of degenerated primers
N-terminal	TQAKIESIETILVDLPTVRPHKLAM	N-term1 GCAARATCGARWSCATCGA
	TQAKIESIETILVDLPTVRPHKLAM	N-term2 GCATCGARACYATCCTDGTDGA
	TQAKIESIETILVDLPTVRPHKLAM	N-term4 CCNCAYAARCTDGCNATG
Is d	DLAEAEHFLDVR	IS-D1 GARCAYTTYCTDGAYGTGC

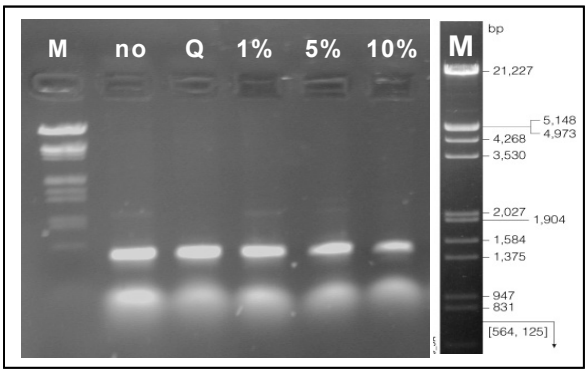

Figure 17. PCR-amplification of a 480 bp gene fragment encoding part of the MCI gene using primers N-term2 and Is D1 and MT1 DNA as template. PCR reactions were performed with no additives (no), 1 x Q-solution (Q) or DMSO at different final concentrations (1 %), (5 %), (10 %). Agarose gel loaded with PCR amplifications and λ DNA digested with *Hind*III and *Eco*RI as molecular weight marker (M).

The extracted 480 bp fragment was cloned into pCR®4-TOPO and successful cloning was confirmed by plasmid extraction and excision of a 480 bp fragment with EcoRI restriction. PCR with the plasmid as template and the plasmid specific primers M13-F and M13-R (Invitrogen, Carlsbad, CA, USA) annealing adjacent to both sides of the insertion site resulted, as expected, in a ca. 650 bp amplification product. PCR with M13-F and N-term2 primers gave an amplification product of 560 bp, whereas PCR with M13-R and N-term2 primers failed to give amplification. This indicated that the MCI fragment was cloned with its N-terminal part adjacent to the M13-R site. The fragment was sequenced in both directions directly from the plasmid using M13-F and M13-R-primers. The obtained sequences were of high quality and allowed to recognize nucleotides of the plasmid and the earlier used protein deduced primers. The sequence was translated into protein sequence and complemented by amino acids identified by N-terminal protein sequencing to proceed the primer binding site. For further investigations residue 7 was defined as serine as

determined by N-terminal sequencing, though DNA sequencing had indicated a cysteine instead. Database searches with that sequence using blastp showed highest homology to CatB of *Pseudomonas putida* CA10 (77 % identities, 88 % similarities), as already observed when the N-terminal sequence was compared with sequences from databases. High similarities were also detected with various other muconate cycloisomerases. (CatB of *P. putida* KT2440, CatB of *P. putida* PRS2000 and CatB of *P. putida* SM25 (72 % identities, 87 % similarities) and CatB *P. putida* P111 and *P. aeruginosa* PAO1 (69 % identities, 86 % similarities)). CatB of *Pseudomonas* sp. MT1 shared less than 42 % identities and 62 % similarities with protein sequences of CMCI.

3.8.1.2 Sequence alignment of MCI from MT1 with other (chloro)muconate cycloisomerases

The phylogenetic tree of selected MCI and CMCI protein sequences demonstrates their relation in terms of homology (Fig. 19). MCI of *Pseudomonas* sp. strain MT1 clustered with CatBs of other Pseudomonads. CMCIs of proteobacteria formed a cluster distinct from that of proteobacterial MCIs. Interestingly CMCI ($TfdD_{II}$) of *Ralstonia eutropha* JMP134 encoded on the degradative plasmid pJP4 could not be certainly assigned to the muconate or chloromuconate cycloisomerase cluster (bootstrap value only 53 out of 100), but was positioned between the two clusters.

Both MCI and CMCI of *Rhodococcus opacus* 1CP did not cluster with any of the cycloisomerases of the proteobacteria indicating that those cycloisomerases of gram-positive and gram-negative bacteria evolved by functionally convergent evolution (34, 151).

MCI of *Pseudomonas* sp. strain MT1 in contrast to all other proteobacterial MCI in the alignment carried instead of an isoleucine (I) a valine (V) at position 53 (numbering according to MCI sequence of MT1). All proteobacterial CMCI in the alignment had a valine at the respective position (except for $TfdD_{II}$ of *R. eutropha* JMP134 carrying a proline (P)). Vollmer et al. had created mutants of MCI of *P. putida* PRS2000 which they speculated to have increased transformation rates with 3-chloromuconate (169). According to their experiments, exchange of the above mentioned isoleucine with valine in mutant I54V lead to an increased k_{cat} and increased affinity for 3-chloromuconate. According to our experiments (see chapter 3.8.1.3 Table 12) we assumed that the amino acid exchanges did not effect the rate of protoanemonin, but of 4-chloromuconolactone formation. We further speculated that MCI of MT1 might have an increased 4-chloromuconolactone formation rate, because it carries a valine instead of an isoleucine.

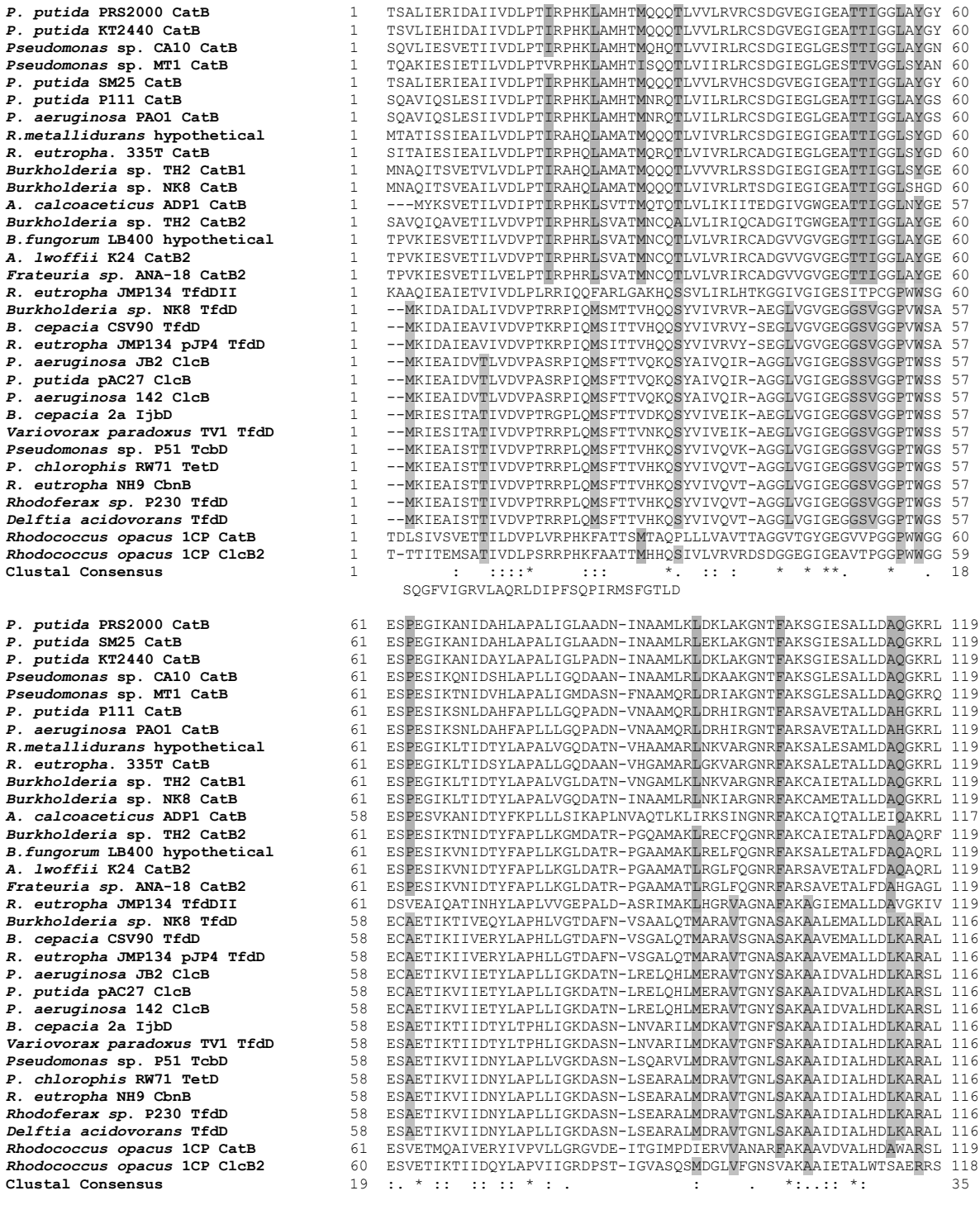
P. putida PRS2000 CatB 1 TSALIERIDAIIVDLPTIRPHKLAMHTMQQQTLVVLRVRCSDGVEGIGEATTIGGLAYGY 60
P. putida KT2440 CatB 1 TSVLIEHIDAIIVDLPTIRPHKLAMHTMQQQTLVVLRLRCSDGVEGIGEATTIGGLAYGY 60
Pseudomonas sp. CA10 CatB 1 SQVLIESVETIIVDLPTIRPHKLAMHTMQHQTLVVIRLRCSDGIEGLGESTTIGGLAYGN 60
Pseudomonas sp. MT1 CatB 1 TQAKIESIETILVDLPTVRPHKLAMHTISQQTLVIIRLRCSDGIEGLGESTTVGGLSYAN 60
P. putida SM25 CatB 1 TSALIERIEAIIVDLPTIRPHKLAMHTMQQQTLVVLRVHCSDGVEGIGEATTIGGLAYGY 60
P. putida P111 CatB 1 SQAVIQSLESIIVDLPTIRPHKLAMHTMNRQTLVILRLRCSDGIEGLGEATTIGGLAYGS 60
P. aeruginosa PAO1 CatB 1 SQAVIQSLESIIVDLPTIRPHKLAMHTMNRQTLVILRLRCSDGIEGLGEATTIGGLAYGS 60
R.metallidurans hypothetical 1 MTATISSIEAILVDLPTIRAHQLAMATMQQQTLVIVRLRCSDGIEGIGEATTIGGLSYGD 60
R. eutropha. 335T CatB 1 SITAIESIEAILVDLPTIRPHQLAMATMQRQTLVIVRLRCADGIEGLGEATTIGGLSYGD 60
Burkholderia sp. TH2 CatB1 1 MNAQITSVETVLVDLPTIRAHQLAMATMQQQTLVVVRLRSSDGIEGIGEATTIGGLSYGE 60
Burkholderia sp. NK8 CatB 1 MNAQITSVEAILVDLPTIRAHQLAMATMQQQTLVIVRLRTSDGIEGIGEATTIGGLSHGD 60
A. calcoaceticus ADP1 CatB 1 ---MYKSVETILVDIPTIRPHKLSVTTMQTQTLVLIKIITEDGIVGWGEATTIGGLNYGE 57
Burkholderia sp. TH2 CatB2 1 SAVQIQAVETILVDVPTIRPHRLSVATMNCQALVLIRIQCADGITGWGEATTIGGLAYGE 60
B.fungorum LB400 hypothetical 1 TPVKIESVETILVDVPTIRPHRLSVATMNCQTLVLVRIRCADGVVGVGEGTTIGGLAYGE 60
A. lwoffii K24 CatB2 1 TPVKIESVETILVDVPTIRPHRLSVATMNCQTLVLVRIRCADGVVGVGEGTTIGGLAYGE 60
Frateuria sp. ANA-18 CatB2 1 TPVKIESVETILVELPTIRPHRLSVATMNCQTLVLVRIRCADGVVGVGEGTTIGGLAYGE 60
R. eutropha JMP134 TfdDII 1 KAAQIEAIETVIVDLPLRRIQQFARLGAKHQSSVLIRLHTKGGIVGIGESITPCGPWWSG 60
Burkholderia sp. NK8 TfdD 1 --MKIDAIDALIVDVPTRRPIQMSMTTVHQQSYVIVRVR-AEGLVGVGEGGSVGGPVWSA 57
B. cepacia CSV90 TfdD 1 --MKIDAIEAVIVDVPTKRPIQMSITTVHQQSYVIVRVY-SEGLVGVGEGGSVGGPVWSA 57
R. eutropha JMP134 pJP4 TfdD 1 --MKIDAIEAVIVDVPTKRPIQMSITTVHQQSYVIVRVY-SEGLVGVGEGGSVGGPVWSA 57
P. aeruginosa JB2 ClcB 1 --MKIEAIDVTLVDVPASRPIQMSFTTVQKQSYAIVQIR-AGGLVGIGEGSSVGGPTWSS 57
P. putida pAC27 ClcB 1 --MKIEAIDVTLVDVPASRPIQMSFTTVQKQSYAIVQIR-AGGLVGIGEGSSVGGPTWSS 57
P. aeruginosa 142 ClcB 1 --MKIEAIDVTLVDVPASRPIQMSFTTVQKQSYAIVQIR-AGGLVGIGEGSSVGGPTWSS 57
B. cepacia 2a IjbD 1 --MRIESITATIVDVPTRGPLQMSFTTVDKQSYVIVEIK-AEGLVGIGEGGSVGGPTWSS 57
Variovorax paradoxus TV1 TfdD 1 --MRIESITATIVDVPTRRPLQMSFTTVNKQSYVIVEIK-AEGLVGIGEGGSVGGPTWSS 57
Pseudomonas sp. P51 TcbD 1 --MKIEAISTTIVDVPTRRPLQMSFTTVHKQSYVIVQVK-AGGLVGIGEGGSVGGPTWGS 57
P. chlorophis RW71 TetD 1 --MKIEAISTTIVDVPTRRPLQMSFTTVHKQSYVIVQVT-AGGLVGIGEGGSVGGPTWGS 57
R. eutropha NH9 CbnB 1 --MKIEAISTTIVDVPTRRPLQMSFTTVHKQSYVIVQVT-AGGLVGIGEGGSVGGPTWGS 57
Rhodoferax sp. P230 TfdD 1 --MKIEAISTTIVDVPTRRPLQMSFTTVHKQSYVIVQVT-AGGLVGIGEGGSVGGPTWGS 57
Delftia acidovorans TfdD 1 --MKIEAISTTIVDVPTRRPLQMSFTTVHKQSYVIVQVT-AGGLVGIGEGGSVGGPTWGS 57
Rhodococcus opacus 1CP CatB 1 TDLSIVSVETTILDVPLVRPHKFATTSMTAQPLLLVAVTTAGGVTGYGEGVVPGGPWWGG 60
Rhodococcus opacus 1CP ClcB2 1 T-TTITEMSATIVDLPSRRPHKFAATTMHHQSIVLVRVRDSDGGEGIEAVTPGGPWWGG 59
Clustal Consensus 1 : :::* ::: *. :: : * * **. * . 18
SQGFVIGRVLAQRLDIPFSQPIRMSFGTLD
P. putida PRS2000 CatB 61 ESPEGIKANIDAHLAPALIGLAADN-INAAMLKLDKLAKGNTFAKSGIESALLDAQGKRL 119
P. putida SM25 CatB 61 ESPEGIKANIDAHLAPALIGLAADN-INAAMLRLEKLAKGNTFAKSGIESALLDAQGKRL 119
P. putida KT2440 CatB 61 ESPEGIKANIDAYLAPALIGLPADN-INAAMLKLDKLAKGNTFAKSGIESALLDAQGKRL 119
Pseudomonas sp. CA10 CatB 61 ESPESIKQNIDSHLAPLLIGQDAAN-INAAMLRLDKAAKGNTFAKSGLESALLDAQGKRL 119
Pseudomonas sp. MT1 CatB 61 ESPESIKTNIDVHLAPALIGMDASN-FNAAMQRLDRIAKGNTFAKSGLESALLDAQGKRQ 119
P. putida P111 CatB 61 ESPESIKSNLDAHFAPLLLGQPADN-VNAAMQRLDRHIRGNTFARSAVETALLDAHGKRL 119
P. aeruginosa PAO1 CatB 61 ESPESIKSNLDAHFAPLLLGQPADN-VNAAMQRLDRHIRGNTFARSAVETALLDAHGKRL 119
R.metallidurans hypothetical 61 ESPEGIKLTIDTYLAPALVGQDATN-VHAAMARLNKVARGNRFAKSALESAMLDAQGKRL 119
R. eutropha. 335T CatB 61 ESPEGIKLTIDSYLAPALLGQDAAN-VHGAMARLGKVARGNRFAKSALETALLDAQGKRL 119
Burkholderia sp. TH2 CatB1 61 ESPEGIKLTIDTYLAPALVGLDATN-VNGAMLKLNKVARGNRFAKCAIETALLDAQGKRL 119
Burkholderia sp. NK8 CatB 61 ESPEGIKLTIDTYLAPALVGQDATN-INAAMLRLNKIARGNRFAKCAMETALLDAQGKRL 119
A. calcoaceticus ADP1 CatB 58 ESPESVKANIDTYFKPLLLSIKAPLNVAQTLKLIRKSINGNRFAKCAIQTALLEIQAKRL 117
Burkholderia sp. TH2 CatB2 61 ESPESIKTNIDTYFAPLLKGMDATR-PGQAMAKLRECFQGNRFAKCAIETALFDAQAQRF 119
B.fungorum LB400 hypothetical 61 ESPESIKVNIDTYFAPLLKGLDATR-PGAAMAKLRELFQGNRFAKSALETALFDAQAQRL 119
A. lwoffii K24 CatB2 61 ESPESIKVNIDTYFAPLLKGLDATR-PGAAMATLRGLFQGNRFARSAVETALFDAQAQRL 119
Frateuria sp. ANA-18 CatB2 61 ESPESIKVNIDTYFAPLLKGLDATR-PGAAMATLRGLFQGNRFARSAVETALFDAHGAGL 119
R. eutropha JMP134 TfdDII 61 DSVEAIQATINHYLAPLVVGEPALD-ASRIMAKLHGRVAGNAFAKAGIEMALLDAVGKIV 119
Burkholderia sp. NK8 TfdD 58 ECAETIKTIVEQYLAPHLVGTDAFN-VSAALQTMARAVTGNASAKAALEMALLDLKARAL 116
B. cepacia CSV90 TfdD 58 ECAETIKIIVERYLAPHLLGTDAFN-VSGALQTMARAVSGNASAKAAVEMALLDLKARAL 116
R. eutropha JMP134 pJP4 TfdD 58 ECAETIKIIVERYLAPHLLGTDAFN-VSGALQTMARAVTGNASAKAAVEMALLDLKARAL 116
P. aeruginosa JB2 ClcB 58 ECAETIKVIIETYLAPLLIGKDATN-LRELQHLMERAVTGNYSAKAAIDVALHDLKARSL 116
P. putida pAC27 ClcB 58 ECAETIKVIIETYLAPLLIGKDATN-LRELQHLMERAVTGNYSAKAAIDVALHDLKARSL 116
P. aeruginosa 142 ClcB 58 ECAETIKVIIETYLAPLLIGKDATN-LRELQHLMERAVTGNYSAKAAIDVALHDLKARSL 116
B. cepacia 2a IjbD 58 ESAETIKTIIDTYLTPHLIGKDASN-LNVARILMDKAVTGNFSAKAAIDIALHDLKARAL 116
Variovorax paradoxus TV1 TfdD 58 ESAETIKTIIDTYLTPHLIGKDASN-LNVARILMDKAVTGNFSAKAAIDIALHDLKARAL 116
Pseudomonas sp. P51 TcbD 58 ESAETIKVIIDNYLAPLLVGKDASN-LSQARVLMDRAVTGNLSAKAAIDIALHDLKARAL 116
P. chlorophis RW71 TetD 58 ESAETIKVIIDNYLAPLLIGKDASN-LSEARALMDRAVTGNLSAKAAIDIALHDLKARAL 116
R. eutropha NH9 CbnB 58 ESAETIKVIIDNYLAPLLIGKDASN-LSEARALMDRAVTGNLSAKAAIDIALHDLKARAL 116
Rhodoferax sp. P230 TfdD 58 ESAETIKVIIDNYLAPLLIGKDASN-LSEARALMDRAVTGNLSAKAAIDIALHDLKARAL 116
Delftia acidovorans TfdD 58 ESAETIKVIIDNYLAPLLIGKDASN-LSEARALMDRAVTGNLSAKAAIDIALHDLKARAL 116
Rhodococcus opacus 1CP CatB 61 ESVETMQAIVERYIVPVLLGRGVDE-ITGIMPDIERVVANARFAKAAVDVALHDAWARSL 119
Rhodococcus opacus 1CP ClcB2 60 ESVETIKTIIDQYLAPVIIGRDPST-IGVASQSMDGLVFGNSVAKAAIETALWTSAERRS 118
Clustal Consensus 19 :. * :: :: :: * : . : . *:..:: *: 35

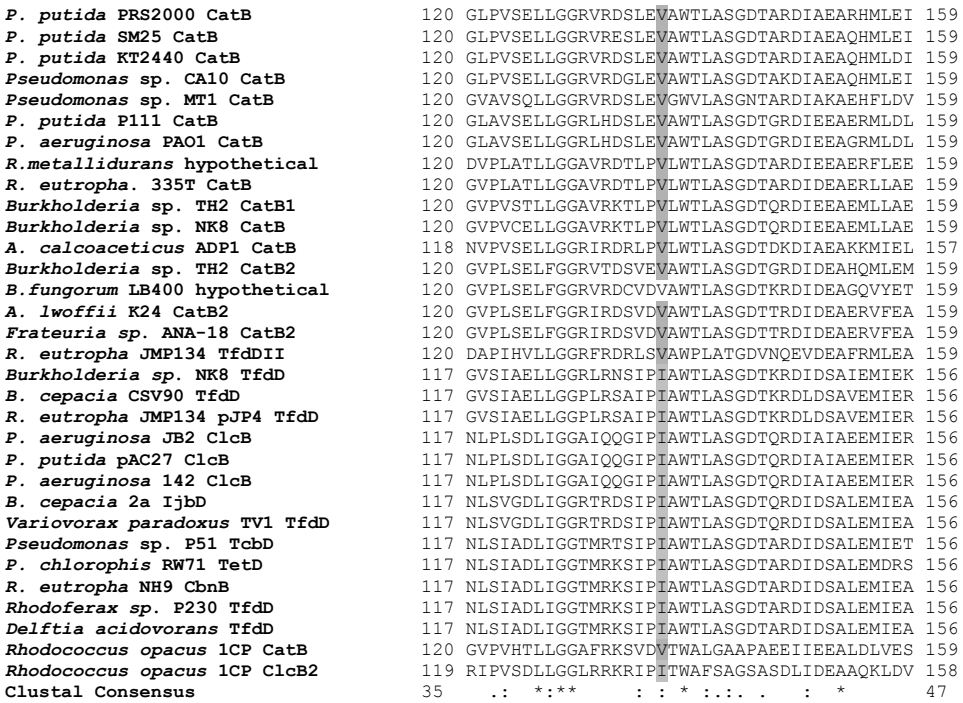

Figure 18: Alignment of protein sequences of muconate cycloisomerases (CatB), chloromuconate cycloisomerases (TfdD, ClcB, TetD, IjbD), TfdDII) and muconate cycloisomerase of *Pseudomonas* sp. strain MT1 based on CLUSTAL W alignment (159). Numbering of sequences are according to the sequence of muconate cycloisomerase of *Pseudomonas* sp. strain MT1. Amino acids conserved in muconate cycloisomerases are highlighted in light grey, those in chloromuconate cycloisomerases in and dark grey. Protein IDs are given in the tree in Figure 19.

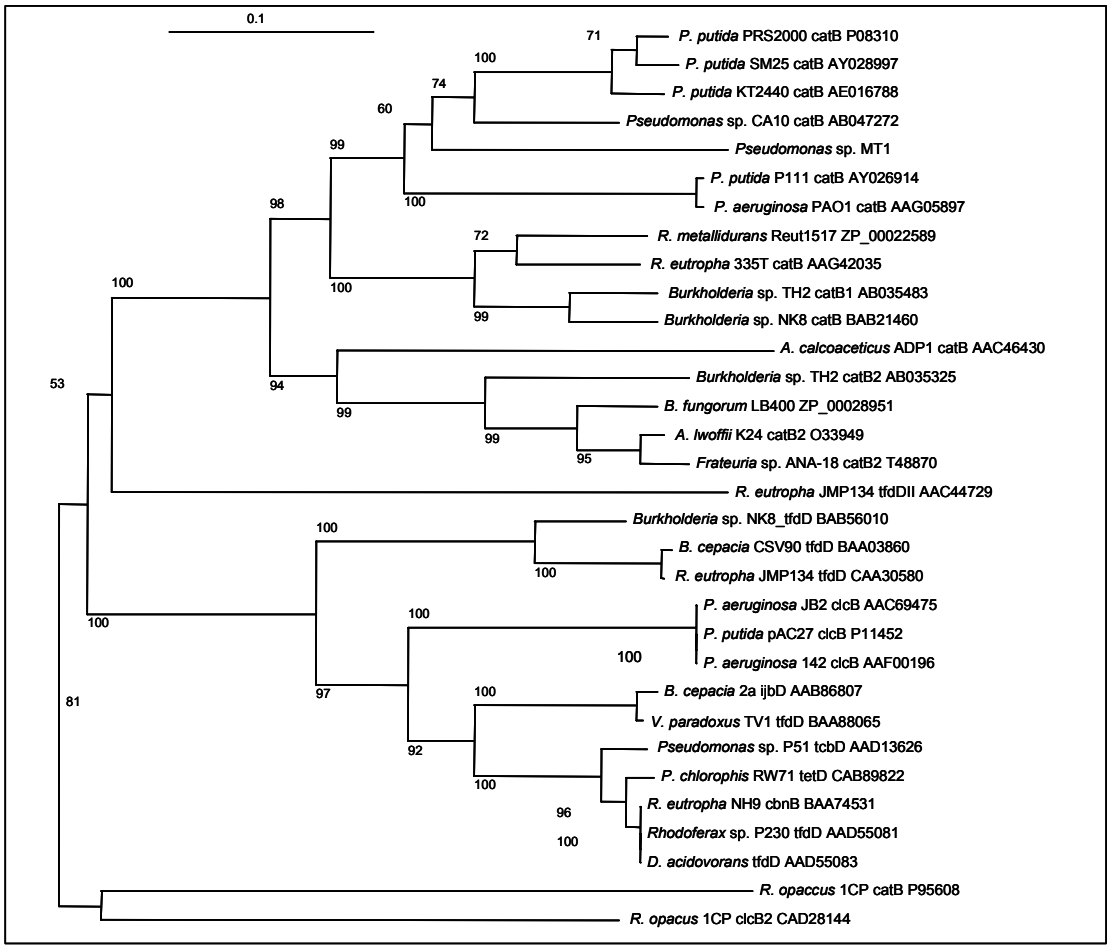

Figure 19: Phylogenetic tree of selected muconate and chloromuconate cycloisomerase protein sequences (indicated by abbreviated organism name, strain designation, name of gene and EMBL/GenBank/DDBJ gene accession number). Alignment of a 159 amino acid length block was performed with CLUSTAL W using default values (159). N-J phylogenetic tree was generated using the option available in CLUSTAL W program. Bootstrap values above 50 % from 1000 neighbour-joining trees are indicated to the left of the nodes. Bar represents 10 amino acid changes per 100 amino acids.

3.8.1.3. Muconate and 3-chloromuconate transformation rates by muconate cycloisomerases

Amino acids conserved throughout muconate cycloisomerases but distinct in chloromuconate cycloisomerases (marked in light grey in the alignment), and amino acids conserved throughout chloromuconate cycloisomerases, but distinct in muconate cycloisomerases (marked in dark grey) might indicate amino acids that are responsible for the functional differences between the two types of cycloisomerases (Fig. 18) (169). Various site-directed mutants of the *P. putida* PRS2000 muconate cycloisomerase have been designed by the authors and analyzed for functional changes compared to the wild-type. As described in chapter 3.4.1 MCI of *Pseudomonas sp*. strain MT1 exhibited a higher activity against 3-chloromuconate than against the unchlorinated muconate and a comparison of k_{cat}/K_m- values indicated 3-chloromuconate to be even the preferred substrate for this enzyme. Such a behavior was unexpected for a MCI, specifically as previous reports on the archetype MCI of *P. putida* PRS2000 according to the studies of Vollmer et al. indicated muconate to be converted with 590 fold the velocity observed with 3-chloromuconate at 0.1 mM substrate concentrations and with a k_{cat}/K_m value more than 1000-fold that of 3-chloromuconate, muconate was assumed to be the by far preferred substrate (169) (Table 6, 12). Even though careful HPLC analysis revealed CatB of PRS2000 to be more active on 3-chloromuconate than previously reported, activity on 0.11 mM muconate was still 30-fold higher than the activity on 3-chloromuconate, whereas MCI of MT1 exhibited higher activity on 3-chloromuconate compared to muconate (3.5.3).

Out of the mutants described by Vollmer et al. two mutants showed increased activities against 3-chloromuconate. In the I54V mutant the amino acid 54 (numbering according to protein sequence of MCI of PRS2000) was changed from Isoleucine to Valine (both nonpolar residues), in mutant A271S amino acid 271 was changed from nonpolar alanine to uncharged, but polar serine. Mutant I54V showed an increased affinity and turnover of 3-chloromuconate, whereas mutant A271S only had a remarkably increased k_{cat} compared to the wild type enzyme (Table 12). Remarkably, in contrast to all the other MCIs, but like the I54V mutants, MCI of MT1 carries a valine (V) at the respective position. As the obtained sequence of MCI of MT1 did not cover the full gene, we could not compare its sequence aligning with amino acid 271 of CatB of PRS2000.

Vollmer et al have used a questionable photometrical method to determine 3-chloromuconate transformation based on an initial decrease in absorption during 3-chloromuconate turnover (169) (3.5.3). Therefore, we re-evaluated the transformation rates of muconate and 3-chloromuconate at initial concentrations of 0.1 mM. The plasmids pCATB1, pCATB51 and pCATB54 (kindly provided from Schlömann and Kaschabeck) contained the wildtype gene *catB* of PRS2000, as well as the I54V and A271S mutated genes respectively. Enzymes were overexpressed in an *E. coli* BL21 derivative and formation of protoanemonin was evaluated by HPLC analysis as described above. Similar to the wild-type, both mutant enzymes converted 0.1 mM muconate with an activity 17 – 34 fold that with 0.1 mM 3-chloromuconate. Thus, according to our study the introduced point mutations did not lead to any significant increase in the transformation rate of 3-chloromuconate to protoanemonin compared to their ability to transform muconate.

Table 12. Relative activities of wildtype and mutant MCI with muconate and 3-chloromuconate at initial substrate concentrations of 0.1 mM.

Muconate cycloisomerases of	**Relative activity (activity with muconate : activity with 3-chloromuconate)**	
	this study	**calculated from Vollmer et al. (169)**
Pseudomonas sp. strain MT1	0.29 ± 0.09	
P. putida PRS2000 CATB1 (wildtype)	30 ± 5	590
P. putida PRS2000 CATB51 (I54V mutant)	34 ± 5	9.2
P. putida PRS2000 CATB54 (A271S mutant)	17 ± 5	15

3.8.2 PCR to amplify gene sequences encoding MCIB

PCR amplification with N-term3 and Is-D1 primers (Table 13) designed based on the determined MCIB protein sequence fragments, and MT1 DNA as template using an annealing temperature of 48° C resulted in amplification of a dominant fragment of about 700 bp. In order to get amounts of the fragment sufficient for sequencing, amplification was repeated in 20 tubes in parallel, which were then combined and purified by gel purification. 30 µg/ml fragment were sent for sequencing with the N-term3 and Is-D1 primers, but unfortunately, sequences obtained were of very poor quality. Therefore the fragment was reamplified and cloned into pCR®4-TOPO. Two clones (named Cyclo1 and Cyclo2) both showing the integration of a 700 bp fragment when the plasmids were restricted with *Eco*RI, were used for further analysis. The plasmid containing the Cyclo1 insert was sent for sequencing using the M13-F and M13-R primer sites located on the vector. The sequences obtained were of good quality and were reverse compliment to each other. Sequence analysis identified the M13 primers and a fragment of expected size inserted into the vectors cloning site. However, when the insert was investigated for sequences of the degenerated primers, which should have been right next to the cloning site, the Is-D1 primer was found in reverse complement at both sides of the insert whereas the N-term3 primer sequence could not be localized in the sequence. Control experiments revealed that the 700 bp fragment could be amplified from genomic DNA or plasmid DNA as template in the presence of primer Is-D1 only. Database searches with the obtained sequences showed 88 % identity with the hypothetical protein Pflu4482 of *P. fluorescens* and 79 % identity to the putative transcriptional regulator PP2884 of *P. putida* KT2440. It can be concluded, that the cloning was successful, but that the 700 bp fragment was not comprising MCIB encoding DNA sequence. Thus, the Is-D1 primer was not sufficiently specific.

Table 13. Amino acid sequences of the N-terminal and internal tryptic peptides of *Pseudomonas* sp. strain MT1 MCIB used for the development of degenerated primers. Peptide sequences underlined were used for the primer design.

Peptide	**Amino acid sequence**	**Name and sequence of degenerated primers**
N-terminal	SQGFVIGRVLAQRLDIPFSQPIRM SFGTLD	N-term3 ATGWSNTTYGGNACNYTNGA
Is d	MLFQENGGLEG	Is-D1 CGCCRCCRTTYTCYTG
Is c	TLSTGSEGGDLAEGER	
Is b	FGSGDPDAELLR	

3.8.3 PCR to amplify gene sequences encoding *trans*-DLH

A dominant 550 bp fragment could be amplified with the primers N-term2 and Is-C2 (designed based on known *trans*-DLH protein sequences of strain MT1, Table 14) and MT1 DNA as template. PCR-product at a concentration of 30 µg/ml was sent for direct sequencing. As only very poor quality sequences were obtained, the fragment was cloned as described above. The resulting plasmid contained an insert of the expected size when excised with EcoRI and control PCRs performed with genomic DNA and plasmid DNA as template using only one primer each demonstrated that the fragment was amplified only when both degenerated primers were present. The insert of the plasmid was sequenced using M13-F and M13-R primers. Detailed investigations of the obtained sequences allowed identification of sequences of the vector adjacent to the M13 primers and the cloning site, as well as sequences of both degenerated primers at the expected locations. However, the deduced amino acid sequence indicated amino acids adjacent to those used for primer design not matching information obtained by protein sequencing. Thus, even though both degenerative primers had annealed and lead to amplification of a 550 bp fragment in a preferred and reproducible manner, the amplified product does not comprise a part of the *trans*-DLH encoding gene. Database searches showed similarities ≥ 92 % and identities ≥ 77 % to genes encoding proteins of the HlyD family of secretion proteins like the multidrug/solvent RND membrane fusion protein of *P. putida* KT2440 (NP_743545) (92 % similarity), the efflux transporter of *Pseudomonas syringae* (NP_794059) (92 % similarity), the multidrug efflux membrane fusion protein MexA precursor of *P. aeruginosa* PAO1 (NP_249116) (85 % similarity).

Table 14. Amino acid sequences of the N-terminal and internal tryptic peptides of *Pseudomonas* sp. strain MT1 *trans*-DLH used for the development of degenerated primers. Peptide sequences underlined were used for the primer design.

Peptide	Amino acid sequence	Name and sequence of degenerated primers
N-terminal	TDTSKSLPTYKQLLERKDAPPGS SWGLFGK	N-term2 GCCTDCCDACYTAYAARCARCT
Is c	VSQGVTLEPGDAVLLR	Is-C2 GGYTCHAGRGTHACRCCYTG
Is d	AFSLDLLATSLYALLAGPSL	
Is e	KLDLDAGASGKALSAKVLEAAR	
Is f	VDVNGAYSVDEAQALR	

3.8.4 Southern Blot analysis of *Pseudomonas* sp. strain MT1 DNA for the presence of muconate cycloisomerase encoding genes

About 600 ng of the 480 bp fragment comprising part of the MCI gene were used as template for DIG labeling according to the protocol of DIG DNA Labeling & Detection Kit (Boehringer Mannheim, Germany). The labeled probe was hybridized with genomic DNA restricted with four distinct restriction enzymes, respectively. In each case strong hybridization with two DNA fragments was observed. As the genome had been restricted at different recognition sites, the possibility that the two bands resulted from hybridization of the probe to a part of the MCI gene, localized on two restriction fragments is rather improbable. It can thus be assumed, that the probe not only hybridized to the MCI gene sequence, but also to a highly homologous sequence present on the genome. As biochemical experiments had shown the presence of a second cycloisomerase MCIB of unknown similarity to MCI in MT1, it can be reasoned that hybridization to a second gene fragment is due to high similarity of MCIB in the tested fragment (Fig. 20).

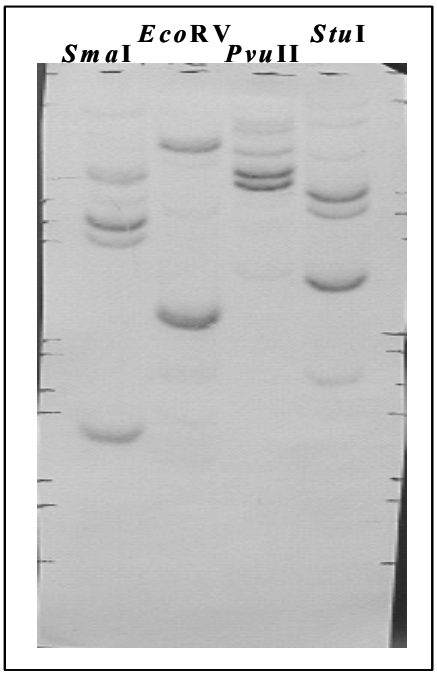

Figure 20: Southern blot analysis of *Pseudomonas* sp. strain MT1 genome. Probe of MCI was hybridized to genomic DNA of MT1 digested with *Sma*I, *Eco*RV, *Pvu*II and *Stu*I. On the right and on the left bands of λ *Hind*III, *Eco*RI as genomic markers are indicated.

4. DISCUSSION

4.1 The upper pathway

Salicylate degradation can be initiated by either a salicylate 1-hydroxylase yielding catechol (50) or a salicylate 5-hydroxylase yielding gentisate (27, 47, 186). Whereas degradative routes involving chlorocatechols produced by 1-hydroxylation of salicylate have been described (82, 127), knowledge on the degradation of chlorogentisates is limited (172). However, in the present study degradation of salicylate and chlorosalicylates by MT1 via a chlorogentisate pathway can be excluded for various reasons. First, only catechol intradiol cleavage but no gentisate ring-cleavage activity was observed. Secondly, transformation of 3-chlorosalicylate results in the formation of 3-chlorocatechol, evidencing the presence of a salicylate 1-hydroxylase activity in MT1. Slow transformation of 3-chlorocatechol by catechol 1,2-dioxygenase results in the formation of 2-chloromuconate. The nearly quantitative accumulation of 3-chlorocatechol plus 2-chloromuconate from 3-chlorosalicylate shows, that no 5-hydroxylating activity against this substrate is present. Third, during the transformation of 4- and 5-chlorosalicylate, 4-chlorocatechol, 3-chloromuconate and maleylacetate were formed as intermediates. All those compounds can only be formed assuming a salicylate 1-hyroxylating activity and a catechol intradiol cleavage pathway.

4.2 Degradation downstream of 4-chlorocatechol

The aerobic degradation of chlorocatechols was until recently assumed to occur exclusively by enzymes of the chlorocatechol pathway involving chlorocatechol dioxygenase, chloromuconate cycloisomerase, dienelactone hydrolase, and maleylacetate reductase. However, recent studies have indicated that bacterial routes for channeling chlorocatechol into central metabolic pathways are more divers than previously thought. In 1995, Arensdorf and Focht (3) described the degradation of 4-chlorobenzoate via 4-chlorocatechol and a *meta*-cleavage pathway, and similarly, Hollender et al. (61) proposed the degradation of 4-chlorophenol via *meta*-cleavage of 4-chlorocatechol to occur in a *Comamonas* isolate. *Pseudomonas putida* GJ31 grows on chlorobenzene via *meta*-cleavage of 3-chlorocatechol (86). Another route of 3-chlorocatechol degradation has recently been reported for *Rhodococcus opacus* (91). It comprises, like all metabolic routes involving cleavage of chlorocatechols described so far, a special chlorocatechol dioxygenase with high activity against chlorocatechols (124). Chlorocatechol dioxygenases have thus far mainly been characterized from proteobacteria, and usually have similar relative maximal activities with catechol, 3-chloro- as well as 4-chlorocatechol (13). A similar specificity profile was observed for chlorocatechol 1,2-

dioxygenase ClcA2 involved in 2-chlorophenol degradation by *Rhodococcus opacus* 1CP (89, 91). The only chlorocatechol dioxygenase differing in substrate specificity from above mentioned chlorocatechol dioxygenases is chlorocatechol dioxygenase ClcA1 of *Rhodococcus opacus* 1CP involved in 4-chlorophenol degradation, which exhibits similar maximal turnover rates for catechol and 4-chlorocatechol, but only 15 % of that activity with 3-chlorocatechol (84). In contrast to all chlorocatechol 1,2-dioxygenases described above, proteobacterial catechol dioxygenases are characterized by a very restricted substrate specificity and V_{max} values with 4-chlorocatechol are usually in the range of 10 % that with catechol (13), and activity with 3-chlorocatechol is negligible (< 1 %, see (13)).

The relative activities with catechol, 4-chloro- and 3-chlorocatechol and the absence of any significant 3-chlorocatechol transforming activity are thus indicative for the induction of catechol 1,2-dioxygenase activity only, independent whether MT1 was growing on salicylate or chlorosalicylate. The negligible activity against 3-chlorocatechol is also the major reason for the failure of MT1 to grow on 3-chlorosalicylate.

MT1 is thus obviously the first organism to be described capable to mineralize chloroaromatics via chlorocatechols in the absence of a specialized chlorocatechol dioxygenase. Such a capability is even more astonishing, as it was recently reported, that chlorocatechol ring-cleavage is a pathway bottleneck even in microorganisms harboring chlorocatechol genes. It has been shown that introduction of single copies of chlorocatechol genes into microorganisms capable to transform chloroaromatics into chlorocatechols is not sufficient to allow mineralization (75, 107). Later on it was proven, that accumulation of chlorocatechols impairs the growth of derivatives harboring single chlorocatechol gene copies and introduction of multiple copies of a chlorocatechol dioxygenase gene, and the consequent high expression of chlorocatechol 1,2-dioxygenase eliminated chlorocatechol accumulation and resulted in fast growing derivatives (108). Those results indicated that mineralization of chloroaromatics necessitates a delicate balance between chlorocatechol producing and chlorocatechol transforming activities. Therefore, the level of chlorocatechol transforming activities necessary to achieve growth depends significantly on the activity of peripheral enzymes. The above mentioned experiments have been performed using 3-chlorobenzoate as model substrate. In case of chlorobenzene degradation it has been observed, that both peripheral enzymes (chlorobenzene dioxygenase and chlorobenzene dihydrodiol dehydrogenase) and chlorocatechol pathway enzymes are localized on the same catabolic plasmid (115, 165) and thus present in the same “gene dosage” inside the cell allowing growth. However,

the recruitment of catechol dioxygenase(s) for growth of MT1 on 4- and 5-chlorosalicylate easily explains the observed failure to grow on high concentrations of substrates (106), which was observed to result in the accumulation of chlorocatechol and cell death.

Similarly, in the absence of a specialized chlorocatechol 1,2-dioxygenase (13), the presence of a typical proteobacterial chloromuconate cycloisomerase (usually active on 2-chloromuconate) (116, 139, 150, 170) and of a *cis*-/*trans*-DLH (highly active on both *cis*- and *trans*-dienelactone) (85, 95, 132, 133, 136, 137) were excluded as cell extracts showed no activity with 2-chloromuconate or *cis*-dienelactone. In contrast, the high activity with muconate indicated the expression of a muconate cycloisomerase involved in the 3-oxoadipate pathway.

Protoanemonin, a highly toxic intermediate, was recently shown to be the dominant product formed from 3-chloromuconate by such muconate cycloisomerases (8). As in *Pseudomonas* sp. strain MT1 (as well as *Pseudomonas sp.* strain RW10), only enzymes of the 3-oxoadipate pathway have been observed and it has been suggested, that those organisms harbor a new route of 4-chlorocatechol degradation via protoanemonin as intermediate (106, 177). However, in none of these organisms, any protoanemonin hydrolyzing activity to form the postulated pathway intermediate *cis*-acetylacrylate could be observed (14, 177, this study).

When 4-chlorocatechol or the pathway intermediate 3-chloromuconate was incubated with cell extract, the substrates were transformed stoichiometrically into *cis*-dienelactone, protoanemonin and, surprisingly, maleylacetate.

Thus, it was obvious that 3-chloromuconate is a central intermediate of the catabolic route in MT1 from where the carbon flow is directed into *cis*-dienelactone, protoanemonin and maleylacetate. Only negligible activities with *cis*-dienelactone and protoanemonin were observed in either cell extracts or by whole cells, indicating *cis*-dienelactone and protoanemonin to be dead-end products of the pathway and therefore most likely to be leaking quantitatively out of the cells (10 ± 5 % *cis*-dienelactone). The actual amount of protoanemonin formed will be higher than the one detected in the supernatant of culture (7 ± 5 %) as protoanemonin was reported to be relatively unstable even under physiological conditions (8).

Therefore, maleylacetate is the dominant metabolite downstream of 3-chloromuconate which can be reduced by the highly expressed MAR. However, transformation of 3-chloromuconate to maleylacetate had to be elucidated and constitutes the core of the novel 4-chlorocatechol degradative pathway.

4.3 The new *ortho*-cleavage pathway of 4-chlorocatechol to maleylacetate

In the present investigation it is shown that the amount of protoanemonin formed from 3-chloromuconate depends on whether single purified cycloisomerases or combinations of enzymes are used for conversion. 3-Chloromuconate conversion by a purified muconate cycloisomerase of *Pseudomonas* sp. strain MT1 resulted in high concentrations of protoanemonin as shown for muconate cycloisomerases from *Pseudomonas* sp. strain B13 or RW10 (8). Simultaneous presence of MCI and *trans*-DLH of MT1, in contrast, yielded considerably smaller protoanemonin concentrations, but higher amounts of maleylacetate and thus, protoanemonin has to be considered not to be the major intermediate of the degradative pathway. Most interestingly, like MT1, also *Pseudomonas* sp. strain RW10 does not form quantitative amounts of protoanemonin when a cell-free extract of chlorosalicylate-grown cells is exposed to 4-chlorocatechol (8) indicating that protoanemonin is not the only product.

4.3.1 Mechanism of cycloisomerization

Schmidt et al. have been the first ones to describe differences between muconate cycloisomerases involved in the 3-oxoadipate pathway and chloromuconate cycloisomerases of the chlorocatechol pathway. They postulated that the analyzed enzymes, derived from *Pseudomonas* sp. B13 differ from one another only by their substrate specificity, with chloromuconate cycloisomerases having an increased activity with chlorosubstituted muconates. They assumed that both muconate and chloromuconate cycloisomerases transform 2-chloro- and 3-chloromuconate, however at different rates, to 5-chloro- and 4-chloromuconolactone, respectively and that those muconolactones dehalogenate spontaneously to *trans*- and *cis*-dienenlactone, respectively. However, doubts on the spontaneous nature of dehalogenation arose when 5-chloro-3-methylmuconolactone, formed from 2-chloro-4-methylmuconate, was reported as a stable compound, even under physiological conditions (113). A year later Vollmer et al. demonstrated the inability of MCI to cause dehalogenation during conversion of 2-chloromuconate. The authors showed that MCI instead catalyze the formation of an equilibrium between 2-chloromuconate and 2-chloro- and 5-chloromuconolactone and proposed that chloromuconate cycloiomerases in contrast to muconate cycloisomerases have evolved the capability to cleave the carbon chloride bond (168). Thus dehalogenation of 5-chloromuconolactone was evidenced to be an enzymatic reaction.

Short time after, Blasco et al. observed that not *cis*-dienelactone, but protoanemonin is the product of 3-chloromuconate transformation by muconate cycloisomerases (8). Therefore they postulated that during 3-chloromuconate transformation muconate and chloromuconate cycloiosmerases catalyze different reactions and they postulated 4-chloromuconolactone as a common intermediate of both reactions. For chloromuconate cycloisomerases they postulated an active site which catalyzes fast elimination of the solvent-derived C5-proton and of the halide, thus generating *cis*-dienelactone from 4-chloromuconolactone, whereas for muconate cycloisomerases they postulated an enzyme catalyzed decarboxylation and a dehalogenation of 4-chloromuconolatone leading to protoanemonin (8).

According to studies on the reaction mechanisms of muconate cycloisomerase and mandelate racemase muconate (as well as 2-chloromuconate) cycloisomerization proceeds via an enol/enolate (Fig. 21 B), to which a proton is added to form muconolactone (Fig. 21 D) (42, 131). Similarly, the formation of protoanemonin from 3-chloro-*cis*,*cis*-muconate involves a protonation reaction, as two hydrogen atoms are present on the exocyclic carbon. In contrast, it was proposed that in the reaction leading to *cis*-dienelactone, the corresponding enol/enolate intermediate is not protonated but rather loses the negative charge by chloride abstraction (Fig. 21 C) (72). However, a direct enzyme-catalyzed dehalogenation of 3-chloromuconate leading to *cis*-dienelactone (Fig. 21 A) cannot be excluded. To prove that protoanemonin formation involves a protonation reaction, Kaulmann et al. exchanged the Lys169 residue of *Pseudomonas putida* MCI, which is known to provide the proton for protonation reaction during muconate transformation (131), by alanine. As expected, substrates requiring protonation, such as muconate as well as 2-methyl, 3-methyl- or 2-chloromuconate were not converted at a significant rate by the variant. However, the variant was still active with 3-chloro- and 2,4-dichloromuconate. Interestingly, *cis*-dienelactone and 2-chloro-*cis*-dienelactone were formed as products, whereas the wild-type forms protoanemonin and 2-chloroprotoanemonin, respectively. The authors assumed, thus, that chloromuconate cycloisomerases may avoid protoanemonin formation by increasing the rate of chloride abstraction from the enol/enolate intermediate compared to that of proton addition to it.

More importantly, the study shows that protonation reaction to be definitely necessary for protoanemonin formation but not for *cis*-dienelactone formation and indicated that 4-chloromuconolactone will be the intermediate of muconate cycloisomerase-catalyzed cycloisomerization, from which decarboxylation and chloride elimination to protoanemonin (Fig. 21 E) occurs, as proposed by Blasco et al. (8).

The study presented here offers two new pieces of information that support Kaulmanns hypothesis:
i) 3-Chloromuconate transformation by proteobacterial muconate cycloisomerases proceeds via a reaction intermediate which is used as a substrate for *trans*-dienelactone hydrolase. This hydrolase which is active with *trans*-dienelactone, 4-fluromuconolactone and enollactone, but not with *cis*-dienelactone, 3-chloromuconate or protoanemonin, obviously acts on 4-chloromuconolactone.
ii) Concomitant action of *trans*-DLH and MCI can prevent protoanemonin formation in favor of maleylacetate formation, but it does not influence the formation of *cis*-dienelactone. Thus, the reaction intermediate, which serves as a substrate for *trans*-DLH (most probably 4-chloromuconolactone) is not an intermediate in the formation of *cis*-dienelactone, but both reaction mechanisms diverge before, probably at the stage of enol/enolate intermediate. Similar observations were made during 3-chloromuconate transformation by concomitant action of MCIB and *trans*-DLH. Figure 21 summarizes the reaction mechanisms we assume for 3-chloromuconate transformation by MCI and MCIB in the presence of *trans*-DLH.

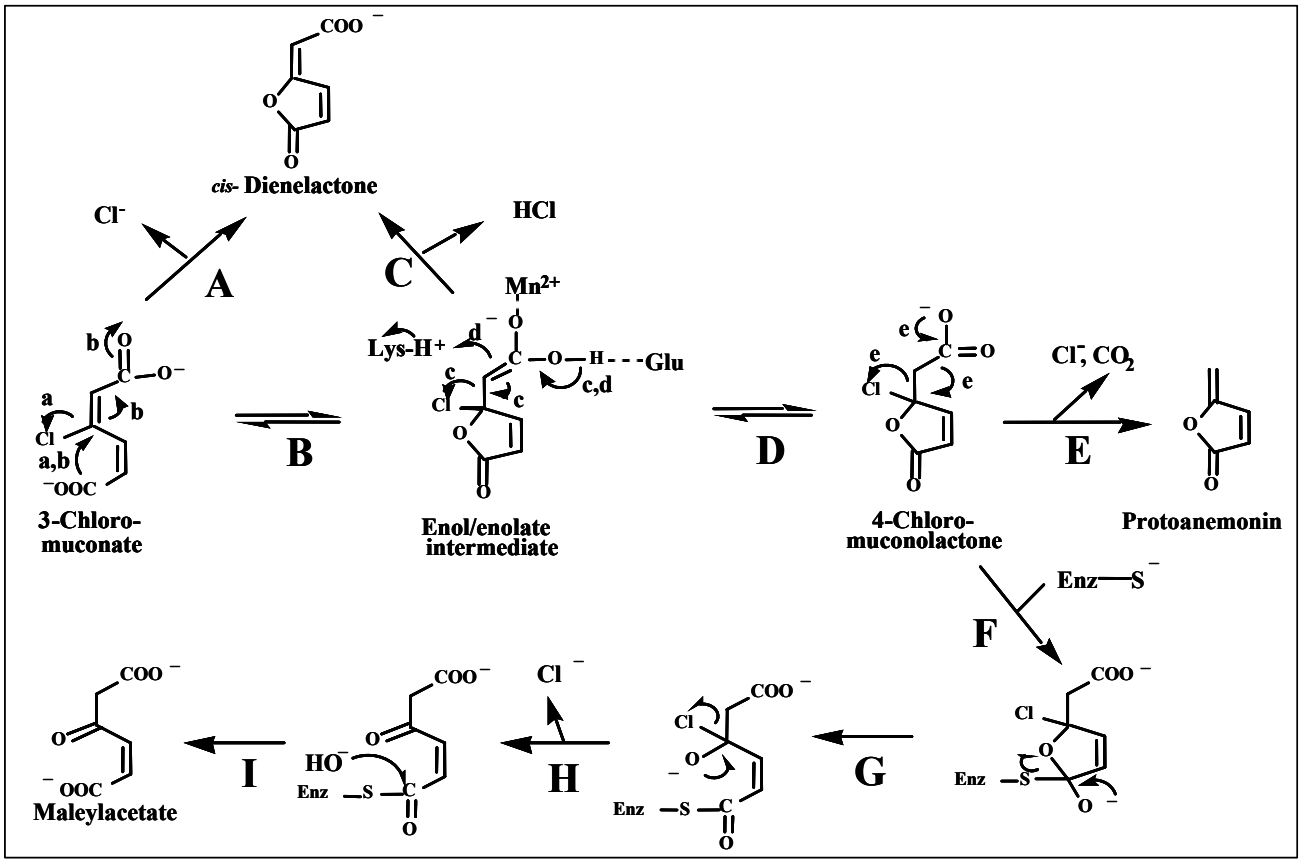

Figure 21: Postulated mechanism for 3-chloromuconate transformation by combined action of a 3-chloromuconate cycloisomerizing enzyme and *trans*-DLH of *Pseudomonas* sp. MT1. Detailed description of steps are given in the text.

4-Chloromuconolactone is the intermediate of 3-chloromuconate cycloisomerization by muconate cycloisomerases, from which decarboxylation and chloride elimination to protoanemonin (Fig. 21 E) occurs (8). Whether this reaction is spontaneous or enzyme catalyzed has not been analyzed thus far.

3-Chloromuconate transformation assays demonstrated that less protoanemonin but more maleylacetate were formed when cell extracts were applied in high compared to low concentration (Table 4). A similar product shift from protoanemonin to maleylacetate was observed when 3-chloromuconate was incubated with increasing concentrations of purified MCI and *trans*-DLH (see 3.5.1, 3.5.2 and below). The kinetic data presented clearly support the notion of protoanemonin formation from 4-chloromuconolactone to be a spontaneous reaction. Assuming that both protoanemonin and maleylacetate formation to be enzyme-catalyzed by muconate cycloisomerase or *trans*-dienelactone hydrolase, respectively, would exclude any effect of the total protein concentration on the product composition. However, if protoanemonin formation is spontaneous and competes with enzymatic hydrolyzation to maleylacetate, an increase in total protein concentration would lower the diffusion time for 4-chloromuconolactone to reach *trans*-DLH, which is in agreement with the observation of protoanemonin formation to be prevented by higher protein concentrations. Accordingly, out of various kinetic models established to describe the obtained kinetic data, only models assuming protoanemonin formation to be spontaneous were in good agreement with the measured data.

Consequently, it can be concluded that *cis*-dienelactone is formed directly by MCI without involving the intermediate formation of 4-chloromuconolactone, whereas protoanemonin and maleylacetate formation necessitate the intermediate formation of this compound. The spontaneous decomposition of 4-chloromuconolactone to protoanemonin is prevented by *trans*-DLH which forms predominantly maleylacetate as reaction product.

It can be further speculated whether *trans*-DLH and MCI or MCIB, respectively, form a loose multienzyme complex which falls apart during cell disruption (25, 110). Nevertheless, in whole cells, proteins will be packed much denser, compared the *in-situ* assays, such that spontaneous reactions and protoanemonin formation are prevented to a significant extent. This explains the low amounts of protoanemonin observed to accumulate in resting cell experiments and during growth of MT1 on chlorosalicylates.

Both cycloisomerases MCI and MCIB of MT1 have been tested for product formation in the presence of *trans*-DLH. In order to compare the influence of the enzyme ratio on the product formation, similar concentrations and ratio of the respective enzymes should be chosen and the amount of *trans*-DLH should be varied as performed for MCI of MT1. Figure 22 demonstrates that the effect of *trans*-DLH on 3-chloromuconate transformation by MCI and MCIB of *Pseudomonas* sp. strain MT1 is in the same order of magnitude.

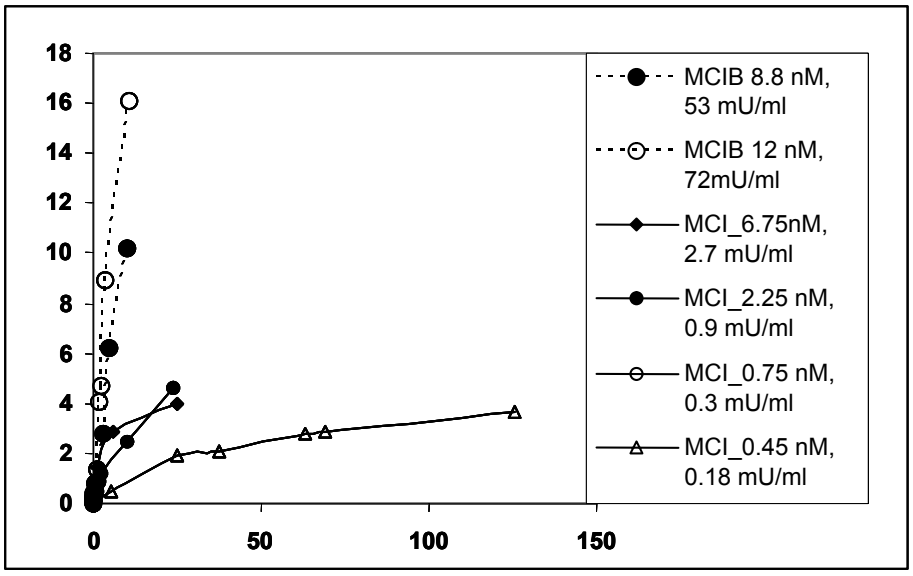

Figure 22: Comparison of influence of *trans*-DLH on MCI and MCIB of *Pseudomonas* sp. strain MT1, respectively. Maleylacetate/protoanemonin ratio versus MCI/*trans*-DLH and MCIB/*trans*-DLH ratios. Curves as in Fig. 14 D and 15, respectively. For better comparison, activities are given as mU/ml transformation of 3-chloromuconate for MCI and MCIB.

4.3.2 Proposed function of *trans*-DLH - Mechanism of hydrolysis of a hypothesized cycloisomerization intermediate

As reasoned above, we propose 4-chloromuconolactone as the reaction intermediate of 3-chloromuconate cycloisomerization, which spontaneously decomposes to protoanemonin. We have further demonstrated that the formation of protoanemonin is reduced in favor of maleylacetate in the presence of *trans*-DLH (see 3.5.1 – 3.5.3). We assume that *trans*-DLH competes with dehalogenation and decarboxylation leading to protoanemonin and hydrolyzes 4-chloro-muconolactone to maleylacetate. Schlömann et al. had previously shown, that 3-fluoromuconate, formed during 4-fluorobenzoate metabolism is transformed by muconate cycloisomerases to 4-fluoromuconolactone without dehalogenation taking place. 4-Fluoromuconolactone was a rather

stable product and decomposed only slowly to maleylacetate with a half-life of 43 hours (135). During their studies on 4-fluorobenzoate metabolism, Schlömann et al. also could identify different types of dienelactone hydrolases, which were analyzed for their capability to transform 4-fluoromuconolactone. Interestingly, *trans*-DLHs as well as *cis*-/*trans*-DLHs were observed to be capable to hydrolyze 4-fluoromuconolactone, whereas *cis*-DLH was not (133, 137). Dehalogenation of 4-chloromuconolactone by MT1 *trans*-DLH can be expected to resemble such 4-fluoromuconolactone conversion to maleylacetate (132, 133). We could demonstrate that t*rans*-DLH of MT1 shares the ability to transform 4-fluoromuconolactone to maleylacetate with 3-oxoadipate enol-lactone hydrolases of *A. calcoaceticus* and *Pseudomonas putida*, as well as *trans*- and *cis*-/*trans*-DLH of *R. eutropha* JMP134 and *Pseudomonas* sp. B13, respectively (132, 133).
Tough the *cis*-/*trans*-DLH $TfdE_I$ of *R. eutropha* JMP134 (as the experiments by Schlömann were performed in cell extracts, it is highly probable that the measured enzyme activity is due to activity of $TfdE_I$, see (114)) was reported to be capable to transform 4-fluoromuconolactone, in the experiment performed by us, this enzyme was not capable to prevent protoanemonin formation from 3-chloromuconate by muconate cycloisomerase. Unfortunately, no detailed characterization of this enzymes capability to transform 4-fluoromuconolactone was available, and therefore it cannot be excluded, that it differed significantly from *trans*-DLH in turnover numbers for 4-fluoromuconolactone. Thus, more detailed analysis will be necessary to evaluate to capabilities of *cis*-/*trans*-DLHs to transform 4-fluoro- and 4-chloromuconolactone.

Additionally, it would be very interesting to screen various purified dienelactone hydrolases, especially *trans*-DLH of *R. eutropha* 335, *Pseudomonas* sp. RW10 and others induced in 4-fluorobenzoate utilizing strains (137) for their ability to transform 4-chloromuconolactone generated *in-situ* by MCI or MCIB of MT1 in order to test if this functional phenotype could specifically be assigned to *trans*-dienelactone hydrolases.

Figure 21 shows a possible reaction mechanism of maleylacetate formation from 4-chloromuconolactone catalyzed by *trans*-DLH in analogy to reaction mechanism suggested by Chea et al. for dienelactone hydrolysis by *cis*-/*trans*-DLH of *Pseudomonas* sp. strain B13 (23). One may expect that the enzyme nucleophile attacks the lactone carbonyl group (Fig. 21, reaction F), giving rise to a halohydrin (Fig. 21, reaction G), which should spontaneously eliminate the halogenide ion (Fig. 21, reaction H). However, the relatedness of MT1 *trans*-DLH to other

hydrolytic enzymes, including the *cis*-/*trans*-DLH family, is not known and *trans*-DLH differs in basic biochemical properties from *cis*-/*trans*-DLH eg. by its high susceptibility to chelators. Thus, this mechanism must be regarded as highly speculative.

Inhibition of *trans*-DLH of MT1 by Hg^{2+}, but not by 4-chloromercuribenzoate, both sulfhydryl-selective agents (88), can be explained by the large molecular size of 4-chloromercuribenzoate which might not be able to access the active site pocket of *trans*-DLH, whereas the small ion can (136). Similarly other small reducing ions have a strong inhibitory effect on *trans*-DLH (Table 8). Unfortunately, there are no inhibition studies using ions on other DLH in the literature. However, not only *trans*-DLH of MT1 but also *trans*-DLH of *Ralstonia eutropha* 335 was shown to be susceptible to chelators, and it was suggested that *trans*-DLH of *R. eutropha* 335 might be Mn^{2+} dependant (132, 133). This observation could indicate a common reaction mechanism of both *trans*-DLH of *Pseudomonas* sp. strain MT1 and *R. eutropha* 335. However, when protein sequence information obtained from MT1 and was compared with the almost complete protein sequence of *trans*-DLH of 335 (personal communication from Schlömann), no significant homology was observed. Against that, *trans*-DLH of 335 was similar to a sequence in *R. metallidurans* (ongoing sequencing project). Thus, the phylogenetic relationship between *trans*-DLHs of *Pseudomonas* and of *Ralstonia* still remain to be established.

4.4 The novel cycloisomerase (MCIB) – product and substrate specificities of (chloro)muconate cycloisomerases

The metabolism of 4-chlorocatechol by MT1 and reaction mechanisms leading to the formation of maleylacetate from 3-chloromuconate have been examined in detail using muconate cycloisomerase and *trans*-DLH of MT1. However, besides MCI, which is the dominant cycloisomerase during growth of MT1 on salicylate, we could identify a second cycloisomerase activity, termed MCIB in MT1, which was specifically induced during growth on 5-chlorosalicylate. MCIB of *Pseudomonas* sp. strain MT1 catalyze 3-chloromuconate transformation to *cis*-dienelactone and protoanemonin in equal amounts and is thus assumed to be an enzyme with catalytical function intermediate to muconate and chloromuconate cycloisomerases of proteobacteria. However, our analysis has shown that even muconate cycloisomerases do (including the archetype enzyme of PRS2000) not exclusively catalyze protoanemonin formation but catalyze, though to a minor extent, dehalogenation to form *cis*-dienelactone (MCI of MT1 8 ± 5 % of the initial substrate concentration,

(see 3.4.1) and muconate cycloisomerase of *P. putida* PRS2000 17 ± 5 % (see 3.5.3)). Such a behavior, to the current knowledge, is however not astonishing. As described above, it is assumed that chloromuconate cycloisomerases avoid protoanemonin formation by increasing the rate of chloride abstraction from the enol/enolate intermediate compared to that of proton addition to it. Clearly, formation of protoanemonin and formation of *cis*-dienelactone require different active site structures, allowing at least theoretically all intermediate solutions. Thus, MCIB from the point of increasing halide elimination, is clearly intermediate to muconate and chloromuconate cycloisomerases.

However, the product profile is not the only extraordinary property of MCIB. Similar to proteobacterial muconate cycloisomerases, MCIB has no significant activity with 2-chloromuconate. This is in contrast to studies on proteobacterial chloromuconate cycloisomerases, which usually have relatively high turnover numbers for 2-chloromuconate. It should, however, be noted that even chloromuconate cycloisomerases analyzed in this aspect thus far (169) differed significantly in their substrate specificity. Whereas the *Pseudomonas* sp. strain P51 and B13 derived enzymes transformed 2-chloromuconate and 3-chloromuconate with similar specificities (k_{cat}/K_m values), 3-chloromuconate was a by one order of magnitude preferred substrate for $TfdD_I$ of *R. eutropha* JMP134 (107). For all chloromuconate cycloisomerases, muconate is a relatively poor substrate (78, 139, 168, 169). Thus it seems, that MCIB exhibits just a slightly more restricted substrate specificity than above chloromuconate cycloisomerases. However, MCIB does not efficiently transform 2,4-dichloromuconate, which for all three chloromuconate cycloisomerases described in this respect, is the preferred substrate (78, 169). Two exceptional chloromuconate cycloisomerases are described in the literature with substrate specificities similar to MCIB of MT1 - $TfdD_{II}$ of *Ralstonia eutropha* JMP134 (114) and ClcB of *Rhodococcus opacus* 1CP (34, 151), both specifically dedicated to convert 3-chloromuconate. The amino acid sequences of both proteins fall outside the clusters of muconate and chloromuconate cycloisomerases (Fig. 19). Alignment of the determined MCIB protein sequences with known muconate and chloromuconate cycloisomerases did not show any homology. However, careful inspection of the N-terminal sequence of MCIB showed the presence of motifs characteristic on one hand for muconate cycloisomerases of *Pseudomonas* (MSQXXVI) but also for chloromuconate cycloisomerases (PIXMSFXT). Further analysis of the MCIB protein sequence will reveal to which extend this protein actually is related to muconate and chloromuconate cycloisomerases and add more knowledge on sequence-function relationships among this important class of proteins.

On the first view, not only MCIB, but also MCI of MT1 has extraordinary properties, as it shows a higher specificity constant for 3-chloromuconate than for muconate (Table 6). Against that, transformation rates of 3-chloromuconate of MCI have generally been assumed to be significantly lower than of muconate, a fact that was first discussed for MCI of *Pseudomonas* sp. B13 (139) and later demonstrated for MCI of *Pseudomonas putida* PRS2000 (169). By site-directed mutagenesis, Vollmer et al. created two mutants I54V and A271S, which, according to the authors, were improved for 3-chloromuconate transformation (169). As MCI of MT1, in contrast to muconate cyloisomerases, but similar to chloromuconate cycloisomerases and like the I54V mutant, contains a valine at the respective position, it could be speculated that this amino acid is majorly responsible for the high turnover of 3-chloromuconate of MT1. However, reevaluation of 3-chloromuconate transformation by the PRS2000 muconate cycloisomerase and site-directed mutants showed, that they do not differ significantly in 3-chloromuconate transformation rates, and moreover, rates of the wildtype enzymes have been significantly underestimated. (Table 12). Therefore we suggest that the differences between muconate and chloromuconate cycloisomerases concerning 3-chloromuconate transformation rates are much less pronounced then previously assumed and that the major difference between these groups of enzymes is the reaction mechanism.

In agreement with the hypothesized mechanism of cycloisomerization we speculate that the photometrical 3-chloromuconate activity test used by Vollmer et al. (169) does not determine the rate of substrate transformation into the final product protoanemonin, but determines slight differences in accumulation of 4-chloromuconolactone (Fig. 21). If so, slight increases in 3-chloromuconate transformation rates would result in accumulation of 4-chloromuconolactone, because spontaneous transformation of 4-chloromuconolactone would become rate limiting. This hypothesis can be tested by incubation of 3-chloromuconate with the wildtype or the mutant CatB together with *trans*-DLH of MT1. If 4-chloromuconolactone formation is in fact enhanced in the mutant enzymes, *trans*-DLH will have higher chances to encounter a 4-chloromuconolactone molecule and thus the shift from protoanemonin to maleylacetate production should be facilitated in the assays containing mutant CatB compared to assays containing the wildtype CatB.

4.5 The maleylacetate reductase (MAR)

Maleylacetate as the product of transformation of 3-chloromuconate by muconate cycloisomerases and *trans*-dienelactone hydrolase of MT1 is converted to 3-oxoadipate by the action of a maleylacetate reductase. Most bacterial maleylacetate reductases, which are characterized in detail thus far, are encoded within the cluster of chlorocatechol pathway genes. However, as there was no indication for the induction of any other enzyme typical for chlorocatechol pathways, MAR of MT1 is evidently not encoded in such a gene cluster.

Concerning kinetic parameters, MAR of MT1 differs from previously described maleylacetate reductases in two aspects. Firstly, the K_m of MAR of MT1 was significantly lower compared to proteobacterial MARs of the chlorocatechol pathway (*Pseudomonas* sp. strain B13 K_m = 58 µM (71); *P. aeruginosa* RHO1 K_m =65 µM (92); *R. eutropha* JMP134 $TfdF_{II}$ K_m = 50 µM (92)).

Secondly, the enzyme was efficient in the reduction of *cis*-acetylacrylate to laevulinate, a reaction analogues to maleylacetate reduction. Though MT1 MAR has a very high K_m-value for *cis*-acetylacrylate (640 µM ± 135 µM), its maximal turnover number with *cis*-acetylacrylate is 34 % that with maleylacetate (see 3.7.1). This activity contrasts that of the $TfdF_I$ maleylacetate reductase of *R. eutropha* JMP134 MAR which exhibits only negligible activity with *cis*-acetylacrylate. In fact the side activity of MAR of MT1 with *cis*-acetylacrylate could explain the capability of MT1 to grow on that substrate (106). However, if MT1 actually does grow on *cis*-acetylacrylate via an initial MAR catalyzed reduction with laevulinate as intermediate remains to be elucidated.

4.6 Regulation and genetic organization of the novel pathway

All enzyme activities measured in cell extracts of 5-chlorosalicylate grown MT1 could also be detected in extracts of salicylate, but not in succinate grown cells (Table 2). Thus all those activities are inducible. MCI and muconolactone isomerase were induced to higher levels in cells grown on salicylate, as expected for enzymes of the 3-oxoadipate pathway (50, 102), whereas salicylate 1-hydroxylase, catechol 1,2-dioxygenase, MCIB, *trans*-DLH and MAR were significantly higher expressed when cells were grown on 5-chlorosalicylate compared to salicylate.

On the first view, the induction pattern of catechol 1,2-dioxygenase is surprising, as catechol 1,2-dioxygenase is commonly known to be part of the 3-oxoadipate pathway and to be encoded within one operon with MCI and muconolactone isomerase (50).

There are growing evidence that catabolic genes of the 3-oxoadipate pathway can be encoded several times throughout a bacterial genome, so that they can underlay different mechanisms of regulation (see 4.8) (62, 144). Similar bacterial genome sequencing projects reveal increasing examples of strains, that harbor more than one catechol 1,2-dioxygenase gene or complete *cat* gene clusters. Jiménez et al. (62) summarized cases where several catechol 1,2-dioxygenases are encoded within a bacterial genome, either as duplicates of the full (93, 158) or partial 3-oxoadipate cluster (20, 62, 64, 73, 74, 94). The recent comparison genome sequences of *Pseudomonas putida* KT2440 with other *Pseudomonas* strains, demonstrated that *P. fluorenscens* Pf0-1 harbors two copies of the cat gene clusters, whereas *P. putida* KT2440 codes for one cluster and one additional catechol 1,2-dioxygenase which is located within the benzoate degrading cluster (*ben* cluster). The *ben* clusters of *P. putida* PRS2000, *P. aeruginosa* and *fluorescens,* in contrast, do not harbor a catechol 1,2-dioxygenase encoding gene. *Ralstonia metallidurans* CH34 encodes two non-identical *cat* clusters and one additional catechol 1,2-dioxygenase gene adjacent to its *ben* gene cluster. In contrast, some strains like *Pseudomonas aeruginosa* PAO1, *Burkholderia pseudomallei* (ongoing genome project) and *Novosphingobium aromaticivorans* (ongoing) contain only one 3-oxoadipate cluster or no such cluster or genes at all like *P. syringae* pv. tomato DC3000.

Hence occurrence, genetic location, and regulation of such isoenzymes is highly diverse. Our observation of a higher induction of catechol 1,2-dioxygenases activity in 5-chlorosalicylate cells concomitant with a reduction in level of muconate cycloisomerase and muconolacton isomerase indicate that MT1 should contain at least one independently regulated catechol 1,2-dioxygenase. Recent experiments (Camara, personal communication) indicate that MT1 harbors at least two catechol 1,2-dioxygenases. Thus it can be speculated, that one of the respective encoding genes is located inside a *cat* gene cluster, whereas the second one is independently regulated.

As stated above, mineralization of chloroaromatics necessitates a delicate balance between chlorocatechol producing and chlorocatechol transforming activities. In this context, the high levels of catechol 1,2-dioxygenase observed during growth on chlorosalicylate are most probably due to a catechol 1,2-dioxygenase independently regulated from the 3-oxoadipate pathway gene cluster and is possibly absolutely necessary to allow growth of MT1 on chlorosalicylates.

According to separation of MT1 cell extracts using different principles of protein chromatography only one MCI should be present in MT1. Nevertheless, in southern blots with a fragment of MCI encoding gene of MT1 applied as probe, two distinct genome fragments hybridized resulting in two

major bands (Fig. 20) and it can be assumed that hybridization is due to sequence homology between the MCIB and the MCI encoding gene sequences. The inverse induction patterns of MCI and MCIB suggest that their genes are not located within one operon, neither does the southern blot show a genetic connection of MCI and MCIB.

Salicylate hydroxylase (Fig. 7) is a flavoprotein monooxygenase that catalyzes the conversion of salicylate to catechol. The enzyme was first purified from *P. putida* S1 (181) and later from various other *Pseudomonas* and *Burkholderia* strains, and cloned and sequenced from various sources (9, 66, 81, 183), dominantly *Pseudomonas* spp.. Usually, salicylate hydroxylase is included in the naphthalene pathway, and the gene encoding salicylate hydroxylase is followed by genes encoding a *meta*-cleavage pathway. Different so-called NAH plasmids harboring these genes have been described from *Pseudomonas* strains (19, 182). In contrast, *P. stutzeri* AN10 harbors chromosomally located *nah* genes (126). Moreover, variations in gene organization have been observed. *P. stutzeri* AN10, besides *nahG* encoding salicylate hydroxylase located in one transcriptional unit with the *meta*-cleavage pathway genes, contains a second gene encoding salicylate hydroxylase, *nahW*, which is situated outside but in close proximity to this transcriptional unit. Both, the *nahG* and *nahW* genes of *P. stutzeri* AN10 are induced and expressed upon incubation with salicylate. Such a gene organization seems to be common to naphthalene degrading *P. stutzeri* strains (10). Despite differences in gene organization and partially low homology (NahW shares 23 – 25 % amino acid sequence identity to other salicylate hydroxylases), most salicylate hydroxylases described thus far exhibit similar substrate ranges with significant activities with salicylate, 4-chloro- and 5-chlorosalicylate, and a lower activity against 3-chlorosalicylate (10, 66, 82, 127). Given the broad substrate specificity of salicylate 1-hydroxylases it is not surprising that chlorosalicylate mineralizing *Pseudomonas* strains could easily be obtained by combining a salicylate 1-hydroxylase with a functioning chlorocatechol pathway (82, 127). Genes similar to those encoding salicylate hydroxylase (approx 25 – 30 % amino acid sequence identity) have been localized in the genome of *P. aeruginosa* PAO1 and *P. putida* KT2440, however, KT2440 is reported not to grow on salicylate (63). The analysis of strain collections has shown, that only a few *Pseudomonas* strains are capable to mineralize salicylate, whereas such a capability seems to be frequent in *Burkholderia cepacia* (155), however, as outlined above, identification of the encoding regions as well as information on the regulation of salicylate hydroxylases independent of those involved in naphthalene degradation is rare. Interestingly, salicylate 1-hydroxylase is more

efficiently induced in MT1 during growth on 5-chlorosalicylate compared to salicylate, and thus shows induction pattern similar to those of catechol 1,2-dioxygenase, MCIB, *trans*-DLH and MAR. However, if those genes are localized in one and the same gene cluster remains speculative.

Extracts of MT1 were highly active with *trans*-dienelactone and maleylacetate. Similarly, concomitant expression of different types of DLH and MAR in the absence of chlorocatechol 1,2-dioxygenase and chloromuconate cycloisomerase of the chlorocatechol pathway were previously described for bacteria growing on 4-fluorobenzoate as only source of carbon and energy (137). The authors had speculated on a novel pathway via *ortho*-cleavage of 4-fluorocatechol, 3-fluoromuconate and 4-fluoromuconolactone.
In *R. eutropha* 335 a *trans*-DLH has been reported as crucial enzyme and shown to be induced during growth of the strain with 4–fluorobenzoate (137). The enzyme may play a dual role in the degradation and be responsible for direct conversion of 4-fluoromuconolactone as well as conversion of *trans*-dienelactone formed from 4-fluoromuconolactone as by-product by 3-oxoadipate enol-lactone hydrolase (132). The natural function of the *R. eutropha trans*-DLH so far is unclear. It is highly unlikely to have been selected especially for 4-fluorobenzoate catabolism and thus seems to be recruited for it by accidental induction. In *Pseudomonas* sp. strain MT1 *trans*-DLH may also be recruited by chance induction. However, it may also be coinduced with MCIB. If this was true, then these enzymes might constitute the core elements of another highly unusual chlorocatechol degradative pathway. Future studies into the genetic background of MT1 cycloisomerase and *trans*-DLH should help to solve this question.

In MT1, MAR is responsible for channeling the substrate into the Krebs cycle. While many chlorocatechol operons do comprise MAR encoding genes (38, 67, 68, 79, 109, 114, 143, 163), some recently characterized chlorocatechol gene clusters did not appear to contain such genes (34, 91, 144) and thus maleylacetate reductases have to be recruited from other metabolic routes.
Maleylacetate reductases have also been shown to contribute to the bacterial catabolism of natural aromatic compounds like quinol, resorcinol, tyrosine and vanillate (15, 142, 153), as well as more complex structures, such as hydroxylated biarylethers (4). Though MAR tends to be encoded within specialized gene clusters for degradation of hydroxylated biarylethers (4), dinitrotoluene (*Burkholderia cepacia* R34 (65)), 2,4,5.trichlorophenoxyacetate (*B. cepacia* AC1100 (26)), pentachlorophenol (*Sphingomonas chlorophenolica* ATCC 39723 (17)) recent bacterial genome

projects, including that of *Ralstonia metallidurans* (acc. no. NZ_AAAI01000075), have revealed that MAR encoding genes are localized in chromosomal regions with unknown functions outside catabolic gene clusters (144) and more such information might be coming up with ongoing and future genome projects. Similarly, in *Rhodococcus opacus* 1CP, a MAR encoding gene of unknown metabolic function , which is only distantly related to proteobacterial MAR of the chlorocatechol pathway (142) and not located within a chlorocatechol cluster has been observed.

A maleylacetate reductase of an obvious function similar to that in MT1, more precisely an enzyme responsible for channeling maleylacetate formed from 4-halomuconolactone by a *trans*-dienelactone hydrolase, into the Krebs cycle, was recently described from *R. eutropha* 335 (MacA, accession number AF130250), as not being part of a specialized gene cluster (137, 141, 144). Recent analysis showed, that the *macA* gene is localized in a small gene cluster comprising, in addition to *mac*A a gene for a hypothetical membrane transport protein, *mac*B, possibly cotranscribed with *mac*A, and a presumed regulatory gene, *mac*R, divergently transcribed from *mac*AB. MacA shared only 50 - 57 % identity with maleylacetate reductases of the chlorocatechol pathway, whereas it turned out to be most similar to TftE, the MAR of 2,4,5-dinitrophenoxyacetate degrading *B. cepacia* AC1100 (62 % identity) (26) and to the putative MAR of the 2,4-dinitrotoluene degrading *B. cepacia* R34 (61 % identity) (65, 144). It was speculated, that maleylacetate itself is the inducer of the *mac*A gene, such that the *mac* cluster of *R. eutropha* JMP335 serves as a bridge between maleylacetate forming pathways and the 3-oxoadipate pathway funneling 3-oxoadipate to Krebs-cycle intermediates in a more general way than just for the degradation of the presumably non-natural compound 4-fluorobenzoate.

However, in contrast to the situation in 335, where maleylacetate reductase was induced exclusively during growth on fluorobenzoate, but not on benzoate, significant induction of maleylacetate reductase activity was observed in MT1 even during growth on salicylate, with increased expression levels during growth on chlorosalicylate suggesting a regulation and/or gene organization completely different from that in 335.

4.7 Strain MT1 with its novel pathway in the 4-strain carbon sharing community

Pseudomonas sp. strain MT1 was isolated by continuous culture enrichment as a member of a 4-strain community growing in very stable community composition on 4-chlorosalicylate (MT1, 84 ± 5 %; *Achromobacter xylosoxidans* MT3 and *Pseudomonas veronii* strain MT4, 8 ± 4 %; *Empedobacter brevis* MT2, 1 %). Interestingly, though MT1 can also grow in monoculture on 4-chlorosalicylate, when inoculated together with MT2, MT3 and MT4, it never outcompetes the other strains. Thus, there must be an advantage to exist in a community compared to growing as a monoculture.

Bacteria metabolize substrates in order to obtain energy and carbon for biosynthesis and growth. The chlorosalicylate degrading community can be regarded as an example of carbon sharing between community members. Much simpler examples of carbon sharing for mineralization of a substrate have been described in the literature. The most simple example are two-membered communities mineralizing bicyclic aromatics. In communities mineralizing eg. chlorodibenzofuran, one community member is responsible for the initial attack and grows on the expense of the hereby activated aromatic ring. As the microorganism does not harbor a pathway for mineralizing the intermediary formed chlorinated single-ring aromatic, chlorosalicylate in the case of dibenzofuran degradation, a second community member can gain its energy by mineralizing that intermediate (177). A similar carbon sharing has been reported for the growth of two species cultures on chlorinated biphenyls or aminonaphthalenesulfonates (1, 51, 97). Nonetheless, collaboration between microorganisms has generally been acknowledged when regarding anaerobic metabolism and has not, yet, been received the respective attention in aerobic metabolism. Additionally, investigations were mainly restricted to above mentioned simple kind of carbon sharing. Feigel et al. were among the first to observe synthrophic interaction between community members during the aerobic degradation of aminobenzenesulfonate (35). Even though one community member harbors all enzymes for mineralization, its growth in monoculture is inhibited by a toxic intermediate, the degradation of which is supported by the second community member. Such interactions between microorganisms, evidently of high importance under environmental conditions, was neglected, as nearly all enrichment to isolate microorganisms for xenobiotic degradation had been performed in batch culture, enriching single species with high growth rates. However, growth in continuous culture under low substrate concentrations resembles more the actual environmental conditions. Nevertheless, it was initially surprising that continuous culture enrichment on a simple carbon source like chlorosalicylate resulted in a stable four-membered community.

Strain MT1 was assumed to degrade 4-chlorosalicylate via 4-chlorocatechol and protoanemonin as intermediates. As MT2, MT3 and MT4 are not capable of growth on 4-chlorosalicylate, but can grow in commensal relationship with MT1, it was assumed that they harbor pathways for mineralization of metabolites excreted by MT1.
The analysis by Pelz using ^{13}C-labelled metabolites and isotopic ratio mass spectrometric analysis of label enrichment in immunocaptured members of the community revealed a complex pathway network of carbon sharing (106). In fact, strain MT3 was rapidly incorporating labeled 4-chlorocatechol, whereas MT4 was rapidly incorporating labeled protoanemonin. In contrast to the assumed identity of protoanemonin as pathway intermediate, MT1 was only very slowly incorporating protoanemonin. The metabolic pathway of 4-and 5-chlorosalicylate degradation has now been elucidated for *Pseudomonas* sp. strain MT1 and the results more clearly evidence the metabolic flux in the 4-membered community. Figure 23 summarizes probable and demonstrated steps of 4-chlorosalicylate degradation in the community.

Cycloisomerization of 3-chloromuconate and hydrolysis of 4-chloromuconolactone are the key reactions in the degradation of 4- and 5-chlorosalicylate by MT1. During this reaction, protoanemonin will be formed by chemical decomposition of 4-chloromuconolactone, a reaction not completely avoidable. Pelz et al. demonstrated that MT4 can take up and metabolize significant protoanemonin (106), thus indicating that this strain harbors a metabolic activity with protoanemonin. Thus, as Pelz indicated, MT4 fulfills its function in detoxifying any protoanemonin accumulating in the culture. However, in contrast to previous assumptions, MT4 seems to be the only community member capable to do so.
cis-Dienelactone is formed as a side product by MCI of MT1, and will be formed in higher amounts when MCIB is simultaneously expressed. Thus, *cis*-dienelactone will be formed during chlorosalicylate degradation by MT1. Pelz et al. had shown, that 4-chlorocatechol is dominantly incorporated by MT3. This rapid incorporation can be due to a functional chlorocatechol pathway in this strain, which is also evidenced by a high 4-chlorocatechol transforming activity, indicative for a chlorocatechol 1,2-dioxygenase in the consortium, and probably in MT3 (106). If MT3 harbors a chlorocatechol pathway it should be capable to metabolize *cis*-dienelactone.

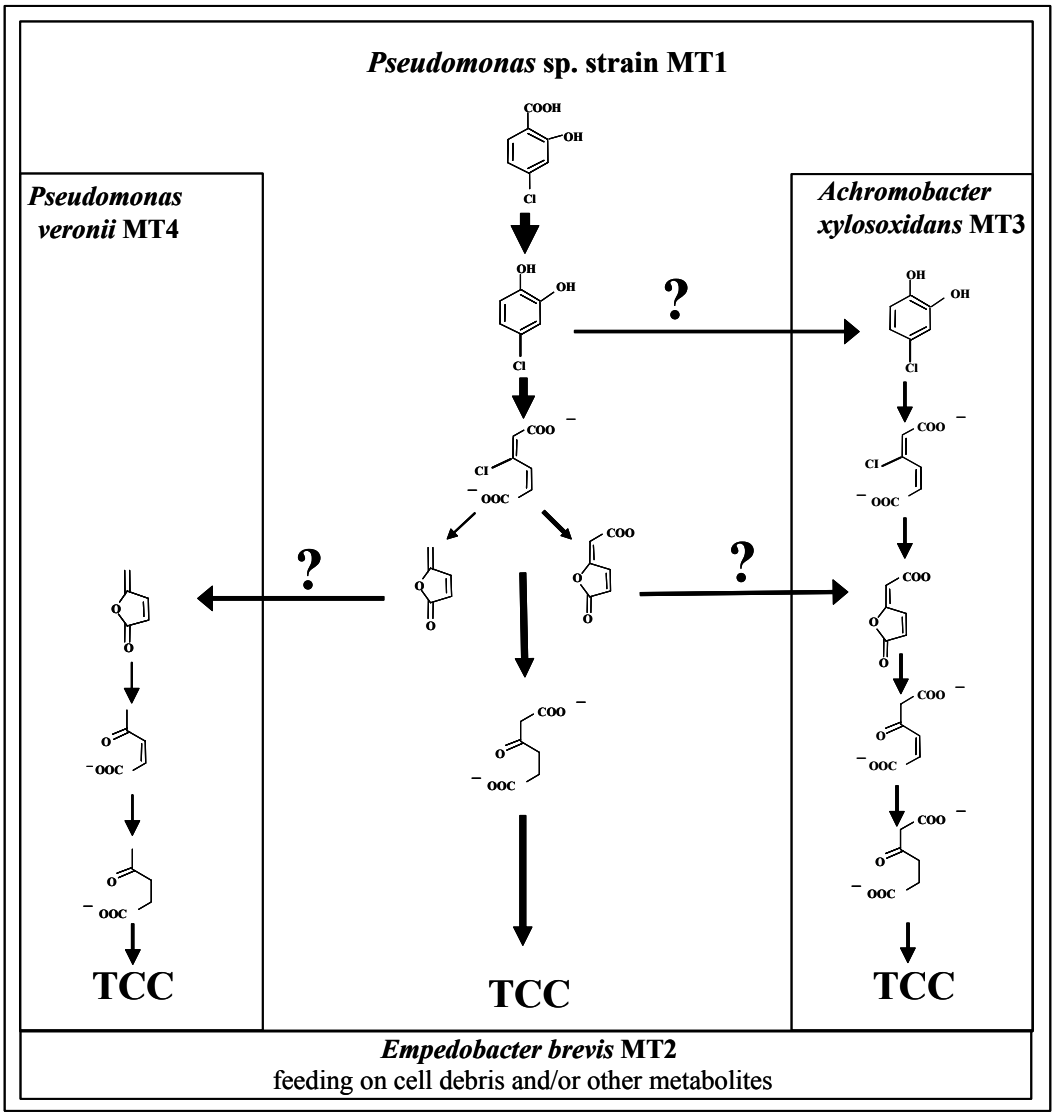

Fig. 23: Modified after Pelz et al. (106). Metabolic pathways in the strain bacterial community. Speculated excretion and uptake of metabolites are marked with ?. Thickness of arrows is chosen according to assumed importance of the catalytical step. Metabolism of *Pseudomonas veronii* MT4 *Achromobacter xylosoxidans* MT3 and *Empedobacter brevis* MT2 are hypothetical. TCC, tricarboxylic acid cycle.

In fact, the relative abundance of MT3 in the community (8 %) agrees well with the proportion of *cis*-dienelactone accumulating during growth of MT1 in pure culture or during resting cell experiments. In contrast, the amounts of protoanemonin accumulation during pure culture growth or during transformation experiments were always slightly lower (4 %) than the relative abundance of MT4. However, the fluxes from 3-chloromuconate to maleylacetate, protoanemonin and *cis*-dienelactone, within the intact cell of MT1, especially under chemostat conditions, are still unknown as they depend on a very fine-tuned interplay of the respective enzymes. However, the stable relative abundances of the strains indicate that most of the substrate is metabolized via the

novel pathway in MT1 and that similar amounts of leaking side-products are degraded by MT3 and MT4. However, it would not be possible to conclude on any detailed fluxes – first of all, because the amounts of leaking metabolites are not quantified and, secondly, because the strains might invest different amounts of energy for the metabolic break-down by enzyme synthesis or other burdens such as synthesis of stress factors. It would be interesting to test whether it was only MT3 taking up *cis*-dienelactone with a pulse feed experiment applying ^{13}C-labeled *cis*-dienelactone.

However, the picture of a simple carbon sharing model based on kinetic properties of the MT1 enzyme system for transformation of 3-chloromuconate to maleylacetate, protoanemonin and *cis*-dienelactone is for sure an oversimplification. First of all, *cis*-dienelactone will not be freely permeable and thus, MT3 would probably need an appropriate transporter system, and secondly, chloromuconates and not dienelactones are the known inducers of the chlorocatechol pathway.
It has been shown, that specifically at higher substrate concentrations, 4-chlorocatechol is leaking out of MT1 and that accumulation of 4-chlorocatechol prevents growth. In fact, the ring cleavage of 4-chlorocatechol by (chloro)catechol 1,2-dioxygenase is crucial for a healthy growth of the bacteria, as 4-chlorocatechol was shown to have a MIC-value of 40 – 200 µM and to negatively effect the viability of different *Ralstonia* strains (108). Pelz et al. speculated that the major function of MT3 is to protect MT1 from the toxicity that would otherwise occur from the accumulation of 4-chlorocatechol. Actually, the take up by MT3 of even small amounts of 4-chlorocatechol excreted by MT1 under chemostat growth would allow the formation 3-chloromuconate and thus, the inducer of the whole chlorocatechol pathway genes.

4.8 Outlook

In the present study a novel metabolic pathway for 4-chlorocatechol degradation was elucidated. Extensive work on substrate transformation by the concomitant action of a cycloisomerase and a *trans*-DLH, revealed that the influence of the second enzyme on product formation was not only dependent on its relative amount, but that the total protein concentration was also highly important. The general kinetics can be explained by *trans*-DLH to act on 4-chloromuconolactone as reaction intermediate and by 4-chloromuconolactone to decompose spontaneously to form protoanemonin. Future experiments should focus on (i) detailed analysis of the influence of *trans*-DLH on products formed by different cycloisomerases to finally obtain a detailed kinetic model on the overall reaction, (ii) analyzing in detail kinetic alterations that have occurred in site-directed CatB variants of PRS2000. Furthermore, it would now be very interesting to investigate how important this pathway is in the environment and how far this pathway is spread among bacteria. Strains isolated by growth on 4-fluorobenzoate (137) might be good candidates for harboring the novel pathway as well.

As the work was focused on the biochemical characterization (metabolites and enzymes) of the pathway, it would be of benefit to explore the genetics of the pathway. Having the gene sequences of the key enzymes will not only allow faster screening of bacteria for the novel pathway, but also to compare the genes with sequences in the databases and thereby investigating the pathway from an evolutionary point of view. Such comparisons will also allow to move forward in the identification of crucial amino acid residues determining selectivity of (chloro)muconate cycloisomerases.

Increasing accumulation of sequence data, including whole bacterial genomes, open up the door to understand enzyme recruitment for catabolic pathways and gene recruitment from different location throughout a bacterial genome. Those mechanisms are considered crucial for bacterial adaptation and evolution of metabolic networks. Localization of the pathway encoding genes in the MT1 genome will form a solid basis for discussing recruitment of enzymes of the novel pathway. More detailed DNA sequence analysis will allow also to characterize the regulation of this new pathway and the manipulation of the pathway. Such manipulation will allow to investigate in more detail the collaboration between different community members of the chemostat community.

5. REFERENCES

1. **Abraham, W. R., B. Nogales, P. N. Golyshin, D. H. Pieper, and K. N. Timmis.** 2002. Polychlorinated biphenyl-degrading microbial communities in soils and sediments. Curr Opin Microbiol **5:**246-53.

2. **Adams, R. H., C. M. Huang, F. K. Higson, V. Brenner, and D. D. Focht.** 1992. Construction of a 3-chlorobiphenyl-utilizing recombinant from an intergeneric mating. Appl Environ Microbiol **58:**647-54.

3. **Arensdorf, J. J., and D. D. Focht.** 1995. A *meta* cleavage pathway for 4-chlorobenzoate, an intermediate in the metabolism of 4-chlorobiphenyl by *Pseudomonas cepacia* P166. Appl Environ Microbiol **61:**443-7.

4. **Armengaud, J., K. N. Timmis, and R. M. Wittich.** 1999. A functional 4-hydroxysalicylate/hydroxyquinol degradative pathway gene cluster is linked to the initial dibenzo-*p*-dioxin pathway genes in *Sphingomonas* sp. strain RW1. J Bacteriol **181:**3452-61.

5. **Asplund, G., and A. Grimvall.** 1991. Organohalogens in Nature. Environ. Sci. Technol. **25:**1346-50.

6. **Assinder, S. J., and P. A. Williams.** 1990. The TOL plasmids: determinants of the catabolism of toluene and the xylenes. Adv Microb Physiol **31:**1-69.

7. **Blasco, R., M. Mallavarapu, K. N. Timmis, and D. H. Pieper.** 1997. Evidence that formation of protoanemonin from metabolites of 4-chlorobiphenyl degradation negatively affects the survival of 4-chlorobiphenyl-cometabolizing microorganisms. Appl Environ Microbiol **63:**427-34.

8. **Blasco, R., R. M. Wittich, M. Mallavarapu, K. N. Timmis, and D. H. Pieper.** 1995. From xenobiotic to antibiotic, formation of protoanemonin from 4-chlorocatechol by enzymes of the 3-oxoadipate pathway. J Biol Chem **270:**29229-35.

9. **Bosch, R., E. Garcia-Valdes, and E. R. Moore.** 1999. Genetic characterization and evolutionary implications of a chromosomally encoded naphthalene-degradation upper pathway from *Pseudomonas stutzeri* AN10. Gene **236:**149-57.

10. **Bosch, R., E. R. Moore, E. Garcia-Valdes, and D. H. Pieper.** 1999. NahW, a novel, inducible salicylate hydroxylase involved in mineralization of naphthalene by *Pseudomonas stutzeri* AN10. J Bacteriol **181:**2315-22.

11. **Brack, W., T. Kind, S. Schrader, M. Moder, and G. Schuurmann.** 2003. Polychlorinated naphthalenes in sediments from the industrial region of Bitterfeld. Environ Pollut **121:**81-5.

12. **Bradford, M. M.** 1976. A rapid and sensitive method for the quantitation of microgram quantities of protein utilizing the principle of protein-dye binding. Anal Biochem **72:**248-54.

13. **Broderick, J. B., and T. V. O'Halloran.** 1991. Overproduction, purification, and characterization of chlorocatechol dioxygenase, a non-heme iron dioxygenase with broad substrate tolerance. Biochemistry **30:**7349-58.

14. **Brückmann, M., R. Blasco, K. N. Timmis, D. H. Pieper, R. M. Wittich, and M. Mallavarapu.** 1998. Detoxification of protoanemonin by dienelactone hydrolase. J Bacteriol **180:**400-2.

15. **Buswell, J. A., P. Ander, B. Pettersson, and K. E. Eriksson.** 1979. Oxidative decarboxylation of vanillic acid by *Sporotrichum pulverulentum*. FEBS Lett **103:**98-101.

16. **Cai, M., and L. Xun.** 2002. Organization and Regulation of Pentachlorophenol-Degrading Genes in *Sphingobium chlorophenolicum* ATCC 39723. J Bacteriol **184:**4672-80.

17. **Cai, M., and L. Xun.** 2002. Organization and regulation of pentachlorophenol-degrading genes in *Sphingobium chlorophenolicum* ATCC 39723. J Bacteriol **184:**4672-80.

18. **Caldwell, D. E., E. Atuku, K. P. Wivcharuk, S. Karthikeyan, D. R. Korber, D. R. Schmid, and G. M. Wolfaardt.** 1997. Germ theory versus community theory in understanding and controlling the proliferation of biofilms. Adv Dental Res **11:**4-13.

19. **Cane, P., and P. A. Williams.** 1982. The plasmid-coded metabolism of naphthalene and 2-methylnaphthalene in *Pseudomonas* strains: Phenotypic changes correlated with structural modification of the plasmid pWW60-1. J Gen Microbiol **128**.

20. **Caposio, P., E. Pessione, G. Giuffrida, A. Conti, S. Landolfo, C. Giunta, and G. Gribaudo.** 2002. Cloning and characterization of two catechol 1,2-dioxygenase genes from *Acinetobacter radioresistens* S13. Res Microbiol **153:**69-74.

21. **Chapman, P. J., and D. W. Ribbons.** 1976. Metabolism of resorcinylic compounds by bacteria: alternative pathways for resorcinol catabolism in *Pseudomonas putida*. J Bacteriol **125:**985-98.

22. **Chari, R. V. J., C. P. Whitman, J. W. Kozarich, K. Ngai, and L. N. Ornston.** 1987. Absolute stereochemical course of the 3-carboxymuconate cycloisomerase of *Pseudomonas putida* and *Acinetobacter calcoaceticus*: Analysis and Implications. J. Am. Chem. Soc. **109:**5514-9.

23. **Cheah, E., G. Ashley, W., J. Gary, and D. Ollis.** 1993. Catalysis by Dienelactone Hydrolase: A Variant on the Protease Mechanism. Proteins **16:**64-73.

24. **Christensen, B. B., J. A. Haagensen, A. Heydorn, and S. Molin.** 2002. Metabolic commensalism and competition in a two-species microbial consortium. Appl Environ Microbiol **68:**2495-502.

25. **Creighton, T., E.** 1993. Proteins - Structures and Molecular Properties., 2nd ed. W. H. Freeman and Company, New York.

26. **Daubaras, D. L., C. D. Hershberger, K. Kitano, and A. M. Chakrabarty.** 1995. Sequence analysis of a gene cluster involved in metabolism of 2,4,5-trichlorophenoxyacetic acid by *Burkholderia cepacia* AC1100. Appl Environ Microbiol **61:**1279-89.

27. **Doddamani, H. P., and H. Z. Ninnekar.** 2001. Biodegradation of carbaryl by a *Micrococcus* species. Curr Microbiol **43:**69-73.

28. **Dorn, E., M. Hellwig, W. Reineke, and H. J. Knackmuss.** 1974. Isolation and characterization of a 3-chlorobenzoate degrading pseudomonad. Arch Microbiol **99:**61-70.

29. **Dorn, E., and H. J. Knackmuss.** 1978. Chemical structure and biodegradability of halogenated aromatic compounds. Substituent effects on 1,2-dioxygenation of catechol. Biochem J **174:**85-94.

30. **Dorn, E., and H. J. Knackmuss.** 1978. Chemical structure and biodegradability of halogenated aromatic compounds. Two catechol 1,2-dioxygenases from a 3-chlorobenzoate-grown pseudomonad. Biochem J **174:**73-84.

31. **Dua, M., A. Singh, N. Sethunathan, and A. K. Johri.** 2002. Biotechnology and bioremediation: successes and limitations. Appl Microbiol Biotechnol **59:**143-52.

32. **Dunn, N. W., and I. C. Gunsalus.** 1973. Transmissible plasmid coding early enzymes of naphthalene oxidation in *Pseudomonas putida*. J Bacteriol **114:**974-9.

33. **Eulberg, D., L. A. Golovleva, and M. Schlömann.** 1997. Characterization of catechol catabolic genes from *Rhodococcus erythropolis* 1CP. J Bacteriol **179:**370-81.

34. **Eulberg, D., E. M. Kourbatova, L. A. Golovleva, and M. Schlömann.** 1998. Evolutionary relationship between chlorocatechol catabolic enzymes from *Rhodococcus opacus* 1CP and their counterparts in proteobacteria: sequence divergence and functional convergence. J Bacteriol **180:**1082-94.

35. **Feigel, B. J., and H. J. Knackmuss.** 1993. Syntrophic interactions during degradation of 4-aminobenzenesulfonic acid by a two species bacterial culture. Arch Microbiol **159:**124-30.

36. **Field, J. A., A. J. Starns, M. Kato, and G. Schraa.** 1995. Enhanced biodegradation of aromatic pollutants in co-culture of anaerobic and aerobic bacterial consortium. Antonie Van Leeuwenhoek J Microviol Serol **67:**47-77.

37. **Fortnagel, P., H. Harms, R. M. Wittich, W. Francke, S. Krohn, and H. Meyer.** 1989. Cleavage of dibenzofuran and dibenzodioxin ring systems by a *Pseudomonas* bacterium. Naturwissenschaften **76:**222-3.

38. **Frantz, B., and A. M. Chakrabarty.** 1987. Organization and nucleotide sequence determination of a gene cluster involved in 3-chlorocatechol degradation. Proc Natl Acad Sci U S A **84:**4460-4.

39. **Frantz, B., K. L. Ngai, D. K. Chatterjee, L. N. Ornston, and A. M. Chakrabarty.** 1987. Nucleotide sequence and expression of clcD, a plasmid-borne dienelactone hydrolase gene from *Pseudomonas* sp. strain B13. J Bacteriol **169:**704-9.

40. **Fuenmayor, S. L., M. Wild, A. L. Boyes, and P. A. Williams.** 1998. A gene cluster encoding steps in conversion of naphthalene to gentisate in *Pseudomonas* sp. strain U2. J Bacteriol **180:**2522-30.

41. **Furukawa, K.** 2000. Engineering dioxygenases for efficient degradation of environmental pollutants. Curr Opin Biotechnol **11:**244-9.

42. **Gerlt, J. A., and P. G. Gassmann.** 1992. Understanding Enzyme-catalyzed Proton Abstraction from Carbon Acids: Details of stepwise mechanisms for *beta*-elimination reactions. J. Am. Chem. Soc. **114:**5928-34.

43. **Gibson, D. T., J. R. Koch, C. L. Schuld, and R. E. Kallio.** 1968. Oxidative degradation of aromatic hydrocarbons by microorganisms. II. Metabolism of halogenated aromatic hydrocarbons. Biochemistry **7:**3795-802.

44. **Goetz, F. E., and L. J. Harmuth.** 1992. Gentisate pathway in *Salmonella typhimurium*: metabolism of *m*-hydroxybenzoate and gentisate. FEMS Microbiol Lett **76:**45-9.

45. **Gottschal, J. C.** 1990. Different types of continuous culture in ecological studies. Methods Microbiol **22:**87-124.

46. **Grimberg, J., S. Maguire, and L. Belluscio.** 1989. A simple method for the preparation of plasmid and chromosomal *E. coli* DNA. Nucleic Acids Res **17:**8893.

47. **Grund, E., B. Denecke, and R. Eichenlaub.** 1992. Naphthalene degradation via salicylate and gentisate by *Rhodococcus* sp. strain B4. Appl Environ Microbiol **58:**1874-7.

48. **Häggblom, M. M.** 1992. Microbial breakdown of halogenated aromatic pesticides and related compounds. FEMS Microbiol Rev **9:**29-71.

49. **Hammer, A., T. Hildenbrand, H. Hoier, K. L. Ngai, M. Schlomann, and J. J. Stezowski.** 1993. Crystallization and preliminary X-ray data of chloromuconate cycloisomerase from *Alcaligenes eutrophus* JMP134 (pJP4). J Mol Biol **232:**305-7.

50. **Harwood, C. S., and R. E. Parales.** 1996. The *beta*-ketoadipate pathway and the biology of self-identity. Annu Rev Microbiol **50:**553-90.

51. **Haug, W., A. Schmidt, B. Nortemann, D. C. Hempel, A. Stolz, and H. J. Knackmuss.** 1991. Mineralization of the sulfonated azo dye Mordant Yellow 3 by a 6-aminonaphthalene-2-sulfonate-degrading bacterial consortium. Appl Environ Microbiol **57:**3144-9.

52. **Haugland, R. A., D. J. Schlemm, R. P. Lyons, 3rd, P. R. Sferra, and A. M. Chakrabarty.** 1990. Degradation of the chlorinated phenoxyacetate herbicides

2,4-dichlorophenoxyacetic acid and 2,4,5-trichlorophenoxyacetic acid by pure and mixed bacterial cultures. Appl Environ Microbiol **56:**1357-62.

53. **Heider, J., and G. Fuchs.** 1997. Anaerobic metabolism of aromatic compounds. Eur J Biochem **243:**577-96.

54. **Heim, S., M. Del Mar Lleo, B. Bonato, C. A. Guzman, and P. Canepari.** 2002. The viable but nonculturable state and starvation are different stress responses of *Enterococcus faecalis*, as determined by proteome analysis. J Bacteriol **184:**6739-45.

55. **Helin, S., P. C. Kahn, B. L. Guha, D. G. Mallows, and A. Goldman.** 1995. The refined X-ray structure of muconate lactonizing enzyme from *Pseudomonas putida* PRS2000 at 1.85 A resolution. J Mol Biol **254:**918-41.

56. **Higson, F. K., and D. D. Focht.** 1989. Bacterial metabolism of hydroxylated biphenyls. Appl Environ Microbiol **55:**946-52.

57. **Hill, G. A., B. Tomusiak, B. Quail, and K. M. v. Cleave.** 1991. Bioreactor design effects on biodegradation capabilities of VOCs in wastewater. Environ. Prog. **10:**147-53.

58. **Hinner, I.** 1998. Biochemische und molekularbiologische Untersuchungen zu Lacton-Hydrolasen des bakteriallen Halogenaromaten-Abbaus. Ph.D. Universitaet Stuttgart, Stuttgart.

59. **Hintner, J. P., C. Lechner, U. Riegert, A. E. Kuhm, T. Storm, T. Reemtsma, and A. Stolz.** 2001. Direct ring fission of salicylate by a salicylate 1,2-dioxygenase activity from P*seudaminobacter salicylatoxidans*. J Bacteriol **183:**6936-42.

60. **Hoier, H., M. Schlömann, A. Hammer, A. Goldman, J. Stezwoski, J., and U. Heinemann.** 1994. Crystal Structure of Chloromuconate Cycloisomerase from *Alcaligenes eutrophus* JMP 134 (pJP4) at 3 A resolution. Acta Crystallographica - Section D - Biological Crystallography **50:**75-84.

61. **Hollender, J., J. Hopp, and W. Dott.** 1997. Degradation of 4-Chlorophenol via the *meta*-Cleavage Pathway by *Chromamonas testosteroni* JH5. Appl Environ Microbiol **63:**4567-72.

62. **Ignacio Jimenez, J., B. Minambres, J. L. Garcia, and E. Diaz.** 2002. Genomic analysis of the aromatic catabolic pathways from *Pseudomonas putida* KT 2440. Environ Microbiol **4:**824-41.

63. **Jimenez, J. I., B. Minambres, J. L. Garcia, and E. Diaz.** 2002. Genomic analysis of the aromatic catabolic pathways from *Pseudomonas putida* KT2440. Environ Microbiol **4:**824-41.

64. **Jiménez, J. I., B. Minambres, J. L. Garcia, and E. Diaz.** 2003. Genomic insights in the metabolism of aromatic compounds. Ramos, J.L. (ed.), The Pseudomonads. Biosynthesis of Macromolecules and Molecular metabolism, Vol. III. Kluwer Academic/Plenum Publishers, New York, in press.

65. **Johnson, G. R., R. K. Jain, and J. C. Spain.** 2002. Origins of the 2,4-dinitrotoluene pathway. J Bacteriol **184:**4219-32.

66. **Jones, R. M., V. Pagmantidis, and P. A. Williams.** 2000. sal genes determining the catabolism of salicylate esters are part of a supraoperonic cluster of catabolic genes in *Acinetobacter* sp. strain ADP1. J Bacteriol **182:**2018-25.

67. **Kasberg, T., D. L. Daubaras, A. M. Chakrabarty, D. Kinzelt, and W. Reineke.** 1995. Evidence that operons *tcb*, *tfd*, and *clc* encode maleylacetate reductase, the fourth enzyme of the modified *ortho* pathway. J Bacteriol **177:**3885-9.

68. **Kasberg, T., V. Seibert, M. Schlömann, and W. Reineke.** 1997. Cloning, characterization, and sequence analysis of the *clcE* gene encoding the maleylacetate reductase of *Pseudomonas* sp. strain B13. J Bacteriol **179:**3801-3.

69. **Kaschabek, S. R., T. Kasberg, D. Müller, A. E. Mars, D. B. Janssen, and W. Reineke.** 1998. Degradation of chloroaromatics: purification and characterization of a novel type of chlorocatechol 2,3-dioxygenase of *Pseudomonas putida* GJ31. J Bacteriol **180:**296-302.

70. **Kaschabek, S. R., and W. Reineke.** 1992. Maleylacetate reductase of *Pseudomonas* sp. strain B13: dechlorination of chloromaleylacetates, metabolites in the degradation of chloroaromatic compounds. Arch Microbiol **158:**412-7.

71. **Kaschabek, S. R., and W. Reineke.** 1995. Maleylacetate reductase of *Pseudomonas* sp. strain B13: specificity of substrate conversion and halide elimination. J Bacteriol **177:**320-5.

72. **Kaulmann, U., S. R. Kaschabek, and M. Schlömann.** 2001. Mechanism of chloride elimination from 3-chloro- and 2,4-dichloro-*cis*,*cis*-muconate: new insight obtained from analysis of muconate cycloisomerase variant CatB-K169A. J Bacteriol **183:**4551-61.

73. **Kim, S. I., S. H. Leem, J. S. Choi, Y. H. Chung, S. Kim, Y. M. Park, Y. K. Park, Y. N. Lee, and K. S. Ha.** 1997. Cloning and characterization of two *catA* genes in *Acinetobacter lwoffii* K24. J Bacteriol **179:**5226-31.

74. **Kim, S. I., S. H. Leem, J. S. Choi, and K. S. Ha.** 1998. Organization and transcriptional characterization of the *cat1* gene cluster in *Acinetobacter lwoffi* K24. Biochem Biophys Res Commun **243:**289-94.

75. **Klemba, M., B. Jakobs, R. M. Wittich, and D. Pieper.** 2000. Chromosomal integration of tcb chlorocatechol degradation pathway genes as a means of expanding the growth substrate range of bacteria to include haloaromatics. Appl Environ Microbiol **66:**3255-61.

76. **Kleywegt, G. J., H. Hoier, and T. A. Jones.** 1996. A re-evaluation of the crystal structure of chloromuconate cycloisomerase. Acta Crystallographica - Section D - Biological Crystallography **D52:**858-63.

77. **Krooneman, J., E. B. Wieringa, E. R. Moore, J. Gerritse, R. A. Prins, and J. C. Gottschal.** 1996. Isolation of *Alcaligenes* sp. strain L6 at low oxygen concentrations and degradation of 3-chlorobenzoate via a pathway not involving (chloro)catechols. Appl Environ Microbiol **62:**2427-34.

78. **Kuhm, A. E., M. Schlömann, H. J. Knackmuss, and D. H. Pieper.** 1990. Purification and characterization of dichloromuconate cycloisomerase from *Alcaligenes eutrophus* JMP 134. Biochem J **266:**877-83.

79. **Laemmli, C. M., J. H. Leveau, A. J. Zehnder, and J. R. van der Meer.** 2000. Characterization of a second tfd gene cluster for chlorophenol and chlorocatechol metabolism on plasmid pJP4 in *Ralstonia eutropha* JMP134(pJP4). J Bacteriol **182:**4165-72.

80. **Laemmli, U. K.** 1970. Cleavage of Structural Proteins during the Assembly of the Head of Bacteriophage T4. Nature **227:**680-5.

81. **Lee, J., K. R. Min, Y. C. Kim, C. K. Kim, J. Y. Lim, H. Yoon, K. H. Min, K. S. Lee, and Y. Kim.** 1995. Cloning of salicylate hydroxylase gene and catechol 2,3-dioxygenase gene and sequencing of an intergenic sequence between the two genes of *Pseudomonas putida* KF715. Biochem Biophys Res Commun **211:**382-8.

82. **Lehrbach, P. R., J. Zeyer, W. Reineke, H. J. Knackmuss, and K. N. Timmis.** 1984. Enzyme recruitment in vitro: use of cloned genes to extend the range of haloaromatics degraded by *Pseudomonas* sp. strain B13. J Bacteriol **158:**1025-32.

83. **Liu, D., R. J. Maguire, B. J. Dutka, and G. J. Pacepavicius.** 1990. Rationale for including metabolites in chemical toxicity bioassay. Toxicol. Assess. **5:**179-88.

84. **Maltseva, O. V., I. P. Solyanikova, and L. A. Golovleva.** 1994. Chlorocatechol 1,2-dioxygenase from *Rhodococcus erythropolis* 1CP. Kinetic and immunochemical comparison with analogous enzymes from gram-negative strains. Eur J Biochem **226:**1053-61.

85. **Maltseva, O. V., I. P. Solyanikova, L. A. Golovleva, M. Schlömann, and H. J. Knackmuss.** 1994. Dienenlactone hydrolase from *Rhodococcus erythropolis* 1 CP purification and properties. Arch Microbiol **162:**368-74.

86. **Mars, A. E., T. Kasberg, S. R. Kaschabek, M. H. van Agteren, D. B. Janssen, and W. Reineke.** 1997. Microbial degradation of chloroaromatics: use of the *meta*-cleavage pathway for mineralization of chlorobenzene. J Bacteriol **179:**4530-7.

87. **Mau, M., and K. N. Timmis.** 1998. Use of subtractive hybridization to design habitat-based oligonucleotide probes for investigation of natural bacterial communities. Appl Environ Microbiol **64:**185-91.

88. **Mc Cormick, S., and G. Tunnicliff.** 2001. Kinetics of inactivation of glutamate decarboxylase by cysteine-specific reagents.acta Biochimica Polonica **48:**573-8.

89. **Moiseeva, O. V., O. V. Belova, I. P. Solyanikova, M. Schlömann, and L. A. Golovleva.** 2001. Enzymes of a new modified *ortho*-pathway utilizing 2-chlorophenol in *Rhodococcus opacus* 1CP. Biochemistry (Mosc) **66:**548-55.

90. **Moiseeva, O. V., E. V. Lin'ko, B. P. Baskunov, and L. A. LGolovleva.** 1999. Degradation of 2-chlorophenol and 3-chlorobenzoate by *Rhodococcus opacus* 1CP. Microbioloy **64:**400-5.

91. **Moiseeva, O. V., I. P. Solyanikova, S. R. Kaschabek, J. Gröning, M. Thiel, L. A. Golovleva, and M. Schlömann.** 2002. A new modified *ortho*-cleavage pathway of 3-chlorocatechol degradation by *Rhodococcus opacus* 1CP: genetic and biochemical evidence. J Bacteriol **184:**5282-92.

92. **Müller, D., M. Schlömann, and W. Reineke.** 1996. Maleylacetate reductases in chloroaromatic-degrading bacteria using the modified *ortho* pathway: comparison of catalytic properties. J Bacteriol **178:**298-300.

93. **Murakami, S., A. Takashima, J. Takemoto, S. Takenaka, R. Shinke, and K. Aoki.** 1999. Cloning and sequence analysis of two catechol-degrading gene clusters from the aniline-assimilating bacterium *Frateuria* species ANA-18. Gene **226:**189-98.

94. **Nakai, C., K. Horiike, S. Kuramitsu, H. Kagamiyama, and M. Nozaki.** 1990. Three isozymes of catechol 1,2-dioxygenase (pyrocatechase), *alpha alpha*, *alpha beta*, and *beta beta*, from *Pseudomonas arvilla* C-1. J Biol Chem **265:**660-5.

95. **Ngai, K. L., M. Schlömann, H. J. Knackmuss, and L. N. Ornston.** 1987. Dienelactone hydrolase from *Pseudomonas* sp. strain B13. J Bacteriol **169:**699-703.

96. **Nicnas.** 2002. Polychlorinated Naphthalenes. National Industrial Chemicals Notification and Assessment Scheme. Australian government.

97. **Nielsen, A. T., T. Tolker-Nielsen, K. B. Barken, and S. Molin.** 2000. Role of commensal relationships on the spatial structure of a surface-attached microbial consortium. Environ Microbiol **2:**59-68.

98. **Norrander, J., T. Kempe, and J. Messing.** 1983. Construction of improved M13 vectors using oligodeoxynucleotide-directed mutagenesis. Gene **26:**101-6.

99. **Ohtsubo, Y., K. Miyauchi, K. Kanda, T. Hatta, H. Kiyohara, T. Senda, Y. Nagata, Y. Mitsui, and M. Takagi.** 1999. PcpA, which is involved in the degradation of pentachlorophenol in *Sphingomonas chlorophenolica* ATCC39723, is a novel type of ring-cleavage dioxygenase. FEBS Lett **459:**395-8.

100. **Ornston, L. N.** 1966. The conversion of catechol and protocatechuate to *beta*-ketoadipate by *Pseudomonas putida*. 3. Enzymes of the catechol pathway. J Biol Chem **241:**3795-9.

101. **Ornston, L. N.** 1966. The conversion of catechol and protocatechuate to *beta*-ketoadipate by *Pseudomonas putida*. II. Enzymes of the protocatechuate pathway. J Biol Chem **241:**3787-94.

102. **Ornston, L. N.** 1966. The conversion of catechol and protocatechuate to *beta*-ketoadipate by *Pseudomonas putida*. IV. Regulation. J Biol Chem **241:**3800-10.

103. **Ornston, L. N., and R. Y. Stanier.** 1966. The conversion of catechol and protocatechuate to *beta*-ketoadipate by *Pseudomonas putida*. I. Biochemistry. J Biol Chem **241:**3776-86.

104. **Parke, D., M. A. Garcia, and L. N. Ornston.** 2001. Cloning and genetic characterization of dca genes required for beta-oxidation of straight-chain dicarboxylic acids in Acinetobacter sp. strain ADP1. Appl Environ Microbiol **67:**4817-27.

105. **Pathak, D., K. L. Ngai, and D. Ollis.** 1988. X-ray crystallographic structure of dienelactone hydrolase at 2.8 A. J Mol Biol **204:**435-45.

106. **Pelz, O., M. Tesar, R. M. Wittich, E. R. Moore, K. N. Timmis, and W. R. Abraham.** 1999. Towards elucidation of microbial community metabolic pathways: unravelling the network of carbon sharing in a pollutant-degrading bacterial consortium by immunocapture and isotopic ratio mass spectrometry. Environ Microbiol **1:**167-74.

107. **Perez-Pantoja, D., L. Guzman, M. Manzano, D. H. Pieper, and B. Gonzalez.** 2000. Role of tfdC(I)D(I)E(I)F(I) and tfdD(II)C(II)E(II)F(II) gene modules in catabolism of 3-chlorobenzoate by *Ralstonia eutropha* JMP134(pJP4). Appl Environ Microbiol **66:**1602-8.

108. **Perez-Pantoja, D., T. Ledger, D. H. Pieper, and B. Gonzalez.** 2003. Efficient Turnover of Chlorocatechols Is Essential for Growth of *Ralstonia eutropha* JMP134(pJP4) in 3-Chlorobenzoic Acid. J Bacteriol **185:**1534-1542.

109. **Perkins, E. J., M. P. Gordon, O. Caceres, and P. F. Lurquin.** 1990. Organization and sequence analysis of the 2,4-dichlorophenol hydroxylase and dichlorocatechol oxidative operons of plasmid pJP4. J Bacteriol **172:**2351-9.

110. **Pessione, E., S. Divari, E. Griva, M. Cavaletto, G. L. Rossi, G. Gilardi, and C. Giunta.** 1999. Phenol hydroxylase from *Acinetobacter radioresistens* is a multicomponent enzyme. Purification and characterization of the reductase moiety. Eur J Biochem **265:**549-55.

111. **Pieper, D. H., K.-H. Engesser, R. H. Don, K. N. Timmis, and H. J. Knackmuss.** 1985. Modified *ortho*-cleavage pathway in *Alcaligenes eutrophus* JMP134 for the degradationof 4--methylcatechol. FEMS Microbiol Lett **29:**63-7.

112. **Pieper, D. H., K. Pollmann, P. Nikodem, B. Gonzalez, and V. Wray.** 2002. Monitoring key reactions in degradation of chloroaromatics by *in situ* (1)H nuclear magnetic resonance: solution structures of metabolites formed from *cis*-dienelactone. J Bacteriol **184:**1466-70.

113. **Pieper, D. H., K. Stadler-Fritzsche, K. H. Engesser, and H. J. Knackmuss.** 1993. Metabolism of 2-chloro-4-methylphenoxyacetate by *Alcaligenes eutrophus* JMP 134. Arch Microbiol **160:**169-78.

114. **Plumeier, I., D. Perez-Pantoja, S. Heim, B. Gonzalez, and D. H. Pieper.** 2002. Importance of different tfd genes for degradation of chloroaromatics by *Ralstonia eutropha* JMP134. J Bacteriol **184:**4054-64.

115. **Pollmann, K., S. Beil, and D. H. Pieper.** 2001. Transformation of chlorinated benzenes and toluenes by *Ralstonia* sp. strain PS12 *tecA* (tetrachlorobenzene dioxygenase) and *tecB* (chlorobenzene dihydrodiol dehydrogenase) gene products. Appl Environ Microbiol **67:**4057-63.

116. **Pollmann, K., S. Kaschabek, V. Wray, W. Reineke, and D. H. Pieper.** 2002. Metabolism of dichloromethylcatechols as central intermediates in the degradation of dichlorotoluenes by *Ralstonia* sp. strain PS12. J Bacteriol **184:**5261-74.

117. **Popp, P., L. Bruggemann, P. Keil, U. Thuss, and H. Weiss.** 2000. Chlorobenzenes and hexachlorocyclohexanes (HCHs) in the atmosphere of Bitterfeld and Leipzig (Germany). Chemosphere **41:**849-55.

118. **Potrawfke, T., J. Armengaud, and R. M. Wittich.** 2001. Chlorocatechols substituted at positions 4 and 5 are substrates of the broad-spectrum chlorocatechol 1,2-dioxygenase of *Pseudomonas chlororaphis* RW71. J Bacteriol **183:**997-1011.

119. **Prucha, M., A. Peterseim, K. N. Timmis, and D. H. Pieper.** 1996. Muconolactone isomerase of the 3-oxoadipate pathway catalyzes dechlorination of 5-chloro-substituted muconolactones. Eur J Biochem **237:**350-6.

120. **Rainey, P. B., and M. Travisano.** 1998. Adaptive radiation in the heterogeneous environment. Nature **394:**69-72.

121. **Reineke, W.** 1998. Development of hybrid strains for the mineralization of chloroaromatics by patchwork assembly. Annu Rev Microbiol **52:**287-331.

122. **Reineke, W., and H. J. Knackmuss.** 1978. Chemical structure and biodegradability of halogenate aromatic compounds. Substituent effects on 1,2-dioxygenation of benzoic acid. Biochim Biophys Acta **542:**412-23.

123. **Reineke, W., and H. J. Knackmuss.** 1984. Microbial metabolism of haloaromatics: isolation and properties of a chlorobenzene-degrading bacterium. Appl Environ Microbiol **47:**395-402.

124. **Reineke, W., and H. J. Knackmuss.** 1988. Microbial degradation of haloaromatics. Annu Rev Microbiol **42:**263-87.

125. **Rojo, F., D. H. Pieper, K. H. Engesser, H. J. Knackmuss, and K. N. Timmis.** 1987. Assemblage of *ortho* cleavage route for simultaneous degradation of chloro- and methylaromatics. Science **238:**1395-8.

126. **Rossello-Mora, R. A., J. Lalucat, and E. Garcia-Valdes.** 1994. Comparative biochemical and genetic analysis of naphthalene degradation among *Pseudomonas stutzeri* strains. Appl Environ Microbiol **60:**966-72.

127. **Rubio, M. A., K. H. Engesser, and H. J. Knackmuss.** 1986. Microbial metabolism of chlorosalicylates: effect of prolonged subcultivation on constructed strains. Arch Microbiol **145:**123-5.

128. **Ruckdeschel, G., G. Renner, and K. Schwarz.** 1987. Effects of pentachlorophenol and some of its known and possible metabolites on different species of bacteria. Appl Environ Microbiol **53:**2689-92.

129. **Sala-Trepat, J. M., K. Murray, and P. A. Williams.** 1972. The metabolic divergence in the meta cleavage of catechols by *Pseudomonas putida* NCIB 10015. Physiological significance and evolutionary implications. Eur J Biochem **28:**347-56.

130. **Sambrook, J., E. Fritsch, and T. Maniatis.** 1989. Molecular Cloning: A Laboratory Manuel., vol. I - III. Cold Spring Harbor Laboratory Press, New York.

131. **Schell, U., S. Helin, T. Kajander, M. Schlömann, and A. Goldman.** 1999. Structural basis for the activity of two muconate cycloisomerase variants toward substituted muconates. Proteins **34:**125-36.

132. **Schlömann, M.** 1988. Die verschiedenen Typen der Dienlacton-Hydrolase und ohre Rolle beim bakteriellen Abbau von 4-Fluorbenzoat. Ph.D. thesis. Universitat Stuttgart, Stuttgart.

133. **Schlömann, M.** 1994. Evolution of chlorocatechol catabolic pathways. Conclusions to be drawn from comparisons of lactone hydrolases. Biodegradation **5:**301-21.

134. **Schlömann, M.** 2002. Two Chlorocatechol Catabolic Gene Modules on Plasmid pJP4. J Bacteriol **184:**4049-53.

135. **Schlömann, M., P. Fischer, E. Schmidt, and H. J. Knackmuss.** 1990. Enzymatic formation, stability, and spontaneous reactions of 4-fluoromuconolactone, a metabolite of the bacterial degradation of 4-fluorobenzoate. J Bacteriol **172:**5119-29.

136. **Schlömann, M., K. L. Ngai, L. N. Ornston, and H. J. Knackmuss.** 1993. Dienelactone hydrolase from *Pseudomonas cepacia*. J Bacteriol **175:**2994-3001.

137. **Schlömann, M., E. Schmidt, and H. J. Knackmuss.** 1990. Different types of dienelactone hydrolase in 4-fluorobenzoate-utilizing bacteria. J Bacteriol **172:**5112-8.

138. **Schmid, A., A. Kollmer, R. G. Mathys, and B. Witholt.** 1998. Developments toward large-scale bacterial bioprocesses in the presence of bulk amounts of organic solvents. Extremophiles **2:**249-56.

139. **Schmidt, E., and H. J. Knackmuss.** 1980. Chemical structure and biodegradability of halogenated aromatic compounds. Conversion of chlorinated muconic acids into maleylacetic acid. Biochem J **192:**339-47.

140. **Schmidt, E., G. Remberg, and H. J. Knackmuss.** 1980. Chemical structure and biodegradability of halogenated aromatic compounds. Halogenated muconic acids as intermediates. Biochem J **192:**331-7.

141. **Seibert, V.** 1997. Evolution des bakteriellen Abbaus von chlorierten Aromaten - molekularbiologische Untersuchungen zur Rekrutierung der Maleylacetat-Reduktasen. Ph. D. Thesis. Universität Stuttgart.

142. **Seibert, V., E. M. Kourbatova, L. A. Golovleva, and M. Schlömann.** 1998. Characterization of the maleylacetate reductase MacA of *Rhodococcus opacus* 1CP and evidence for the presence of an isofunctional enzyme. J Bacteriol **180:**3503-8.

143. **Seibert, V., K. Stadler-Fritzsche, and M. Schlömann.** 1993. Purification and characterization of maleylacetate reductase from *Alcaligenes eutrophus* JMP134(pJP4). J Bacteriol **175:**6745-54.

144. **Seibert, V., M. Thiel, I. Hinner, and M. Schlömann.** 2003. Characterization of a gene cluster encoding the maleylacetate reductase from *Ralstonia eutropha* 335, an enzyme recruited for growth with 4-fluorobenzoate. J Bacteriol **in press**.

145. **Shapiro, J. A.** 1998. Thinking about bacterial populations as multicellular organisms. Annu Rev Microbiol **52:**81-104.

146. **Skiba, A., V. Hecht, and D. H. Pieper.** 2002. Formation of protoanemonin from 2-chloro-*cis*,*cis*-muconate by the combined action of muconate cycloisomerase and muconolactone isomerase. J Bacteriol **184:**5402-9.

147. **Smith, M. R.** 1990. The biodegradation of aromatic hydrocarbons by bacteria. Biodegradation **1:**191-206.

148. **Snyder, R., G. Witz, and B. D. Goldstein.** 1993. The toxicology of benzene. Environ Health Perspect **100:**293-306.

149. **Solyanikova, I. P., O. V. Maltseva, and L. A. Golovleva.** 1995. A modified *ortho*-cleavage pathway in *Pseudomonas putida* strain 87: Purification and properties of dienelactone hydrolase. Biochemistry Moscow **60:**945-51.

150. **Solyanikova, I. P., O. V. Maltseva, M. D. Vollmer, L. A. Golovleva, and M. Schlömann.** 1995. Characterization of muconate and chloromuconate cycloisomerase from *Rhodococcus*

erythropolis 1CP: indications for functionally convergent evolution among bacterial cycloisomerases. J Bacteriol **177:**2821-6.

151. **Solyanikova, I. P., O. V. Maltseva, M. D. Vollmer, L. A. Golovleva, and M. Schlömann.** 1995. Characterization of muconate and chloromuconate cycloisomerase from *Rhodococcus erythropolis* 1CP: indications for functionally convergent evolution among bacterial cycloisomerases. J Bacteriol **177:**2821-6.

152. **Spain, J., and D. T. Gibson.** 1991. Pathway for Biodegradation of *p*-Nitrophenol in a *Moraxella* sp.. Appl Environ Microbiol **57:**812-9.

153. **Spain, J. C., and S. F. Nishino.** 1987. Degradation of 1,4-dichlorobenzene by a *Pseudomonas* sp.. Appl Environ Microbiol **53:**1010-9.

154. **Spiers, A. J., A. Buckling, and P. B. Rainey.** 2000. The causes of *Pseudomonas* diversity. Microbiology **146:**2345-50.

155. **Stanier, R. Y., N. J. Palleroni, and M. Doudoroff.** 1966. The aerobic pseudomonads: a taxonomic study. J Gen Microbiol **43:**159-271.

156. **Stryer, L.** 1988. Biochemistry. Freeman and Company, New York.

157. **Studier, F. W., A. H. Rosenberg, J. J. Dunn, and J. W. Dubendorff.** 1990. Use of T7 RNA polymerase to direct expression of cloned genes. Methods Enzymol **185:**60-89.

158. **Suzuki, K., A. Ichimura, N. Ogawa, A. Hasebe, and K. Miyashita.** 2002. Differential expression of two catechol 1,2-dioxygenases in *Burkholderia* sp. strain TH2. J Bacteriol **184:**5714-22.

159. **Thompson, J. D., T. J. Gibson, F. Plewniak, F. Jeanmougin, and D. G. Higgins.** 1997. The CLUSTAL_X windows interface: flexible strategies for multiple sequence alignment aided by quality analysis tools. Nucleic Acids Res **25:**4876-82.

160. **Timmis, K. N., and D. H. Pieper.** 1999. Bacteria designed for bioremediation. Trends Biotechnol **17:**200-4.

161. **van der Meer, J. R.** 1994. Genetic adaptation of bacteria to chlorinated aromatic compounds. FEMS Microbiol Rev **15:**239-49.

162. **van der Meer, J. R.** 1997. Evolution of novel metabolic pathways for the degradation of chloroaromatic compounds. Antonie Van Leeuwenhoek **71:**159-78.

163. **van der Meer, J. R., R. I. Eggen, A. J. Zehnder, and W. M. de Vos.** 1991. Sequence analysis of the *Pseudomonas* sp. strain P51 *tcb* gene cluster, which encodes metabolism of chlorinated catechols: evidence for specialization of catechol 1,2-dioxygenases for chlorinated substrates. J Bacteriol **173:**2425-34.

164. **van der Meer, J. R., and V. Sentchilo.** 2003. Genomic islands and the evolution of catabolic pathways in bacteria. Curr Opin Biotechnol **14:**248-54.

165. **van der Meer, J. R., A. R. van Neerven, E. J. de Vries, W. M. de Vos, and A. J. Zehnder.** 1991. Cloning and characterization of plasmid-encoded genes for the degradation of 1,2-dichloro-, 1,4-dichloro-, and 1,2,4-trichlorobenzene of *Pseudomonas* sp. strain P51. J Bacteriol **173:**6-15.

166. **Verband der chemischen Industrie.** 1989. Umwelt und Chemie., 7 ed. Herder Verlag, Frankfurt, Germany.

167. **Vollhardt, K., P., C., and N. Schore, E.** 2000. Organische Chemie., third edition ed. Wiley-VCH Verlag, Weinheim, Germany.

168. **Vollmer, M. D., P. Fischer, H. J. Knackmuss, and M. Schlömann.** 1994. Inability of muconate cycloisomerases to cause dehalogenation during conversion of 2-chloro-*cis*,*cis*-muconate. J Bacteriol **176:**4366-75.

169. **Vollmer, M. D., H. Hoier, H. J. Hecht, U. Schell, J. Gröning, A. Goldman, and M. Schlömann.** 1998. Substrate specificity of and product formation by muconate cycloisomerases: an analysis of wild-type enzymes and engineered variants. Appl Environ Microbiol **64:**3290-9.

170. **Vollmer, M. D., U. Schell, V. Seibert, S. Lakner, and M. Schlömann.** 1999. Substrate specificities of the chloromuconate cycloisomerases from *Pseudomonas* sp. B13, *Ralstonia eutropha* JMP134 and *Pseudomonas* sp. P51. Appl Microbiol Biotechnol **51:**598-605.

171. **Vollmer, M. D., and M. Schlömann.** 1995. Conversion of 2-chloro-*cis*,*cis*-muconate and its metabolites 2-chloro- and 5-chloromuconolactone by chloromuconate cycloisomerases of pJP4 and pAC27. J Bacteriol **177:**2938-41.

172. **Werwath, J., H. A. Arfmann, D. H. Pieper, K. N. Timmis, and R. M. Wittich.** 1998. Biochemical and genetic characterization of a gentisate 1, 2-dioxygenase from *Sphingomonas* sp. strain RW5. J Bacteriol **180:**4171-6.

173. **Wery, J., D. I. Mendes da Silva, and J. A. de Bont.** 2000. A genetically modified solvent-tolerant bacterium for optimized production of a toxic fine chemical. Appl Microbiol Biotechnol **54:**180-5.

174. **White-Stevens, R. H., and H. Kamin.** 1972. Studies of a flavoprotein, salicylate hydroxylase. I. Preparation, properties, and the uncoupling of oxygen reduction from hydroxylation. J Biol Chem **247:**2358-70.

175. **White-Stevens, R. H., H. Kamin, and Q. H. Gibson.** 1972. Studies of a flavoprotein, salicylate hydroxylse. I. Enzyme mechanism. J Biol Chem **247:**2371-81.

176. **Williams, P. A., and K. Murray.** 1974. Metabolism of benzoate and the methylbenzoates by *Pseudomonas putida* (*arvilla*) mt-2: evidence for the existence of a TOL plasmid. J Bacteriol **120:**416-23.

177. **Wittich, R. M., C. Strömpel, E. R. B. Moore, R. Blasco, and K. N. Timmis.** 1999. Interaction of *Sphingomonas* and *Pseudomonas* strains in the degradation of chlorinated dibenzofurans. J. Ind. Microbiol. Biotechnol. **23:**353-8.

178. **Wittich, R. M., H. Wilkes, V. Sinnwell, W. Francke, and P. Fortnagel.** 1992. Metabolism of dibenzo-p-dioxin by *Sphingomonas* sp. strain RW1. Appl Environ Microbiol **58:**1005-10.

179. **Wycisk, P., H. Weiss, A. Kaschl, S. Heidrich, and K. Sommerwerk.** 2003. Groundwater pollution and remediation options for multi-source contaminated aquifers (Bitterfeld/Wolfen, Germany). Toxicol Lett **140-141:**343-51.

180. **Xun, L., J. Bohuslavek, and M. Cai.** 1999. Characterization of 2,6-dichloro-p-hydroquinone 1,2-dioxygenase (PcpA) of *Sphingomonas chlorophenolica* ATCC 39723. Biochem Biophys Res Commun **266:**322-5.

181. **Yamamoto, S., M. Katagiri, H. Maeno, and O. Hayaishi.** 1965. Salicylate Hydroxylase, a Monooxygenase Requiring Flavin Adenine Dinucleotide. I. Purification and General Properties. J Biol Chem **240:**3408-13.

182. **Yen, K. M., and I. C. Gunsalus.** 1982. Plasmid gene organization: naphthalene/salicylate oxidation. Proc Natl Acad Sci U S A **79:**874-8.

183. **You, I. S., D. Ghosal, and I. C. Gunsalus.** 1991. Nucleotide sequence analysis of the *Pseudomonas putida* PpG7 salicylate hydroxylase gene (*nahG*) and its 3'-flanking region. Biochemistry **30:**1635-41.

184. **You, I. S., and I. C. Gunsalus.** 1986. Regulation of the *nah* and *sal* operons of plasmid NAH7: evidence for a new function in *nahR*. Biochem Biophys Res Commun **141:**986-92.

185. **Zhou, N. Y., J. Al-Dulayymi, M. S. Baird, and P. A. Williams.** 2002. Salicylate 5-hydroxylase from *Ralstonia* sp. strain U2: a monooxygenase with close relationships to and shared electron transport proteins with naphthalene dioxygenase. J Bacteriol **184:**1547-55.

186. **Zhou, N. Y., S. L. Fuenmayor, and P. A. Williams.** 2001. nag genes of *Ralstonia* (formerly *Pseudomonas*) sp. strain U2 encoding enzymes for gentisate catabolism. J Bacteriol **183:**700-8.